

NEW DESIGN METHODS FOR POLYHEDRAL LINKAGES

A THESIS SUBMITTED TO
THE GRADUATE SCHOOL OF NATURAL AND APPLIED SCIENCES
OF
MIDDLE EAST TECHNICAL UNIVERSITY

BY

GÖKHAN KİPER

IN PARTIAL FULFILLMENT OF THE REQUIREMENTS
FOR
THE DEGREE OF MASTER OF SCIENCE
IN
MECHANICAL ENGINEERING

SEPTEMBER 2006

Approval of the Graduate School of Natural and Applied Sciences

Prof. Dr. Canan Özgen
Director

I certify that this thesis satisfies all the requirements as a thesis for the degree of Master of Science

Prof. Dr. S. Kemal İder
Head of Department

This is to certify that we have read this thesis and that in our opinion it is fully adequate, in scope and quality, as a thesis for the degree of Master of Science

Assoc. Prof. Dr. A. U. Özgür Kişisel
Co-Supervisor

Prof. Dr. Eres Söylemez
Supervisor

Examining Committee Members

Prof. Dr. Nevzat Özgüven (METU, ME) _____

Prof. Dr. Eres Söylemez (METU, ME) _____

Assoc. Prof. Dr. A. U. Özgür Kişisel (METU, MATH) _____

Prof. Dr. Reşit Soylu (METU, ME) _____

Asst. Prof. Dr. Ergin Tönük (METU, ME) _____

I hereby declare that all information in this document has been obtained and presented in accordance with academic rules and ethical conduct. I also declare that, as required by these rules and conduct, I have fully cited and referenced all material and results that are not original to this work.

Name, Last name : Gökhan Kiper

Signature :

ABSTRACT

NEW DESIGN METHODS FOR POLYHEDRAL LINKAGES

Kiper, Gökhan

M.Sc., Mechanical Engineering Department

Supervisor : Prof. Dr. Eres Söylemez

Co-Supervisor: Assoc. Prof. Dr. A. U. Özgür Kişisel

September 2006, 115 pages

This thesis analyses the existing types of polyhedral linkages and presents new linkage types for resizing polyhedral shapes. First, the transformation characteristics, most specifically, magnification performances of existing polyhedral linkages are given. Then, methods for synthesizing single degree-of-freedom planar polygonal linkages are described. The polygonal linkages synthesized are used as faces of polyhedral linkages. Next, the derivation of some of the existing linkages using the method given is presented. Finally, some designs of cover panels for the linkages are given. The Cardan Motion is the key point in both analyses of existing linkages and synthesis of new linkages.

Keywords: Deployable Structures, Polyhedral Linkages, Cardan Motion

ÖZ

ÇOK YÜZLÜ MEKANİZMALARI İÇİN YENİ TASARIM YÖNTEMLERİ

Kiper, Gökhan

Yüksek Lisans, Makine Mühendisliği Bölümü

Tez Yöneticisi : Prof. Dr. Eres Söylemez

Ortak Tez Yöneticisi : Doç. Dr. A. U. Özgür Kişisel

Eylül 2006, 115 sayfa

Bu tez çalışmasında mevcut çok yüzlü mekanizmaları analiz edilmekte ve yeni çok yüzlü mekanizması çeşitleri sunulmaktadır. İlk olarak, mevcut çok yüzlü mekanizmalarının dönüşüm karakteristikleri, özellikle büyütme performansları verilmektedir. Sonra, tek serbestlik dereceli düzlemsel çokgen mekanizmaları için tasarım yöntemleri anlatılmaktadır. Bu çokgen mekanizmaları çok yüzlü mekanizmalarının yüzleri olarak kullanılmaktadır. Daha sonra, bazı mevcut mekanizmaların sunulan yöntemlerle türetilmesine yer verilmektedir. Son olarak, mekanizmalar için kaplama paneli tasarımları verilmektedir. Hem mevcut mekanizmaların analizinde, hem de yeni mekanizmaların tasarımında Cardan hareketi anahtar rol oynamaktadır.

Anahtar kelimeler: Açılır-kapanır Yapılar, Çok Yüzlü Mekanizmalar, Cardan Hareketi

ACKNOWLEDGMENTS

The author is most sincerely grateful to his supervisor Prof. Dr. Eres Söylemez and co-supervisor Assoc. Prof. Dr. A. U. Özgür Kişisel for their most valuable efforts in guiding, teaching, understanding and encouraging throughout the study.

The author also would like to gratefully thank Prof. Dr. Peter Spellucci (Department of Mathematics, Technical University of Darmstadt), Prof. Dr. Gerhard Wilhelm Weber (Institute of Applied Mathematics, Middle East Technical University) and Prof. Dr. Cem Tezer (Department of Mathematics, Middle East Technical University) for their very precious time-sparing and contributions.

The technical assistance of Mr. Kıvanç Uyanık is gratefully acknowledged.

TABLE OF CONTENTS

PLAGIARISM	iii
ABSTRACT	iv
ÖZ	v
ACKNOWLEDGMENTS	vi
TABLE OF CONTENTS	vii
LIST OF FIGURES	ix
CHAPTER	
1. INTRODUCTION	1
1.1 Some Basics of Polyhedral Geometry	2
1.2 Cardan Motion	5
1.3 Recent Studies on Deployable Structures	8
1.4 Polyhedral Linkages	18
2. TRANSFORMATION CHARACTERISTICS OF PRESENT POLYHEDRAL LINKAGES	35
2.1 Linear Similarity Transformations in 3D Space	35
2.2 Motion Characteristics of Present Polyhedral Linkages	37
2.2.1 Dipolygonoids	37
2.2.2 The Fulleroid	45
2.2.3 Hoberman Designs	48
2.2.4 Wohlhart Designs	54
2.2.4.1 Polyhedral Star-Transformers	55

2.2.4.2	Linkages with Multiple Slider-Cranks	58
2.2.4.3	Linkages with Planar Link Groups for Double Pyramids	61
2.2.4.4	Linkages with Planar Link Loops for Regular Polyhedra	67
2.2.4.5	Polyhedral Zig-Zag Linkages	69
2.2.5	Agrawal et. al. Designs	72
2.2.6	Kovács et al. Designs	73
2.3	Comparison of the Present Designs	75
3.	NEW DESIGN METHODS FOR POLYHEDRAL LINKAGES	77
3.1	Sectioning Polyhedra	77
3.2	Synthesizing Linkages for the Triangular Sections	81
3.3	On the Motion of the Designed Mechanism	89
3.4	Polygon Scaling	95
3.5	Some Modifications - Relations with Existing Polygonal Linkages	97
3.6	Cover Plates for Planar Linkages	100
3.7	Solid Angle Preserving Links and Polyhedron Scaling	103
4.	DISCUSSION AND CONCLUSIONS	107
	REFERENCES	110
	APPENDIX – SYMMETRY GROUPS OF POLYHEDRA	114

LIST OF FIGURES

FIGURES

Figure 1.1 The five Platonic solids: tetrahedron, cube, octahedron, dodecahedron, icosahedron	4
Figure 1.2 Possible trajectories of points in Cardan motion	6
Figure 1.3 a) Isosceles slider-crank <i>OCS</i> and b) Double slide <i>AB</i>	7
Figure 1.4 The Iris Dome of Hoberman	9
Figure 1.5 A conic retractable dome of Hoberman which uses angulated scissor hinges	9
Figure 1.6 A planar arch structure making use of angulated elements	10
Figure 1.7 An angulated scissor element	10
Figure 1.8 Hoberman outside structures: a) the iris dome used in EXPO 2000, Hannover b) the gate used in 2002 Olympic Winter Games, Utah .	11
Figure 1.9 You and Pellegrino's planar and spherical retractable roof designs	12
Figure 1.10 Noncircular retractable roof design examples	12
Figure 1.11 Kokawa's roof design	13
Figure 1.12 Kokawa's arch-marionettic structure design	13
Figure 1.13 Kassabian and Pellegrino's two spherical covered retractable roof designs	14
Figure 1.14 Kassabian and Pellegrino's two planar covered retractable roof designs	15
Figure 1.15 Example of a single-layer network of Bennett linkages	16

Figure 1.16 Deployment sequence of a deployable arch	17
Figure 1.17 A prototype for the transforming partitions project of KDG	18
Figure 1.18 A student project of KDG	18
Figure 1.19 Jitterbug's motion: an octahedron – an icosahedron – a cuboctahedron – an icosahedron – an octahedron	19
Figure 1.20 Fulleroid's motion: the planar link pairs always remain on a rhombic dodecahedron	20
Figure 1.21 The scissor elements and geared joints used in Hoberman designs	21
Figure 1.22 Hoberman's expanding polyhedra designs	21
Figure 1.23 Wohlhart's linkages with the shapes of the Platonic solids proposed in [30]	23
Figure 1.24 Truncated icosahedral linkages with planar and spatial link groups	24
Figure 1.25 Polyhedral linkage complexes: a hexagonal prism and a linkage complex having unit cell as the cubic linkage	25
Figure 1.26 Wohlhart's linkages with the shapes of the Platonic solids proposed in [32]	27
Figure 1.27 Some irregular polyhedral linkages: A frustum pyramid linkage, a Catalan solid linkage and a toroidal linkage complex	28
Figure 1.28 Two octahedral double pyramidal linkages of the two types	28
Figure 1.29 The cubic and the octahedral linkages of [35]	29
Figure 1.30 Exploded form of a tetrahedral linkage with prismatic joints	30
Figure 1.31 Some alternative meshes: vertex mating (tetrahedra as the example), face mating (closed pack meshes; cubes as the example), edge mating (icosahedra, tetrahedra and dodecahedra as the examples)	31

Figure 1.32 Two different kinds of meshes used to approximate a chair	31
Figure 1.33 A cardboard model and computer simulation demonstrating the expansion process of a polyhedral virus	33
Figure 1.34 A realistic model for the motion of cowpea chlorotic mottle virus and a mechanical model for the same virus	34
Figure 2.1 Magnification of a triangle ABC about a <i>magnification center</i> O ..	36
Figure 2.2 An example of a dipolygon – A is a 120° rotation and B is a 90° rotation about two intersecting axes with a separation of angle θ ..	37
Figure 2.3 A possible way of construction of the dipolygonid $8\{3\} + 6\{4\} 54^\circ 44' 08''$ (8 triangles, 6 squares, $\theta = 54^\circ 44' 08''$)	38
Figure 2.4 The motion of the Jitterbug ($4\{3\} + 4\{3\} 70^\circ 31' 44''$): transforms from an octahedron to a cuboctahedron, and vice versa. In between the icosahedron is realized	39
Figure 2.5 The circumscribing cylinders for the uniform motion of a dipolygon	40
Figure 2.6 Joints allowing rotation of plates while keeping the angle between the planes of the plates constant	41
Figure 2.7 $12\{2\} + 6\{3\} 45^\circ$ has its polygonal faces on a cube at any configuration	41
Figure 2.8 The distance of a vertex and an edge of a regular n -gon	43
Figure 2.9 The projection of P on yz plane at the minimal configuration (M_{min}) and the maximal configuration (P_{max})	44
Figure 2.10 The expansion/contraction motion of the Fulleroid between the two limit configurations	46
Figure 2.11 Polygonal faces of the Fulleroid on rhombic dodecahedron	46
Figure 2.12 A pair of coplanar links at the face of a Fulleroid – at extreme configurations	47
Figure 2.13 a) The scissor elements [27] b) Geared joints	49

Figure 2.14 An octahedral symmetric linkage with gear joints a, c) in two possible folded configurations b) in an expanded configuration ..	49
Figure 2.15 A design constructed with polygonal elements [29] – a dipolygonid: $20\{3\} + 20\{3\} 41^{\circ}48'37''$	50
Figure 2.16 A general angulated scissor element in two configurations	51
Figure 2.17 A mechanism with an angulated scissor element	51
Figure 2.18 The famous Hoberman sphere	52
Figure 2.19 A polyhedral linkage making use of angulated elements – magnifies a truncated icosahedron	53
Figure 2.20 The maximal and minimal positions of an angulated element with $ AE = CE = BE = DE = l$ and $\angle AEB = \angle CED = \pi - \alpha$	54
Figure 2.21 Polyhedral star-transformer for the truncated icosahedron	56
Figure 2.22 A design of Hoberman a, b) minimal configurations with (a) 5-valent vertices pointing outward and (b) 3-valent vertices pointing outward c) an intermediate configuration between two maximal configurations	56
Figure 2.23 Relating circumscribing circle of a face to the circumscribing sphere for a Platonic solid	58
Figure 2.24 A planar link groups for an irregular pentagon	59
Figure 2.25 The magnification of the vertices are fully realized, but the edges are missing and the faces have blanks	59
Figure 2.26 Platonic solids by implementing planar link groups with multiple slider cranks on the faces	60
Figure 2.27 An irregular tetrahedral linkage	60
Figure 2.28 The two types of link groups proposed in [34]	62
Figure 2.29 An octahedral linkage	62
Figure 2.30 The edges and faces realized partially	62

Figure 2.31 The motion of the joint connecting an outer triangle and the central triangle with respect to frame (O, x, y)	63
Figure 2.32 Ratio of magnification versus central link rotation for an equilateral triangular linkage	66
Figure 2.33 Faces magnified as an opening flower	67
Figure 2.34 Vertices blank, edges through two points, faces partially blank ...	68
Figure 2.35 The Cardan motion of a link pair	68
Figure 2.36 Articulations for tetrahedral, cubic, dodecahedral linkages	70
Figure 2.37 Articulations for octahedral and icosahedral linkages	71
Figure 2.38 The tetrahedral, the cubic and the dodecahedral linkages	72
Figure 2.39 A cubic double link expandohedra	74
Figure 2.40 Vertices and edges blank, faces partially realized	74
Figure 3.1 A triangulation of a pentagon	78
Figure 3.2 Magnification of a triangle centered at one of its vertices	78
Figure 3.3 A six link kinematic chain which is supposed to scale a triangle ...	80
Figure 3.4 Simplified mechanism for half of a triangle	80
Figure 3.5 The known parameters of the system	81
Figure 3.6 The link parameters and the joint parameters of the mechanism ...	81
Figure 3.7 The largest desired size of 1OPR	85
Figure 3.8 The mechanism revised	86
Figure 3.9 The designed scissor linkage for an isosceles triangle $OP_{\max}R_{\max}$..	88
Figure 3.10 Cardan Motion for single slider - The motion of the moving centrede with respect to the fixed centrede	90

Figure 3.11 Segment PQ makes a Cardan Motion when connected to a multiple slider assembly	91
Figure 3.12 Geometrical illustration for maintaining a Cardan Motion with multiple slider assemblies	92
Figure 3.13 Two possible mechanisms to realize a specified straight line coupler path	93
Figure 3.14 Possible constructions for triangle scaling linkages	94
Figure 3.15 The fixed and moving centrodes for the coupler and intermediate links for a three-slider-linkage	95
Figure 3.16 Magnification of the vertices of a hexagon	96
Figure 3.17 Magnification of the vertices of a hexagon by using the linkages with slider axes through the vertices	97
Figure 3.18 Some of Hoberman's designs	98
Figure 3.19 Foldable ring structures of You et. al.	98
Figure 3.20 Linkages obtained by rigidly connected angulated elements	99
Figure 3.21 Wohlhart's linkages	100
Figure 3.22 Some extensions for the links to cover the faces	101
Figure 3.23 Phases of magnification of a square with links covering the surface fully at the maximal and the minimal configurations	101
Figure 3.24 A K'nex [®] model of a linkage magnifying a square	102
Figure 3.25 A link that can be used to connect a cubic vertex	103
Figure 3.26 A cubic linkage	104
Figure 3.27 Right cones intersecting at the tip for a 3-valent vertex	105
Figure 3.28 The gyro-elongated square dipyramid	106
Figure A.1 An algorithm to find the symmetry group of a polyhedron	115

CHAPTER 1

INTRODUCTION

Umbrellas, eye glasses, tents, foldable chairs, tables, ladders... Some goods need to be collapsible for transportability or storage purposes. Also satellite wings and retractable roofs for pools and sports centers must be deployable. In all these movable constructions, the aim is not motion but to transform rigid bodies from a stable state to another. Hence, such systems are termed as *deployable structures*.

Recently, functionality, cost reduction and ease-of-use requirements of applications for which deployable structures can be used accelerated the researches on development of new deployable systems. Even a symposium on deployable structures was held in Cambridge in 1998 [1].

Among many type of deployable structures, this thesis deals with the *polyhedral linkages*. Polyhedral linkages are the deployable structures used for spatial deployment, where a shape transformation between certain polyhedral shapes is realized. This type of linkages finds application in spatial magnification of objects, virus modeling, architecture and toy industry.

In this chapter, some basic terminology and theory and the recent studies on deployable structures will be presented. In Chapter 2, the polyhedral linkages of various designers are analyzed in detail. New design methods for polyhedral linkages are presented in Chapter 3. Conclusions and discussions are given in Chapter 4. Also there is a section about polyhedral geometry in the appendices.

1.1 Some Basics of Polyhedral Geometry

A *polygon* is a closed planar region bounded by straight lines. The line segments constituting the boundaries are called the *sides* of a polygon, while the intersection points of the sides are called the *vertices* of a polygon. In general, only two edges intersect at a vertex. Generally, degenerate cases where more than two edges intersect at a vertex are disregarded. Polygons are usually named by the number of sides, such as pentagon, hexagon, etc. As two special cases, polygons with three sides are called triangles and polygons with four sides are called quadrilaterals. Also some polygons may have special names due to special geometry, such as a parallelogram or an isosceles triangle. If any line segment drawn between two inner points of a polygon totally remains in the inner region, then such a polygon is called a *convex polygon*. Otherwise, the polygon is a *concave polygon*. Convex polygons with equal side lengths and angles are called *regular polygons*. If all vertices of a polygon are on a circle, the polygon is called a *cyclic polygon* [2].

A *polyhedron* is a closed spatial region bounded by planes. The name polyhedron comes from the two Latin words *poly*, meaning many, and *hedron*, meaning face. The plural form is *polyhedra*. The planar boundaries of the polyhedra, which are indeed polygons, are called *faces*, while the line segments that are the intersections of the faces are called the *edges* and the intersection points of the edges are called the *vertices*. If an edge is intersection of more than two faces or if there is shrinkage at a vertex, the polyhedral shape is degenerate. Physically interpreting, an object with a small but finite volume must be able to freely travel inside a polyhedron, otherwise, the polyhedron is said to be degenerate. Degenerate polyhedra are generally disregarded. If any line segment drawn between two inner points of a polyhedron totally remains

in the inner region, then such a polyhedron is called a *convex polyhedron*, and otherwise a *concave polyhedron*. If all vertices of a polyhedron are on a sphere, the polyhedron is called a *spherical polyhedron* [2].

The number of edges meeting at a vertex is termed as the *valency* of a vertex. The angle between two adjacent edges on a polygonal face is called a *plane angle*. The angle between two neighboring faces is called the *dihedral angle*. A small neighborhood around a vertex is called the *solid angle* of a vertex. As angles are measured by distances on a unit circle, solid angles are measured by areas on unit spheres and the unit of measure is *steradians* [2].

Polyhedra are named according to the number of faces, such as tetrahedron, octahedron, decahedron, etc. Again, some special names due to special geometry exist. If a convex polyhedron has only regular polygons of the same type as the faces and the solid angles of all the vertices are the same, then the polyhedron is a *regular polyhedron (Platon Solid)*. There are five regular polyhedra: the regular tetrahedron, the cube, the regular octahedron, the regular dodecahedron and the regular icosahedron (Figure 1.1). Some other well known special polyhedra are the *Prism, Antiprisms, Archimedean Solids (Semi-regular Polyhedra)*, Catalan Solids (duals of Archimedean Solids) and *Johnson Solids* [2].

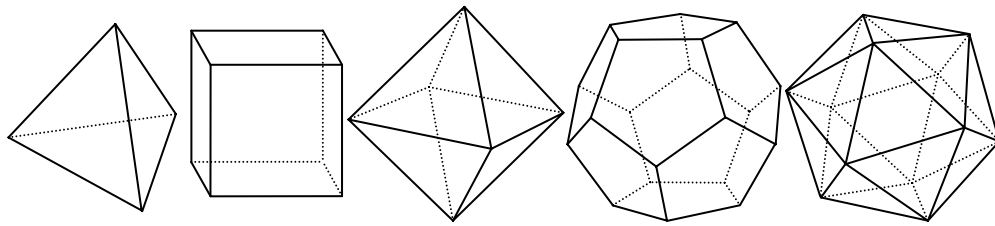


Figure 1.1 The five Platonic solids: tetrahedron, cube, octahedron, dodecahedron, icosahedron

Most of the time, polyhedra are classified according to the symmetries they preserve (See Appendix for the details of symmetry groups of polyhedra). The symmetry groups of polyhedra obviously constitute equivalence classes. Usually, two elements of a class can be obtained from one another by either truncating or expanding. *Truncation* is cutting pyramids on the vertices of a polyhedron and *expansion* is adding pyramids on the faces of a polyhedron, while preserving the symmetries. Archimedean solids can be obtained if one continuously truncates a polyhedron until the cuts finally meet or expands until two neighboring faces become coplanar, the *dual (reciprocal)* of the original polyhedron is found. The dual of a polyhedron is obtained by interchanging the vertices with faces and vice versa. Every polyhedron has a dual and the dual of the dual of a polyhedron is itself. Specifically, the tetrahedron is self-dual, the cube and the octahedron are duals and the dodecahedron and the icosahedron are duals [2].

1.2 Cardan Motion

The Cardan motion plays an important role in this thesis, as it appears in analysis and synthesis of many linkages. To define and analyze Cardan motion, some basic definitions are necessary.

Consider a fixed plane Γ_f and a moving plane Γ_m . If Γ_m is not in pure translation, at any instant, there exists a fixed point on Γ_m and this point is called the *pole* or the *instantaneous center*. The curve traced by the pole in Γ_f is called the *fixed centrode* and the curve tracked by the pole in Γ_f is called the *moving centrode*. In general, the fixed centrode envelopes the moving centrode. If the centrodes are both circles with fixed centrode diameter twice of moving centrode diameter, then the circles are called the *Cardan circles* and the motion is called the *Cardan motion* [3].

A general point in the moving centrode has an elliptic trajectory in Γ_f , hence the Cardan motion is also referred as the *elliptic motion* (trajectory of point E and F in Figure 1.2). The center of such an ellipse is the center of the fixed centrode. As a limiting case, if the point of interest is on the moving centrode in Γ_m , the path of this point is a straight line passing through the center of the fixed centrode (Trajectory of point S in Figure 1.2). As a special case, the path of the center of the moving centrode in Γ_f is a circle with the same radius as the moving centrode and center coincident with the center of the fixed centrode (trajectory of point O in Figure 1.2) [3].

The Cardan motion most simply can be visualized as the rolling of a circle inside a circle with diameter twice larger. If these circles are gears, the

planetary gear pair obtained realizes the Cardan motion. Other two well known Cardan motion mechanisms are the isosceles slider-crank mechanism (equal crank and coupler length) (Figure 1.3.a) and a double slide along two intersecting lines (Figure 1.3.b) [3]. For the isosceles slider-crank mechanism, one joint of the coupler link traces a circle while the other one traces a straight line. Since the motion of a plane can be fully described by two distinct points, the motion of the coupler link is the Cardan motion. Similarly, both joints of the double slider trace a straight line, hence the motion is the Cardan motion.

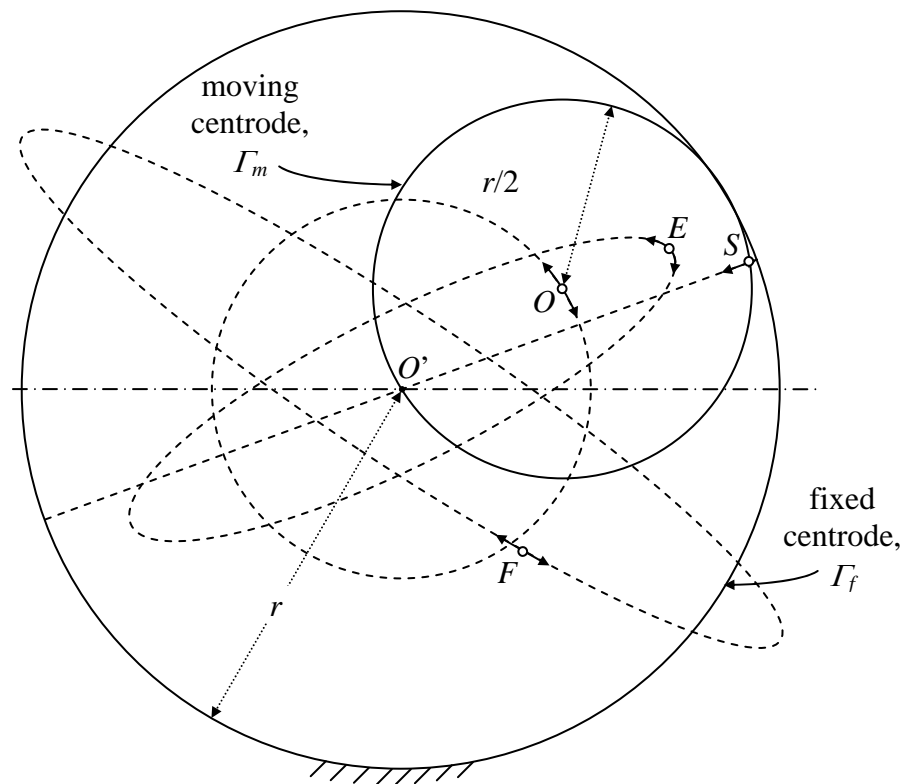


Figure 1.2 Possible trajectories of points in Cardan motion

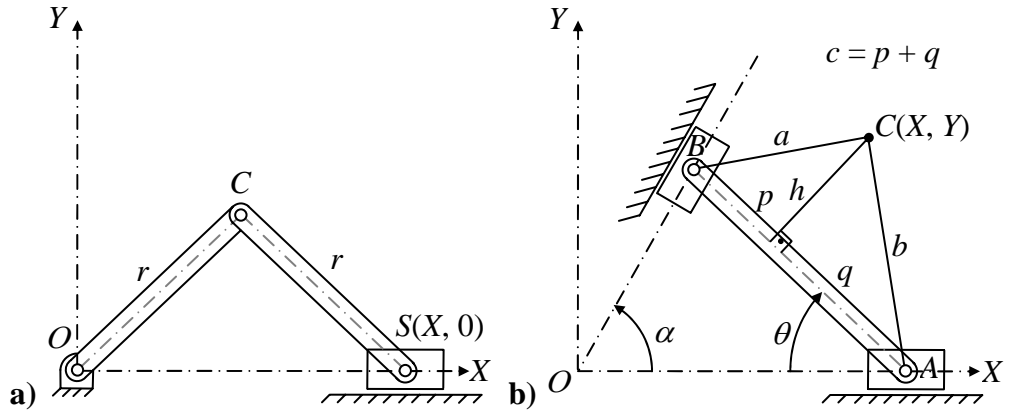


Figure 1.3 a) Isosceles slider-crank *OCS* and b) Double slide *AB*

The analysis of the double slider is necessary in the following chapter. Consider the double slide *AB* in Figure 1.3. A coupler point *C* has the coordinates

$$X = \left(\frac{c}{\tan \alpha} + h \right) \sin \theta + p \cos \theta \quad \text{and} \quad Y = q \sin \theta + h \cos \theta \quad (1.1a, b)$$

Solving (1.1a) and (1.1b) for $\cos \theta$ and $\sin \theta$, by the Pythagorean Theorem the following ellipse equation is obtained

$$b^2 X^2 + \left[p^2 + \left(h + \frac{c}{\tan \alpha} \right)^2 \right] Y^2 - 2c \left(h + \frac{q}{\tan \alpha} \right) XY = \left(pq - h^2 - \frac{ch}{\tan \alpha} \right)^2 \quad (1.2)$$

For $h = -b \cos \alpha$ and $p = q = b \sin \alpha$ (1.2) is a circle equation with radius $a = b$

and for $b^2 \left[p^2 + \left(h + \frac{q}{\tan \alpha} \right)^2 \right] = c^2 \left(h + \frac{q}{\tan \alpha} \right)^2$ (1.2) is a straight line equation.

1.3 Recent Studies on Deployable Structures

In this section a brief summary of previous work on deployable structures is presented.

The very systematic studies on deployable structures were started by Prof. Sergio Pellegrino when he founded the Deployable Structures Laboratory (DSL) at the University of Cambridge in 1990 [4]. Pellegrino et al. study on folding conditions for two-dimensional and three-dimensional structures with scissors joints, packaging conditions for thin membranes, computational tools to identify singular configurations (kinematic bifurcations) along a deployment path, shape optimization methods for variable geometry trusses [5].

Among various projects of the DSL, retractable roofs need to be paid attention as far as this thesis is concerned. A detailed review of past work relating retractable roofs can be obtained from [5].

The Spanish engineers Pinero, Escrig and Zeigler used scissor hinges for retracting roofs [6]. Rather new designs shown in Figures 1.4-1.6 belong to Hoberman. The Iris dome (Figure 1.4) is constructed from a number of angulated elements (Figure 1.7) arranged on concentric circles. These form a circular shape and the circles are connected to each other by joints connecting the end nodes of the angulated elements, creating a series of pin-jointed parallelograms. This allows the structure to retract towards its perimeter thus creating a central opening at the center when retracted [7]. Some of Hoberman's models were built (Figure 1.8).

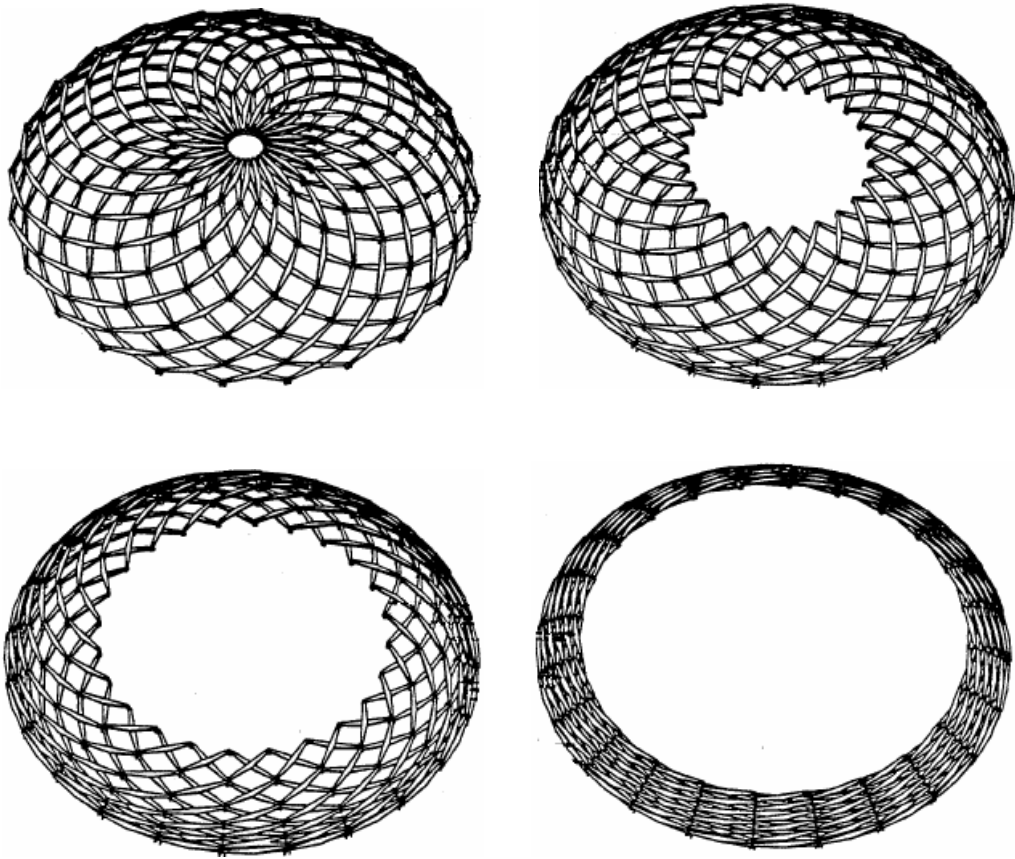


Figure 1.4 The Iris Dome of Hoberman [8]



Figure 1.5 A conic retractable dome of Hoberman which uses angulated scissor hinges [9]

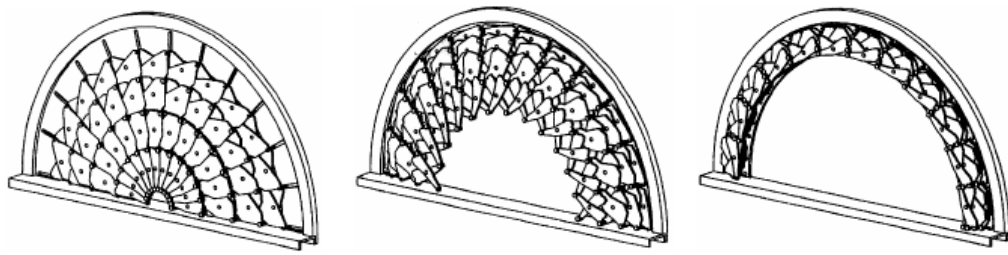


Figure 1.6 A planar arch structure making use of angulated elements [9]

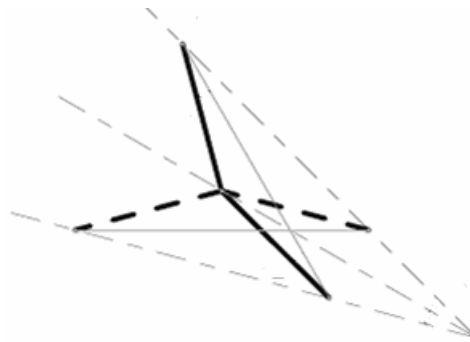


Figure 1.7 An angulated scissor element [4]

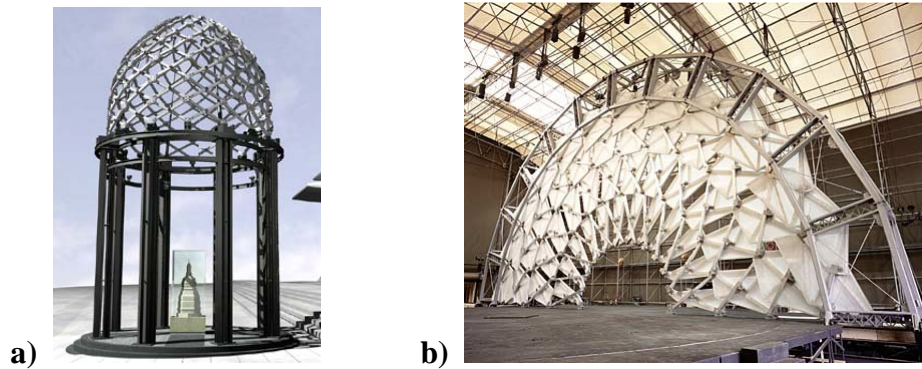


Figure 1.8 Hoberman outside structures: **a)** the iris dome used in EXPO 2000, Hannover **b)** the gate used in 2002 Olympic Winter Games, Utah [7]

Back to the retractable domes, the next development was by You and Pellegrino with the multi-angulated elements [10]. Each multi-angulated element is composed of a number of bars, which are rigidly connected to each other, instead of separate angulated elements as used by Hoberman [4]. Examples of such deployable structures are given in Figure 1.9. The mechanism in this figure consists of 24 identical angulated elements, each of which is a bar having 3 bends. There is a revolute joint at each bend. Also You and Pellegrino present noncircular foldable structures in [10], as illustrated in Figure 1.10. Kovacs and Tarnai studied foldable spherical bar structures [11].

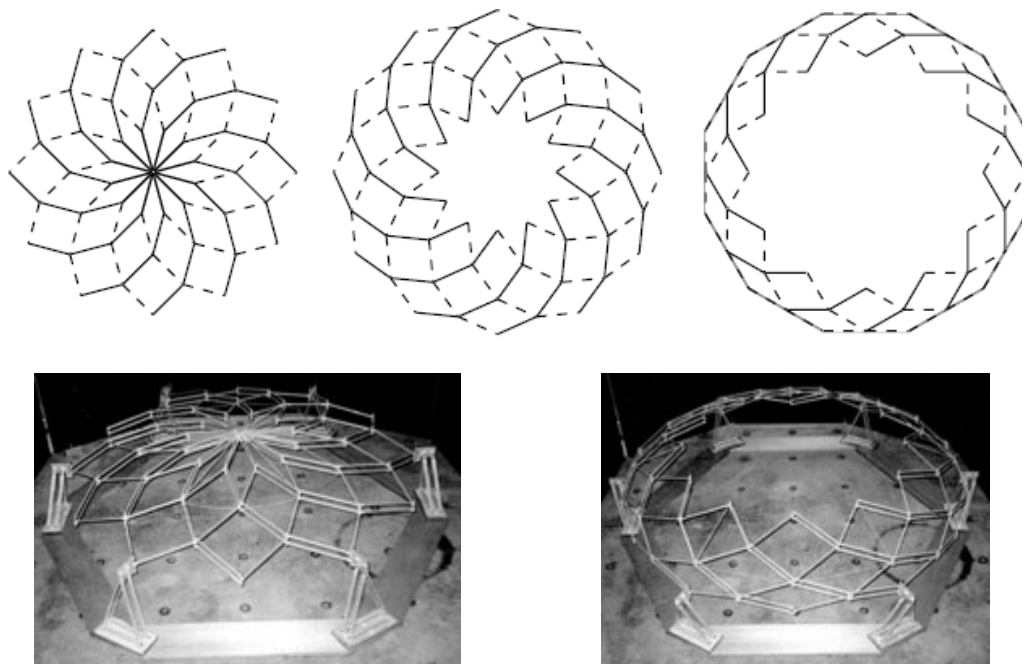


Figure 1.9 You and Pellegrino's planar and spherical retractable roof designs [5]

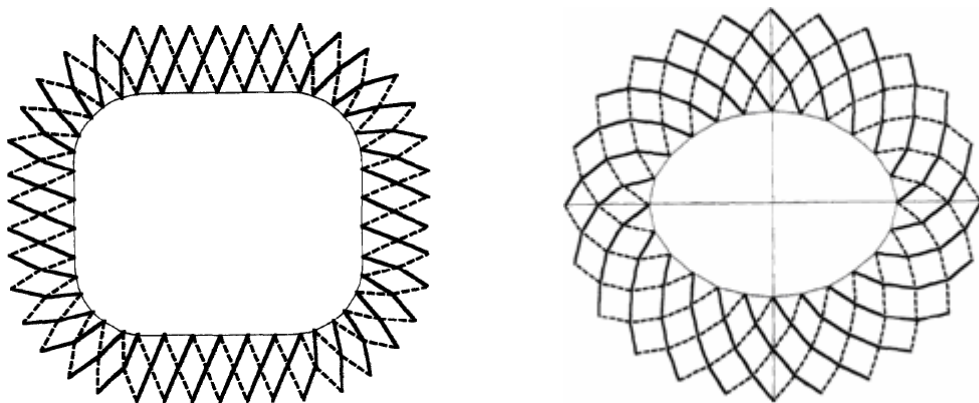


Figure 1.10 Noncircular retractable roof design examples [10]

Based on studies of You and Pellegrino, Kokawa proposed a new type of retractable dome structure (Figure 1.11). Kokawa also worked on a deployable tent design (Figure 1.12).

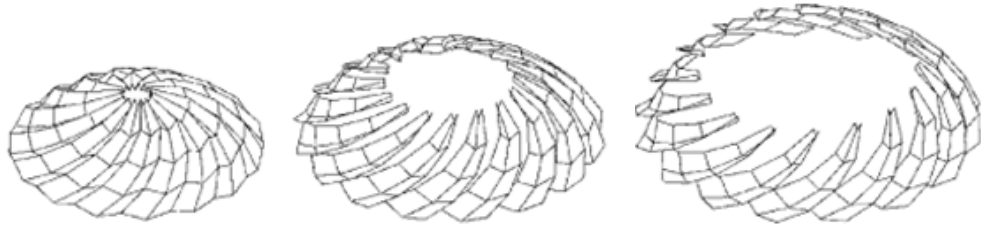


Figure 1.11 Kokawa's roof design [12]



Figure 1.12 Kokawa's arch-marionettic structure design [13]

By further studies of Kassabian and Pellegrino cover elements were designed to cover the surface spanned by the multi-angulated elements (Figures 1.13, 1.14). The main idea that allows the design was the fact that if a rigid body

rotation of the structure is allowed, then the motion of each angulated element is a pure rotation about a fixed point and hence can be described by a circle. Therefore it is possible to support the structure on a number of fixed points each corresponding to the centre of one of these circles [4]. The design details of these cover plates can be found in [5]. Later, Buhl, Jensen and Pellegrino studied on shape optimization of these cover elements [14].

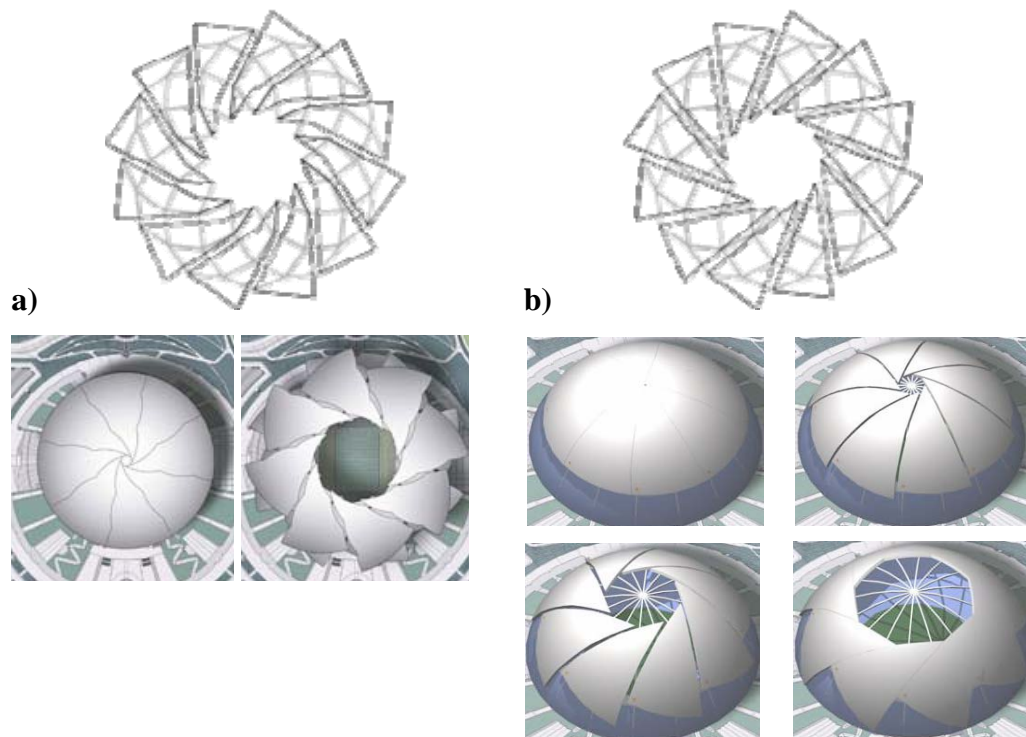


Figure 1.13 Kassabian and Pellegrino's two spherical covered retractable roof designs [4]

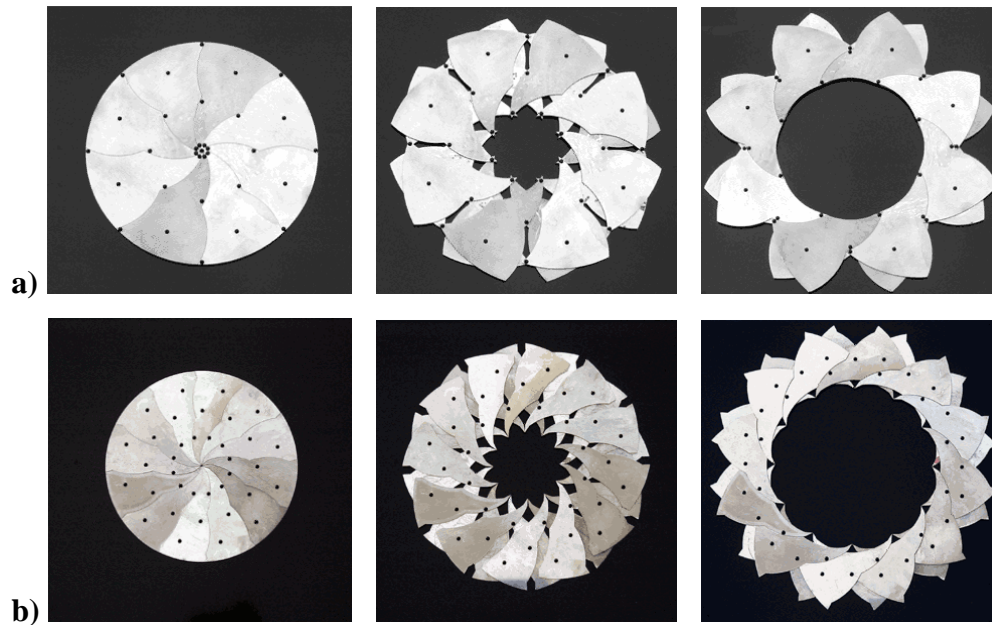


Figure 1.14 Kassabian and Pellegrino's two planar covered retractable roof designs [4]

Some other active research areas of DSL are tensegrity structures [15, 16], solid surface deployable antenna, mesh reflector [17], bi-stable shells with embedded actuators, deployable Synthetic Aperture Radar (SAR) systems [18], wrinkling of membrane surfaces [19], dynamic analysis of catenary mooring cables, design and actuation of multi-stable structures and foldable composite structures.

Another way to build deployable structures is to make use of Bennett linkages. Synthesis of Bennett linkages can be reviewed in [20]. Chen and You used these linkages as unit elements for deployable structures [21]. The Bennett linkage consists of a chain of four rigid links connected by four revolute, axes of which are neither parallel nor concurrent. The linkage is the only 4R linkage

with this property [20]. Some examples of deployable networks of Bennett linkages are illustrated in Figures 1.15, 1.16 [21]. Notice that Bennett linkages are joined to each other not at the joints of the linkages, but by revolute joints at the bars, constructing some small scale Bennett linkages in the neighborhood of the joints. Chen and You also used 6R linkages, specifically the Bricard linkages to synthesize deployable structures [22].

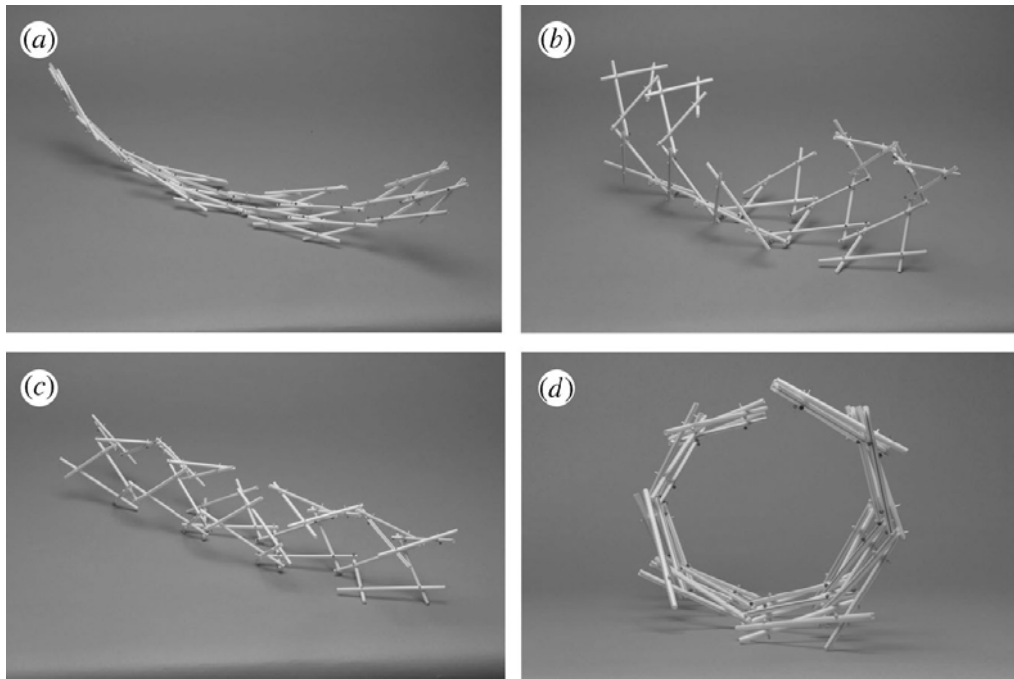


Figure 1.15 Example of a single-layer network of Bennett linkages [21]

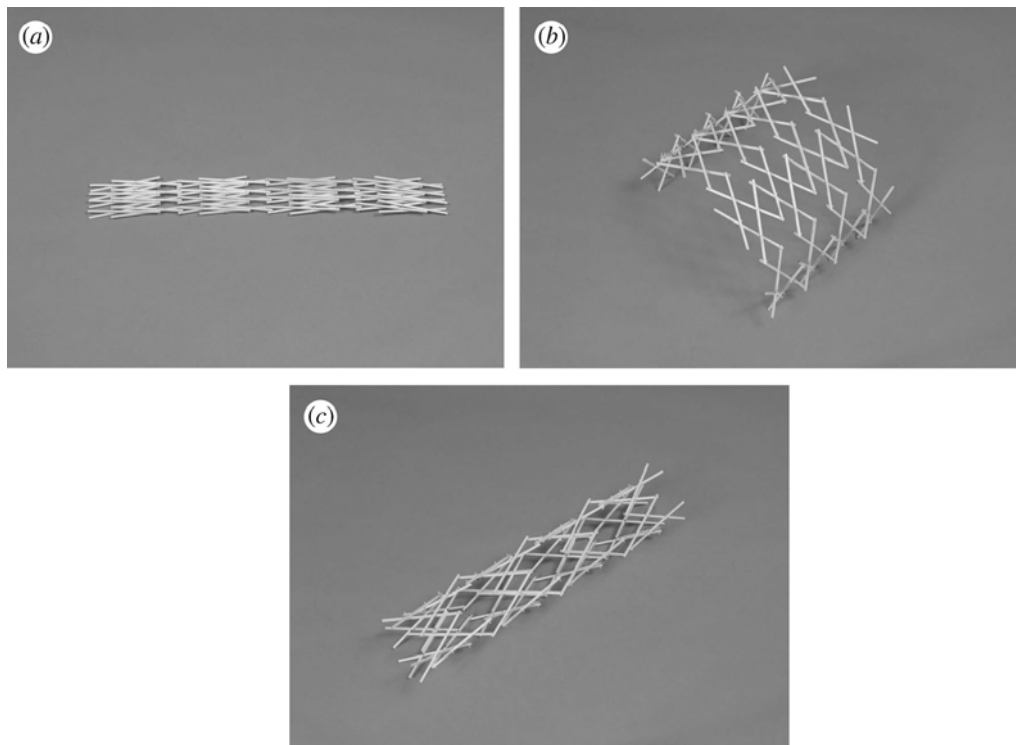


Figure 1.16 Deployment sequence of a deployable arch [21]

Another academic group studying deployable structures is the Kinetic Design Group (KDG) of Massachusetts Institute of Technology. The group studies deployable structures-related subjects such as folding egg and transforming partitions [23] (See Figures 1.17, 1.18).

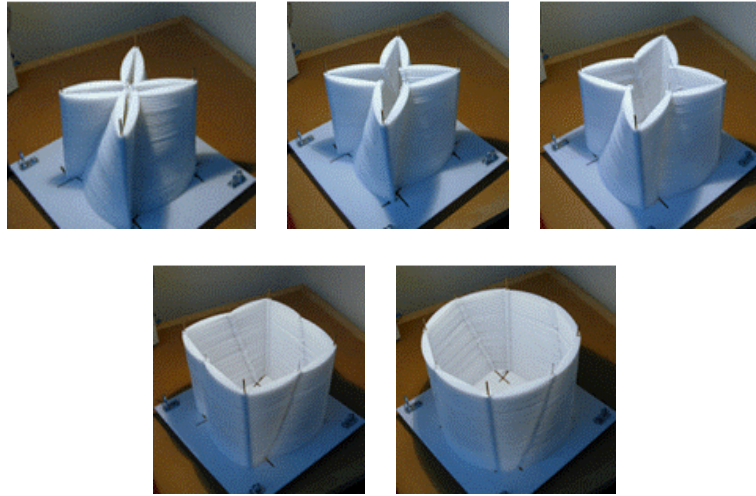


Figure 1.17 A prototype for the transforming partitions project of KDG [23]



Figure 1.18 A student project of KDG [23]

1.4 Polyhedral Linkages

Although, the term polyhedral linkage is defined as “space linkages made entirely of rigid plates hinged together” by Michael Goldberg in 1942 [24], this term refers to a more general class today, where only the shape is of concern

while the joint type is not limited to the hinged joints: Polyhedral linkages are the deployable structures used for spatial deployment, where a shape transformation between certain polyhedral shapes is realized. In this thesis, only a special class of polyhedral linkages for which the linkages transform between similar polyhedral shapes with variable size will be considered.

The present polyhedral linkages will be introduced in this section, however, detailed analysis is given in Chapter 2.

First serious work on this type of polyhedral linkages is probably R. Fuller Buckminster's discovery: the *jitterbug* [25]. The jitterbug is a polyhedral linkage which consists of eight equilateral triangular shaped links. The joints at the vertices of the triangles allow the linkage to have a one degree-of-freedom (dof) motion (Figure 1.19). The special thing about the linkage is that the triangular faces rotation and radial expansion (dilation symmetry) motion along the four three-fold symmetry axes of the octahedron. Later on, many jitterbug-like linkages were discovered and Verheyen fully defined and classified these linkages giving them a new name: the *dipolygonids* [25].

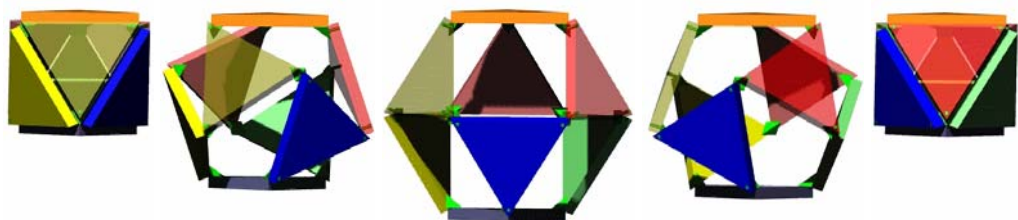


Figure 1.19 Jitterbug's motion: an octahedron – an icosahedron – a cuboctahedron – an icosahedron – an octahedron (simulation prepared using MSC.visualNastran 4D 2002)

Another important design of Fuller is the Fulleroid (Figure 1.20). Fulleroid contains isosceles triangle shaped links. The twelve link pairs connected by revolute joints remain coplanar on the faces of a fictitious rhombic dodecahedron at all configurations. The rhombic dodecahedron shape can be fully visualized in the minimal configuration. In 1997 Wohlhart presented the kinematic and dynamic analysis of the Fulleroid [26].

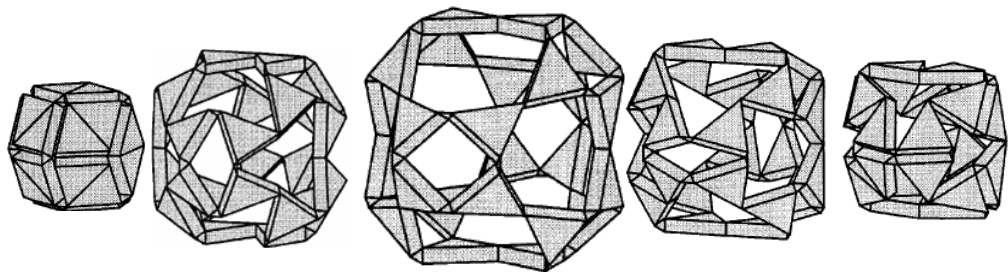


Figure 1.20 Fulleroid's motion: the planar link pairs always remain on a rhombic dodecahedron [26]

Recently, the famous Hoberman toys called attention to polyhedral linkages. The Hoberman toys retract and contract via linkages constructed in radial symmetry or by frames on the surface of polyhedra. Hoberman uses angulated scissor elements, polygonal link groups or geared joints for the expansion motion (Figure 1.21). Usually he uses spherical polyhedra, i.e. polyhedra having all the vertices on a sphere, with many faces so that the final configuration is almost a sphere (Figure 1.22)

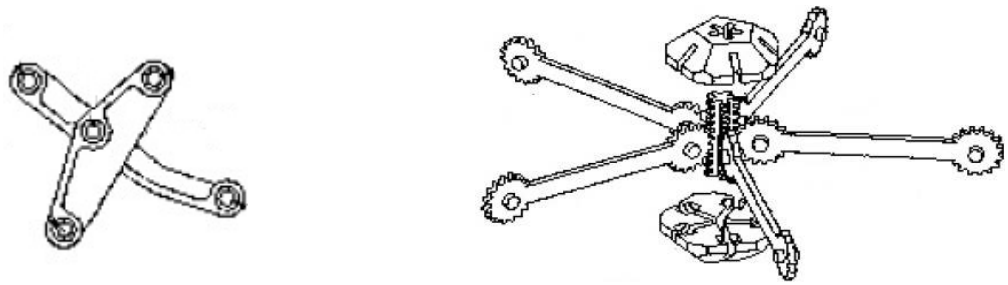


Figure 1.21 The scissor elements and geared joints used in Hoberman designs [27, 28]

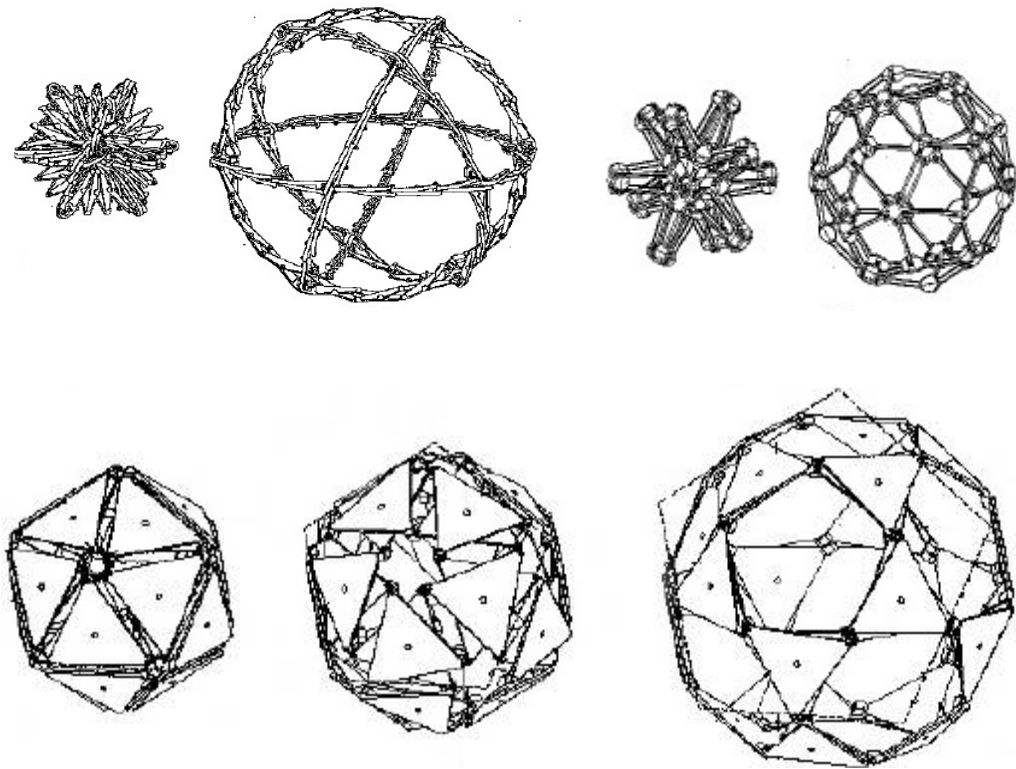


Figure 1.22 Hoberman's expanding polyhedra designs [27, 28, 29]

The scientific studies relating polyhedral linkages became more popular in the last few years. Among the latest studies, some of the most important studies belong to Karl Wohlhart. In 2001, Wohlhart proposed regular polyhedral linkages, where regular polyhedra are defined as all polyhedra which have similar arrangements of non-intersecting regular plane polygonal faces of two or more types about each vertex with all edges of equal length [30]. In this paper Wohlhart first defines the characteristics of the linkages and applies a mobility analysis to illustrate the overconstraintness of the linkages. Basically, Wohlhart synthesizes planar link groups on the faces of the polyhedron and interconnects these groups by special gussets. Later, Wohlhart gives the synthesis details of the linkages. Also the numerical details of the linkages having the shapes of the five Platonic solids are given (Figure 1.23). For the Archimedean solids, Wohlhart compares two different mechanisms: the linkages with planar link groups proposed in [30] and spatial link groups proposed in [31] (Figure 1.24). Finally Wohlhart presents linkage complexes which are obtained by combining same type of linkages (Figure 1.25).

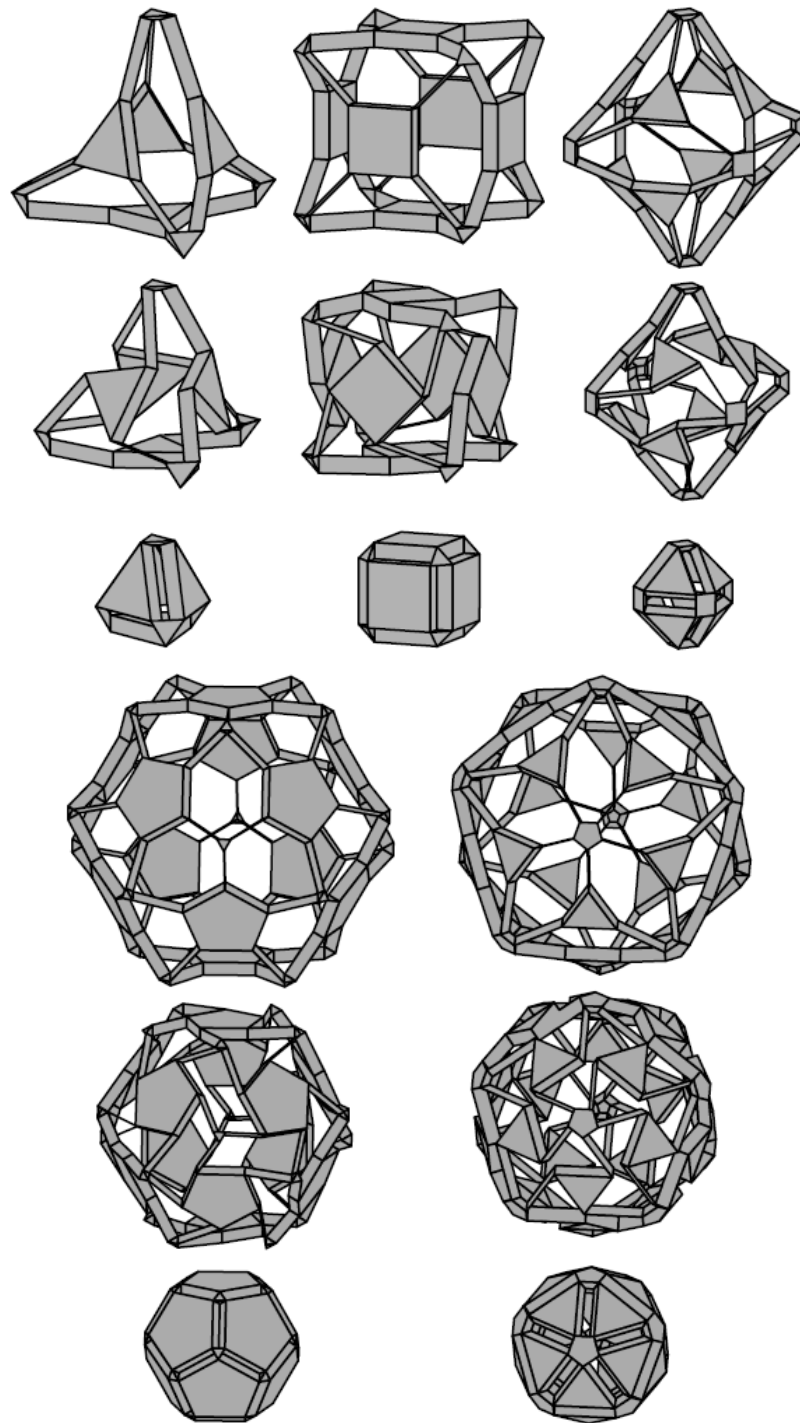


Figure 1.23 Wohlhart's linkages with the shapes of the Platonic solids proposed in [30]

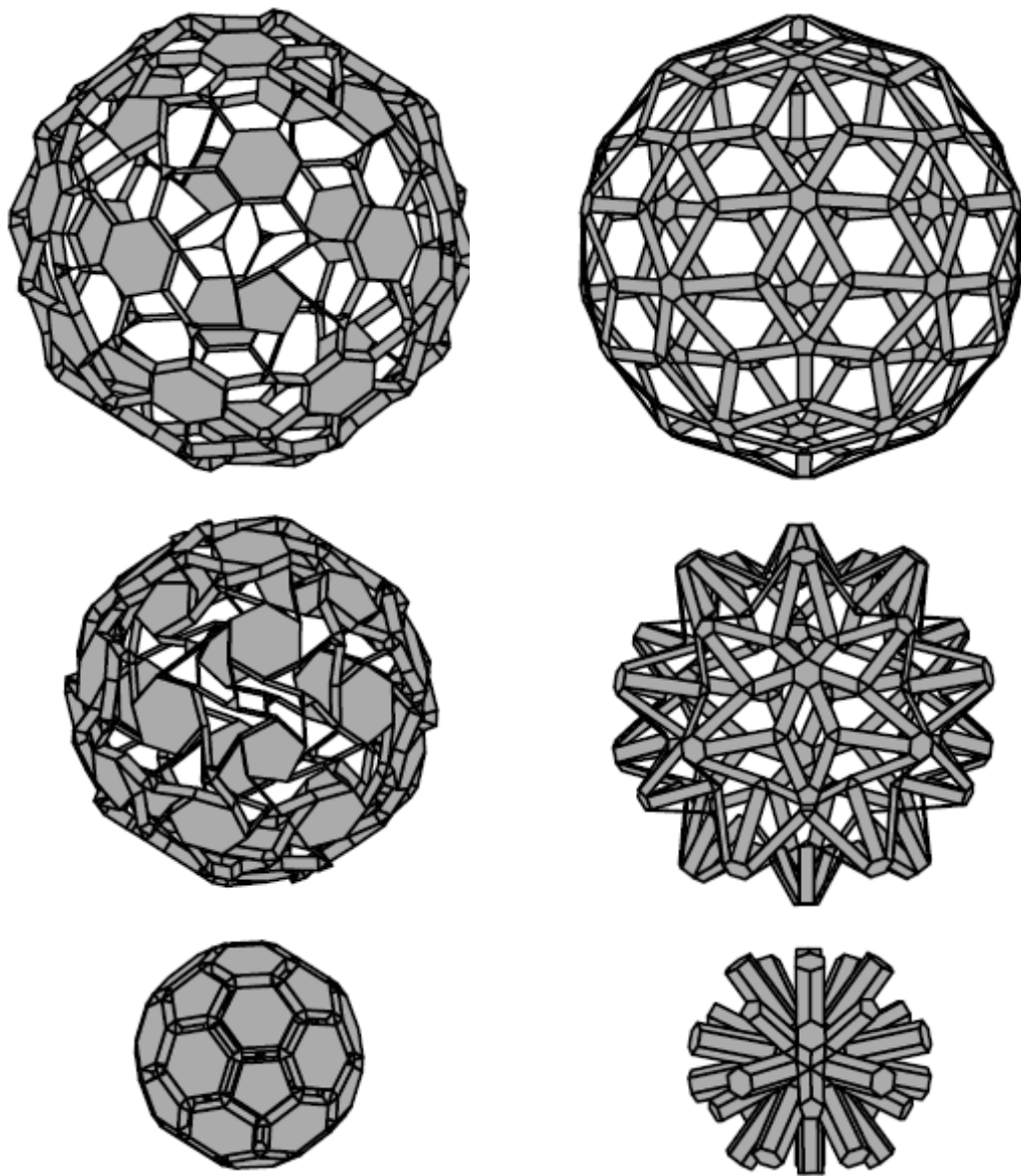


Figure 1.24 Truncated icosahedral linkages with planar and spatial link groups [30]

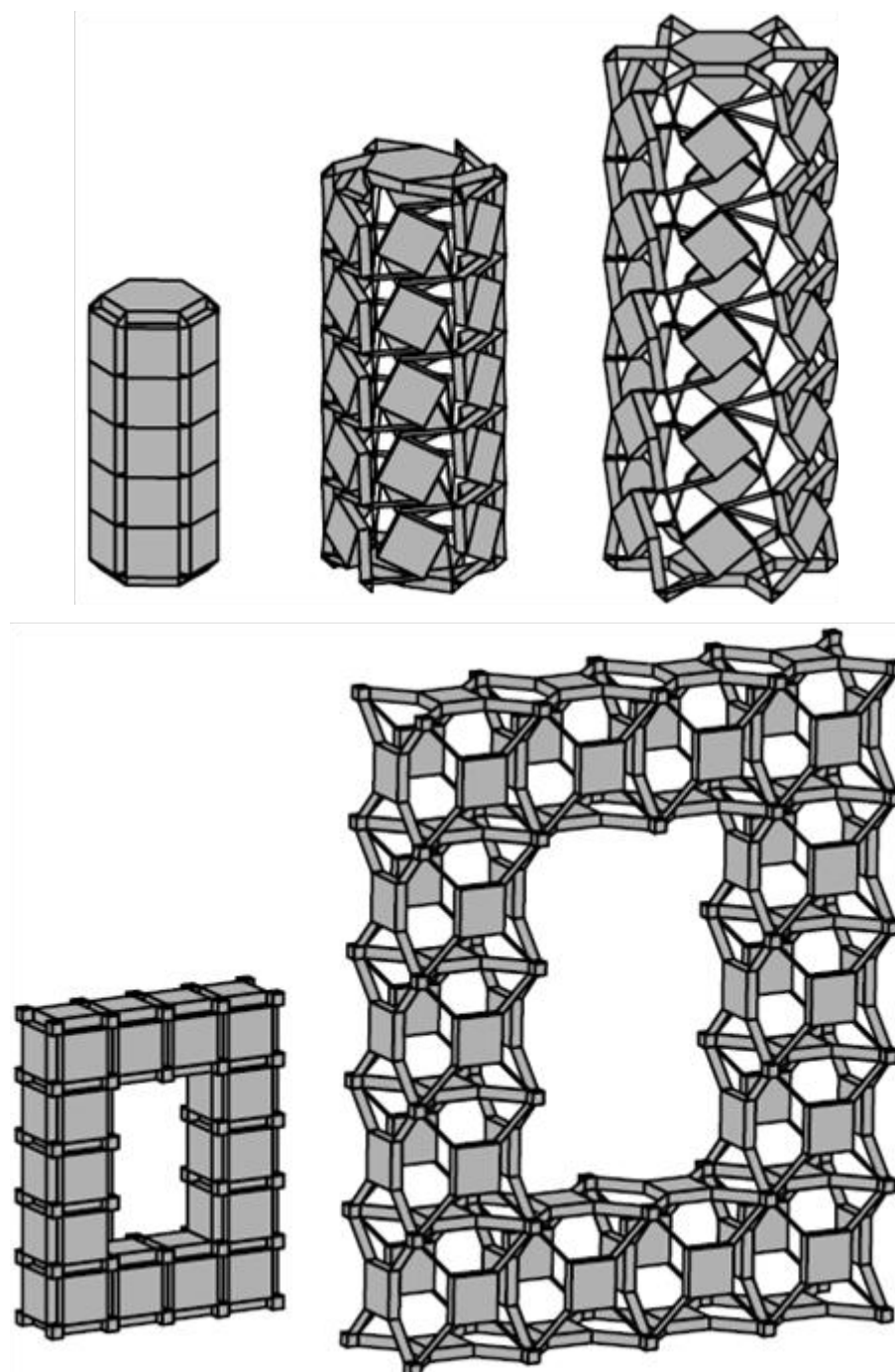


Figure 1.25 Polyhedral linkage complexes: a hexagonal prism and a linkage complex having unit cell as the cubic linkage [30]

The same year, Wohlhart proposed new regular polyhedral linkages, this time with a new synthesis method [32]. Closed kinematic chains are used on the faces with triangular links interconnected with revolute joints (Figure 1.26).

Contrary to the construction of the previous linkages [30], the vertices of the polyhedra in [32] are not located on the linkage but are blank. However, the gussets have simpler shapes in these new designs.

Wohlhart's later work [33] proposes design of irregular polyhedral linkages. As for the regular polyhedra, planar linkages can be designed for the faces of irregular polyhedra and gussets can be used to combine the faces. The planar link groups are like the ones used in [30] and the gussets are the same as in [30]. Figure 1.27 illustrates some of these designs.

Another similar design study of Wohlhart relates double pyramidal linkages [34]. Double pyramids are obtained by attaching two identical pyramids at the bases, hence all the faces of the resulting polyhedra are triangular. Wohlhart proposes two different types of face-bound planar link groups for double pyramidal linkages: one with four links (an open chain) and other with six links (a closed chain). The second type is same as the type proposed in [32]. The first type involves less links and less revolute joints, but the resulting polyhedra are shakier than the second type. For both types, gussets are no different than the gussets introduced in [32]. Some linkage examples are given in Figure 1.28.

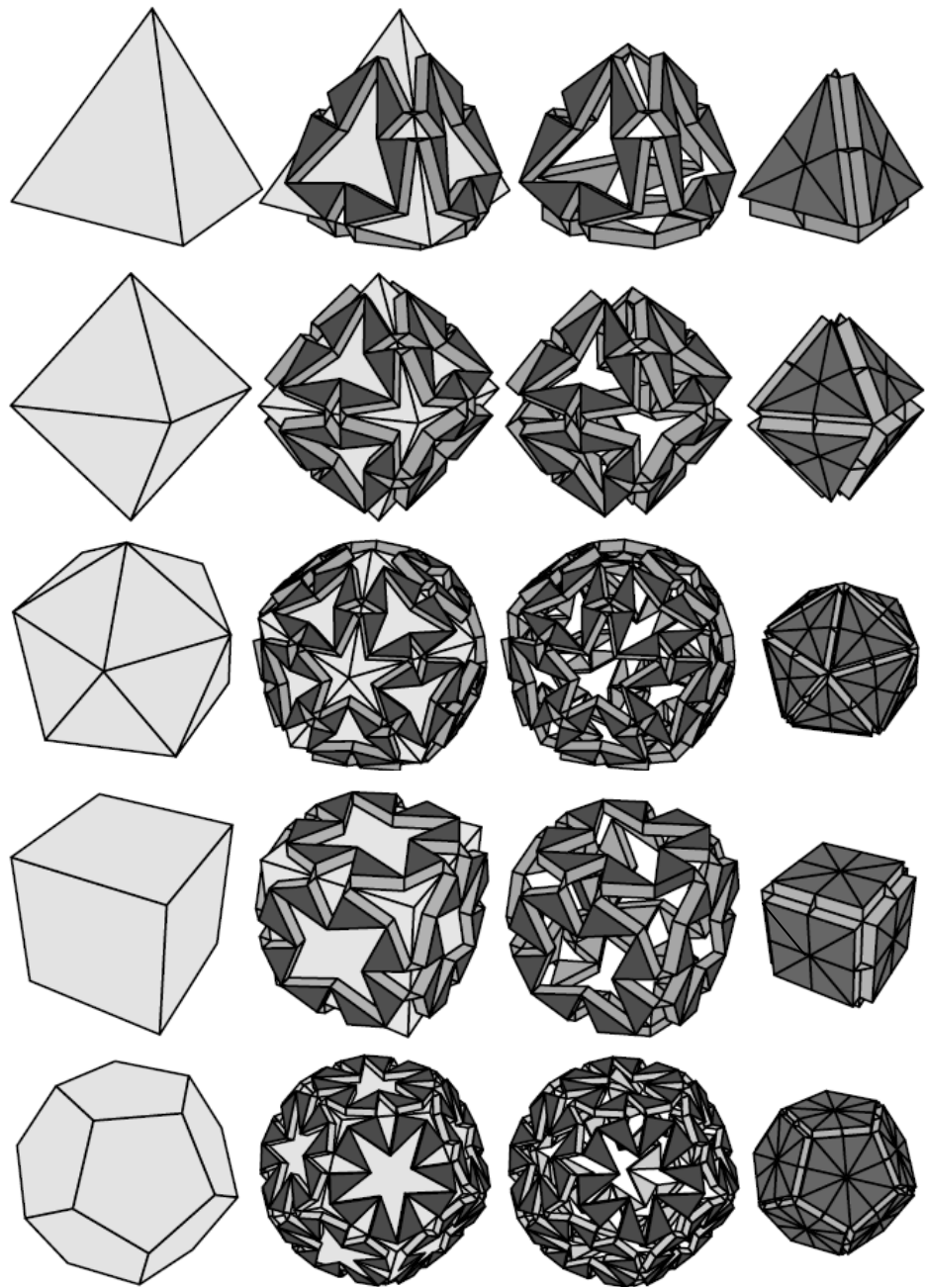


Figure 1.26 Wohlhart's linkages with the shapes of the Platonic solids proposed in [32]

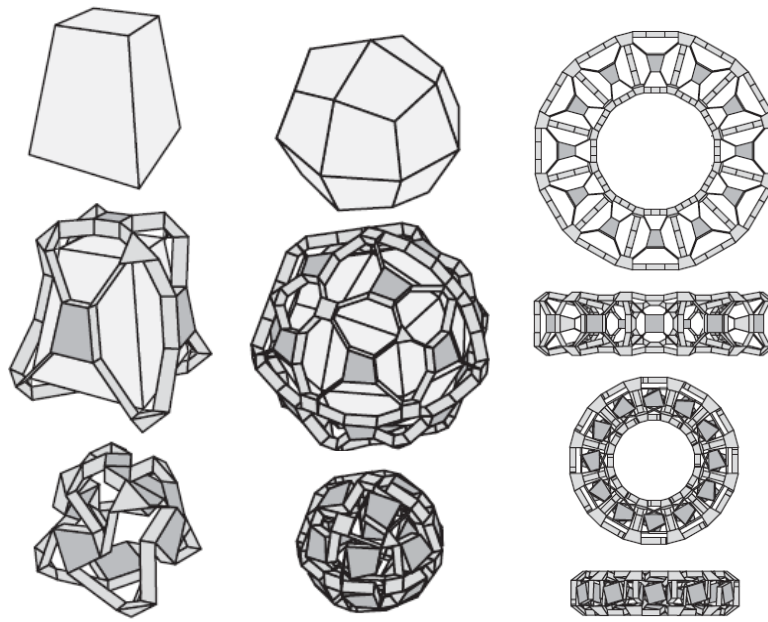


Figure 1.27 Some irregular polyhedral linkages: A frustum pyramid linkage, a Catalan solid linkage and a toroidal linkage complex [33]

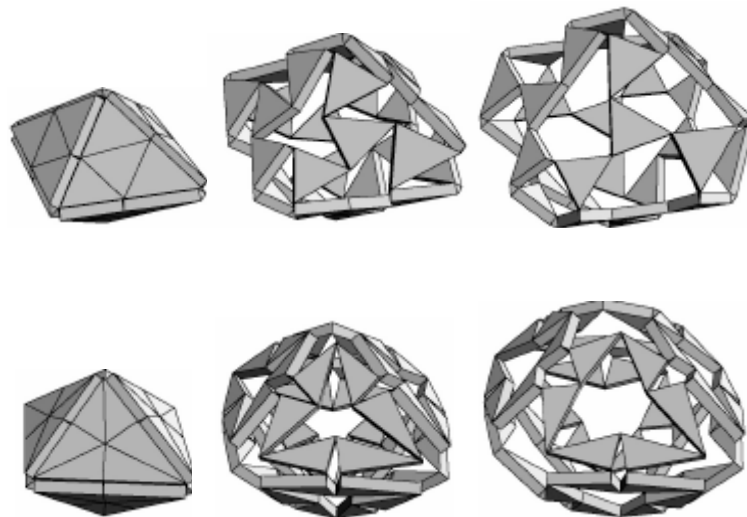


Figure 1.28 Two octahedral double pyramidal linkages of the two types [34]

Another design method of Wohlhart involves scissor mechanisms at edges of Platonic polyhedra [35]. Wohlhart names these linkages as Zig-Zag linkages. Some of the resulting linkages are given in Figure 1.29.

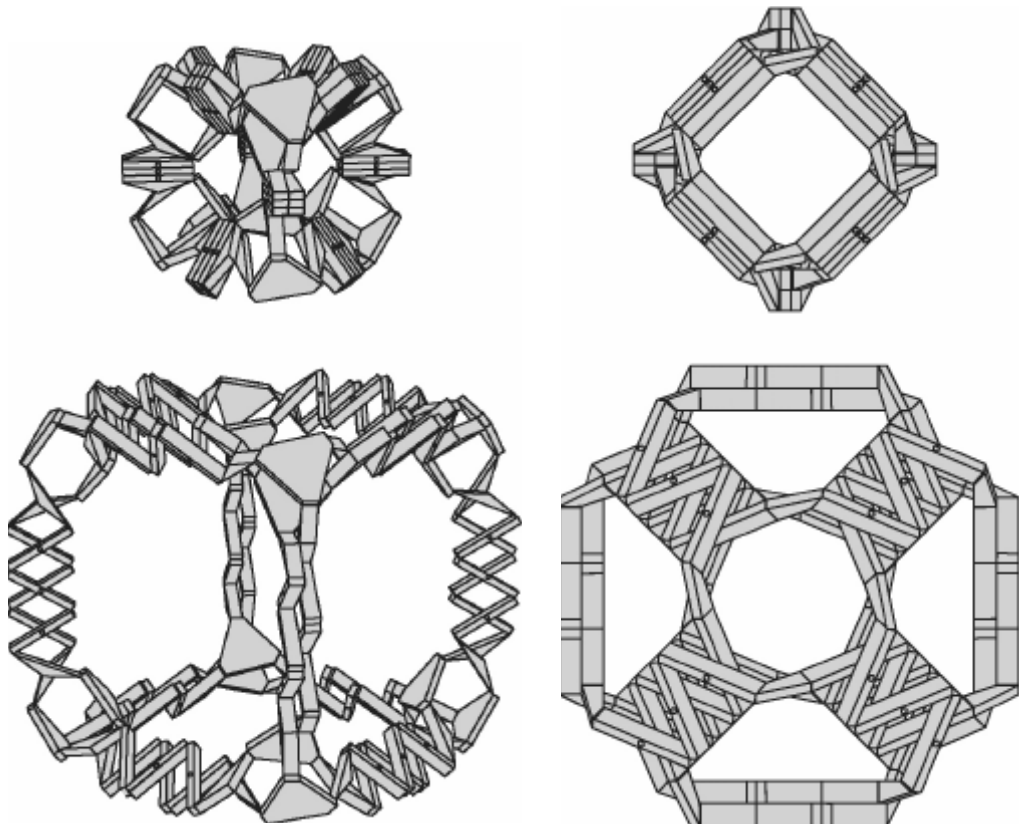


Figure 1.29 The cubic and the octahedral linkages of [35]

A different design approach for the polyhedral linkages was developed by Agrawal, Kumar and Yim [36]. They simply use prismatic joints along the edges of polyhedra. In [36], only the polyhedra which have regular faces and

same valency at all vertices are considered. These polyhedra are the Platonic solids, Archimedean solids, cube faced prisms and equilateral triangle faced antiprisms (Figure 1.30).

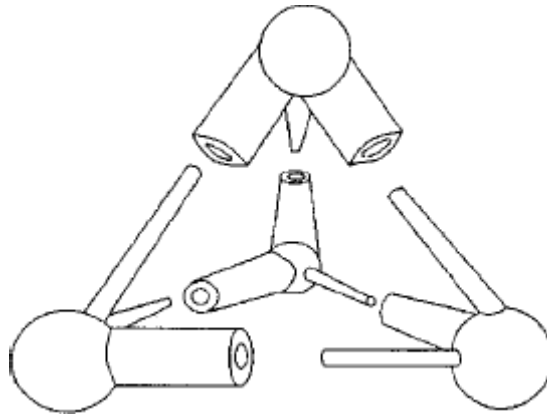


Figure 1.30 Exploded form of a tetrahedral linkage with prismatic joints [36]

The idea is simple, but the applications are very interesting. Using these linkages as unit cells, any object of any shape can be approximated and becomes an expanding structure. Also different kinds of meshes are introduced in [36]. Figure 1.31 illustrates some mesh examples. A chair approximated using two alternative meshes is given in Figure 1.32.

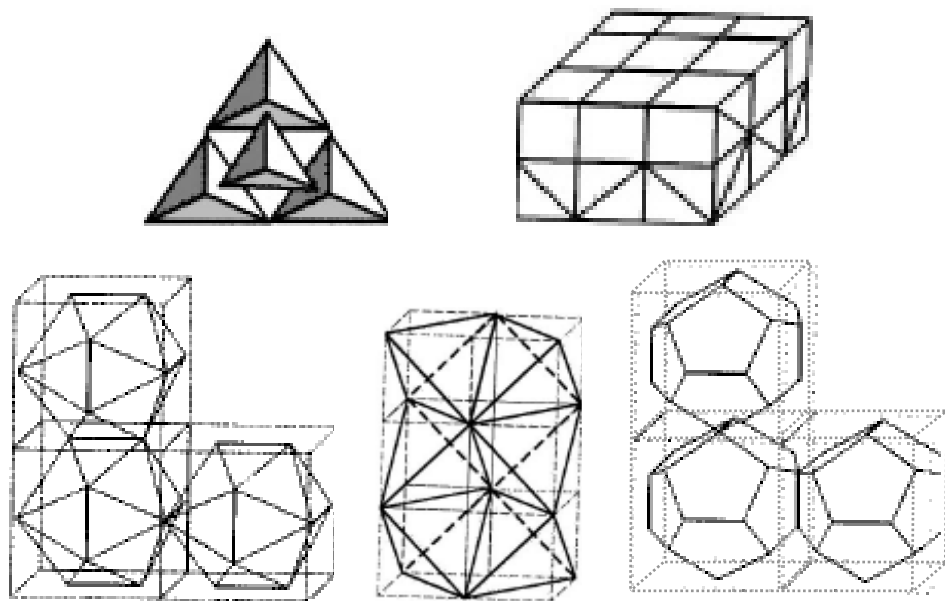


Figure 1.31 Some alternative meshes: vertex mating (tetrahedra as the example), face mating (closed pack meshes; cubes as the example), edge mating (icosahedra, tetrahedra and dodecahedra as the examples) [36]

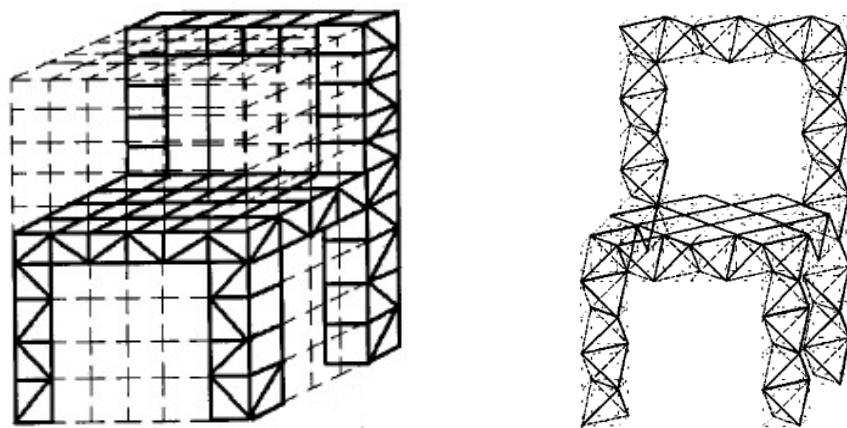


Figure 1.32 Two different kinds of meshes used to approximate a chair [36]

Agrawal et al. also gives a dynamic analysis methodology for all kind of meshes. Lagrange's dynamic equations are used and masses are assumed to be lumped at the vertices. The actuation force necessary can be calculated from these equations [36].

Some scientists make use of polyhedral linkages in modeling polyhedral viruses. First of the publications on this subject concentrates on viruses having truncated icosahedral shape [37]. The motion of the virus of interest is a nonlinear screw motion of the pentagonal faces of a dodecahedron finally constituting a truncated icosahedron (Figure 1.33). This continuous transformation from the dodecahedron to the truncated icosahedron is an example of the *leapfrog transformation* in fullerene chemistry [38]. This screw motion of the faces is also the subject of the later publications relating polyhedral linkage models of viruses [39 - 42]. [39] investigates the mobility and symmetries of the linkage given in Figure 1.33. It is notable that the mobility analysis is made using group theory so that the symmetries are taken into account. [40] additionally investigates the relative motion of the faces of the same linkage.

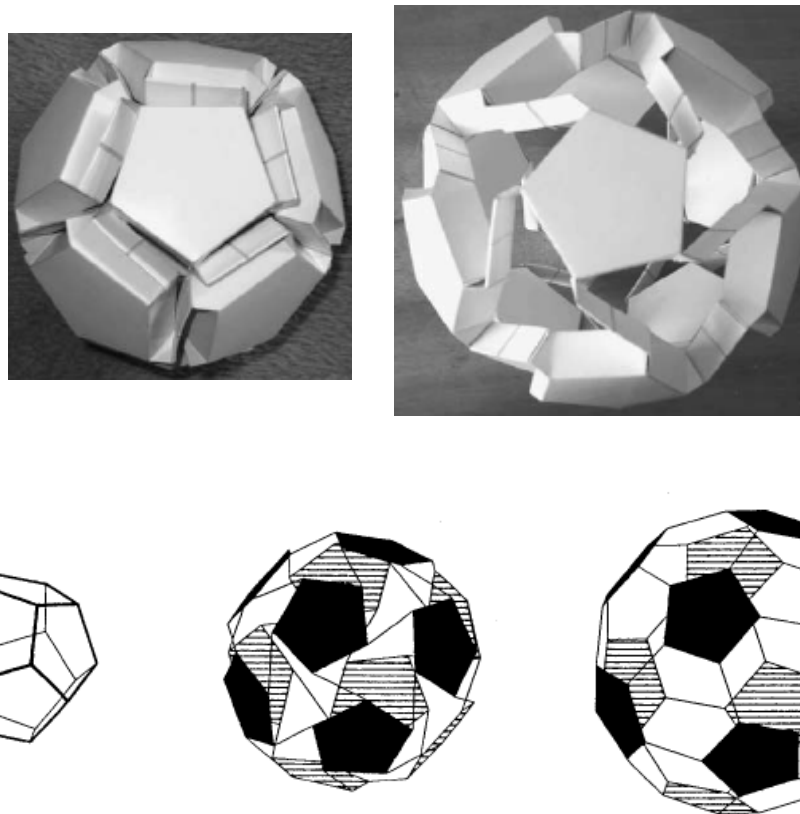


Figure 1.33 A cardboard model and computer simulation demonstrating the expansion process of a polyhedral virus [39, 40]

Two other studies [41, 42] introduce a new linkage type for the leapfrog transformation. In these linkages, the faces are connected by two parallel bars (Figure 1.34). The mobility analysis of these new kinds of linkages is given in [41]. The analysis is done by the method described in [40]. [41] explains how to construct a mechanical model of a cowpea chlorotic mottle virus.

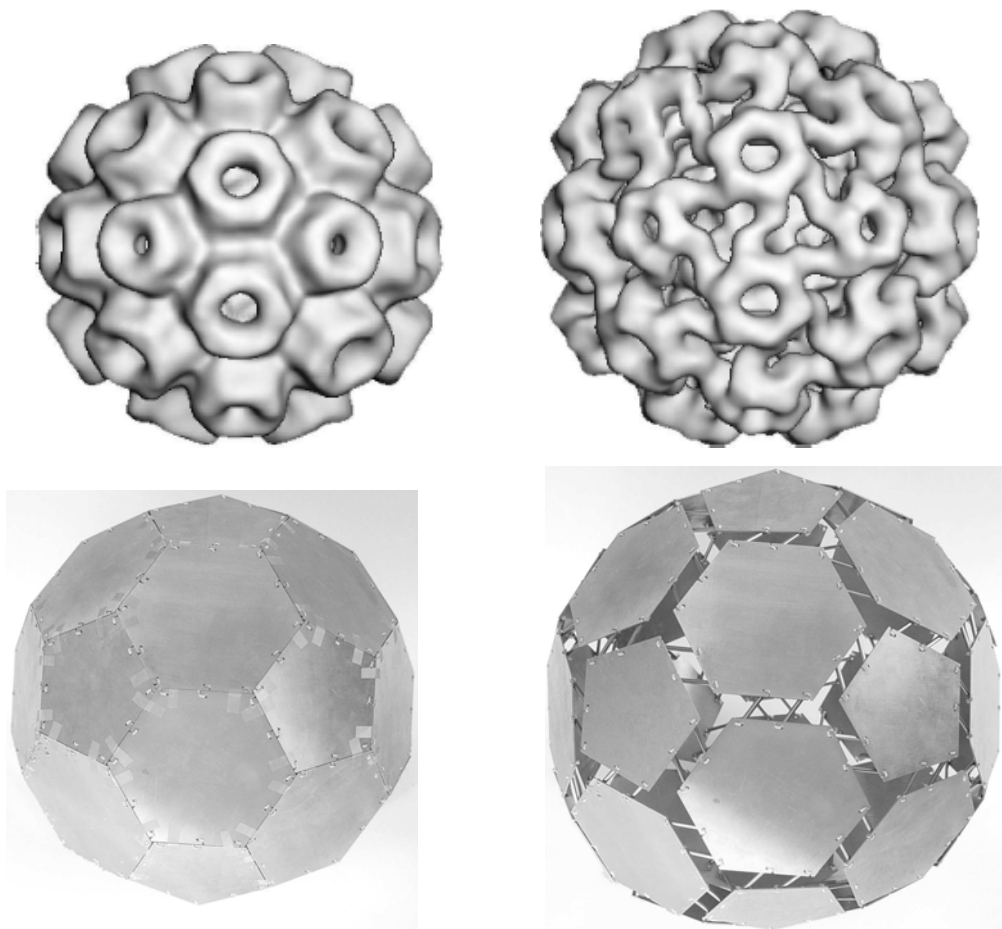


Figure 1.34 A realistic model for the motion of cowpea chlorotic mottle virus and a mechanical model for the same virus [41]

CHAPTER 2

TRANSFORMATION CHARACTERISTICS OF PRESENT POLYHEDRAL LINKAGES

In this chapter, the motion characteristics of present polyhedral linkages are analyzed. As far as polyhedral linkages are concerned, the main aim is to magnify a given polyhedral shape or transform a polyhedral shape to another one. To relate polyhedral shapes corresponding to different configurations of such a linkage one needs to make use of not only isometric (length preserving) transformations, but also some special non-isometric transformations. These motion classes are introduced before the details about the linkage types.

Almost all of the present polyhedral linkages have a single dof and this motion can be described by a single transformation. It is desired that the linkage performs a large amount of magnification. Hence, magnification capabilities of the linkages are investigated and a comparison is given at the end of the chapter.

2.1 Linear Similarity Transformations in 3D Space

Isometries of the 3-dimensional Euclidean space are *translations*, *rotations*, *reflections* or combination of these three transformations. There are no other isometries in 3D space. Translations and rotations (and their combinations) are

considered to be the rigid body motions of the space (or sense preserving isometries) [43].

In scaling an object, not only translations and rotations, but also *magnifications* should be taken into account. Magnifications are similarity transformations that preserve parallelism and relative length (other than length ratio 1; that would be a translation) and direction of line segments (See Figure 2.1). All linear similarity transformations are combinations of isometries and magnifications. Every magnification leaves a point invariant and this point is called the *center of magnification*. The measure of magnification is termed as the *ratio of magnification* [43].

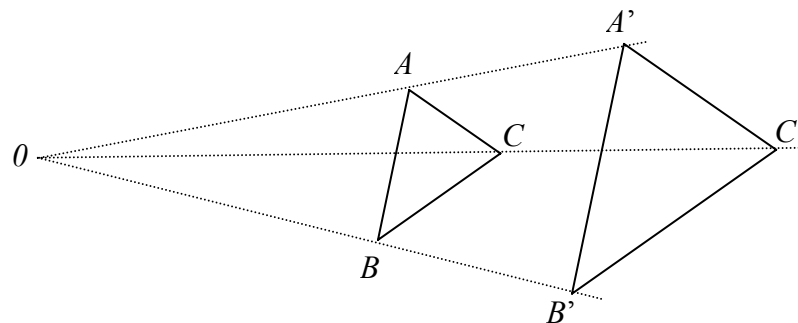


Figure 2.1 Magnification of a triangle ABC about a *magnification center* O

These three motion types, and their combinations, are sufficient to explain the motion of polyhedral linkages. As a special name, a magnification plus a rotation is called a *spiral similarity* [43].

2.2 Motion Characteristics of Present Polyhedral Linkages

2.2.1 Dipolygonids

The complete list of dipolygonids is given by Verheyen in [25]. The key point of these linkages is the translation and rotation of the faces along the symmetry axes. In [25], these linkages are constructed by starting from two polygons. These polygons are obtained by imaging a point P via two rotations A and B along two intersecting axes (Figure 2.2). Verheyen names such a pair of polygons as a *dipolygon*. A *dipolygonid* is defined as the image of a dipolygon over the group of rotations generated by A and B . Figure 2.3 illustrates an example for construction of a dipolygonid.

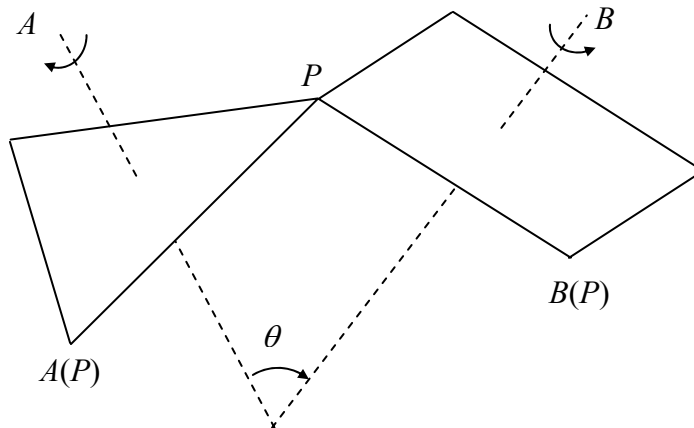


Figure 2.2 An example of a dipolygon – A is a 120° rotation and B is a 90° rotation about two intersecting axes with a separation of angle θ

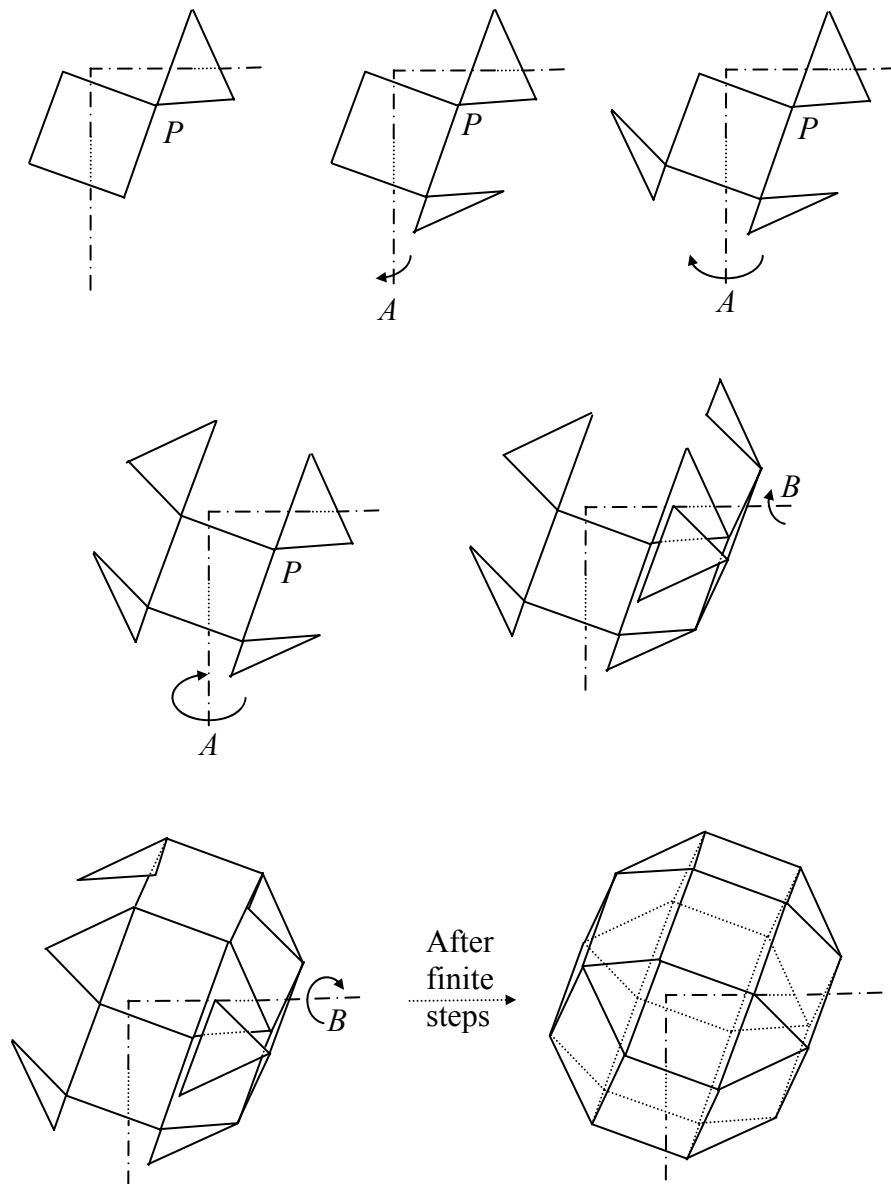


Figure 2.3 A possible way of construction of the dipolygonid $8\{3\} + 6\{4\} | 54^\circ 44' 08''$ (8 triangles, 6 squares, $\theta = 54^\circ 44' 08''$)

Observing that if one allows the polygons of a dipolygon to move along the rotation axes, the vertices of the polygons move along two cylinders, axes of which are the rotation axes of A and B . Then the dipolygon has a single dof motion (Figures 2.4, 2.5). In Figure 2.5, Point P moves along the intersection of the cylinders while the polygons rotate and translate along the rotation axis. This motion is still realized for a dipolygonid [25]. Verheyen names this motion as the *uniform motion* of the dipolygon. During the uniform motion, the sense of rotation and translation of the polygons change at some certain positions. These positions and the consequences of these sense reversions are discussed in [25] in detail.

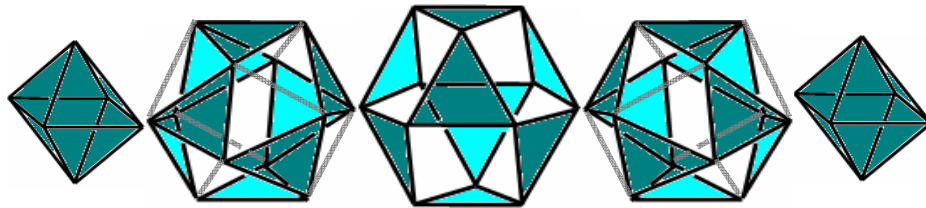


Figure 2.4 The motion of the Jitterbug ($4\{3\} + 4\{3\} | 70^\circ 31' 44''$): transforms from an octahedron to a cuboctahedron, and vice versa. In between the icosahedron is realized

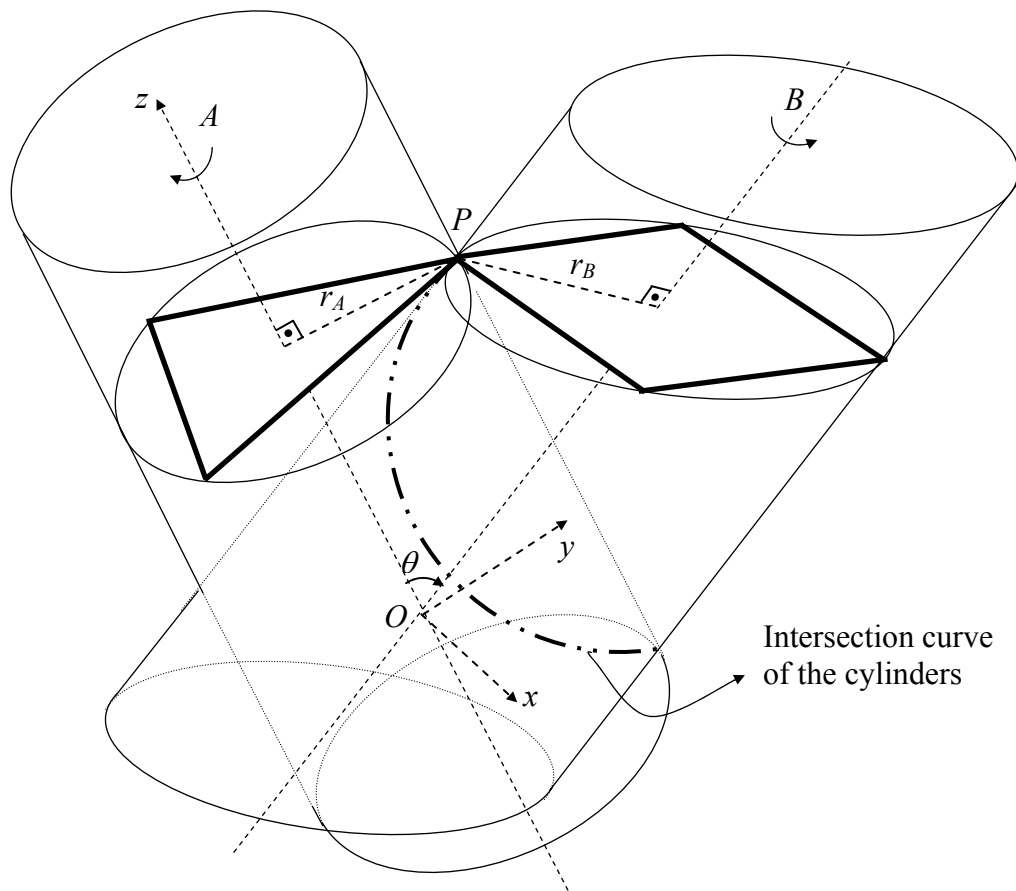


Figure 2.5 The circumscribing cylinders for the uniform motion of a dipolygon

Using thin walled plates as linkages and joints such as given in Figure 2.6, one may construct many dipolygonids as single dof polyhedral linkages. A position analysis is presented in [25].

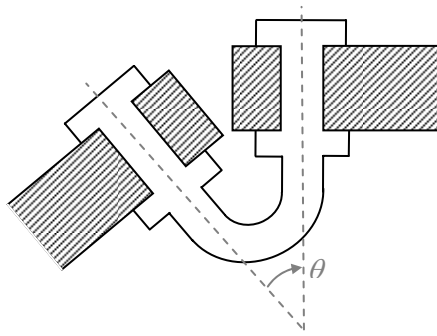


Figure 2.6 Joints allowing rotation of plates while keeping the angle between the planes of the plates constant [25]

The dipolygonids seem to be transforming between different polyhedral shapes. However, they can also be thought to be magnifying a certain shape. If the planes of the polygonal links are intersected, the volume inside will always be the same polyhedron at any configuration (Figure 2.7).

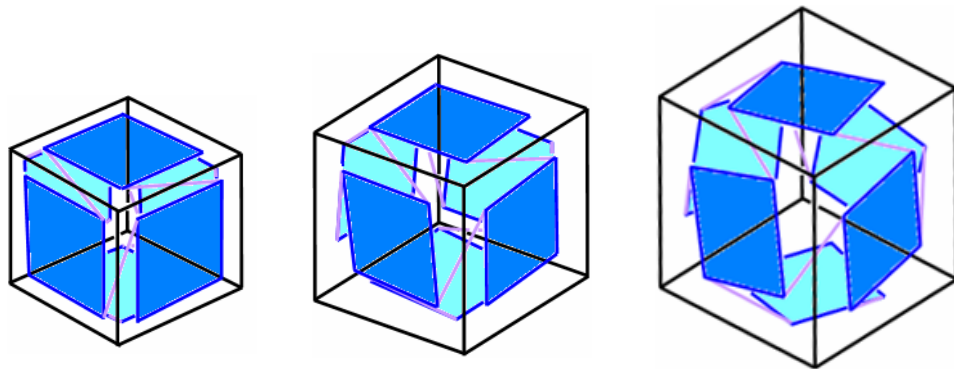


Figure 2.7 $12\{2\} + 6\{3\} | 45^\circ$ has its polygonal faces on a cube at any configuration

Lastly, the magnification ratio between the minimal and maximum physically realizable configurations shall be found. Note that the polyhedral shape defined by the polygonal faces is considered to be magnified, hence only the centers of polygons of a dipolygonid are subjected to a magnification. The other points on the polygon are subject to a spiral similarity. For ease of calculations, the center of magnification shall be chosen as the intersection point of the axes of A and B – point O in Figure 2.5.

Given a dipolygon with the rotations A, B and radii r_A, r_B as shown in Figure 2.5, consider a right-handed frame (x, y, z) with origin at O , z -axis along axis of A and y -axis such that axis of B is contained in the yz -plane. Without loss of generality, choose A such that $r_A \geq r_B$. Intersection point O and the angle θ between rotation axes are fixed once A and B are defined. Once $r_A \geq r_B$ and z is selected along the axis of A , the y component of P , P_y , always has the same sign. Choose the sense of y and z such that P_y is always positive. With this frame, the magnification ratio between the minimal and maximal configurations can be easily found as the ratio of elevations of the polygon defined by the rotation A at the maximal and minimal configurations. This ratio is also equal to the ratio of the z components of P at these configurations.

For the dipolygonids, the minimal configuration is when the edges of two neighboring polygons of a dipolygon meet. At this configuration, the plane constituted by the rotation axes of A and B (yz plane in Figure 2.5) is a symmetry axis for the common edge [43]. Notice that there are two such configurations and are reflection images of one another with respect to plane yz . The maximal configuration is when the generating point P is on yz plane [43]. Although the trajectory of P , which is an ellipse – being intersection of two cylinders, intersects yz plane at two points, the one that is more distant to point O corresponds to the maximal configuration. At the maximal

configuration, obviously the distance of P to the rotation axes are r_A and r_B . At the minimal configuration, the intersection point of the meeting edge and yz plane, say point M , is h_A and h_B distant to the axes of rotations, where h_A and h_B are the radius of the inscribing circles of the polygons of the dipolygon. The reason to this is that the polygons are regular and point M is the midpoint of an edge. h_A and h_B can be related to r_A and r_B as (Figure 2.8)

$$h_A = r_A \cos(\pi/n_A) \quad (2.1)$$

$$h_B = r_B \cos(\pi/n_B) \quad (2.2)$$

where n_A and n_B are the orders of A and B .

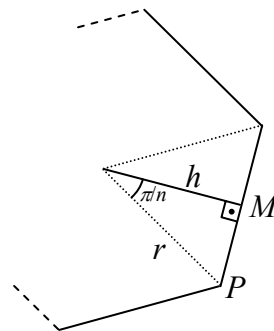


Figure 2.8 The distance of a vertex and an edge of a regular n -gon

Finally the z components of P at the maximal and minimal configurations can be found with a little geometry on yz plane (Figure 2.9). The y components of P at the minimal and maximal configuration are

$$y_{P,min} = h_A \quad (2.3)$$

$$y_{P,max} = r_A \quad (2.4)$$

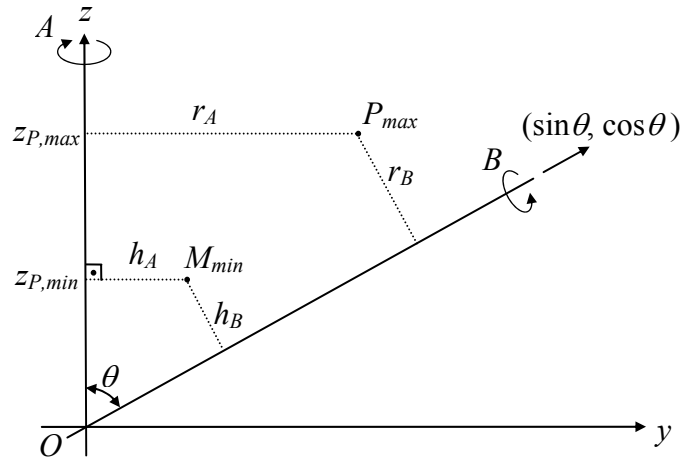


Figure 2.9 The projection of P on yz plane at the minimal configuration (M_{min}) and the maximal configuration (P_{max})

Distance of M_{min} and P_{max} to axis of B yields

$$|(y_{P,min}, z_{P,min}) \times (\sin \theta, \cos \theta)| = h_B \quad (2.5)$$

$$|(y_{P,max}, z_{P,max}) \times (\sin\theta, \cos\theta)| = r_B \quad (2.6)$$

Hence, by (2.1), (2.2), (2.3), (2.4), (2.5) and (2.6), the ratio of magnification is found as

$$\frac{z_{P,max}}{z_{P,min}} = \frac{r_A \cos\theta + r_B}{r_A \cos\theta \cos\frac{\pi}{n_A} + r_B \cos\frac{\pi}{n_B}} \quad (2.8)$$

As a special case for $n_A = n_B = n$ the ratio of magnification is simply $\sec(\pi/n)$. The ratio is 2 for the tetrahedron, the octahedron (the Jitterbug) and the icosahedron, 1.414 for the cube and 1.236 for the dodecahedron.

2.2.2 The Fulleroid

The Fulleroid, named after R. Buckminster Fuller, is a linkage that has its faces of the polygonal links on a rhombic dodecahedron (Figure 2.10) [26]. Johannes Kepler was the first to give special importance to this polyhedron by classifying it as a half-regular polyhedron [26]. Today, the rhombic dodecahedron is known to be a Catalan solid, being the dual of the cuboctahedron - an Archimedean/semi-regular solid [44].

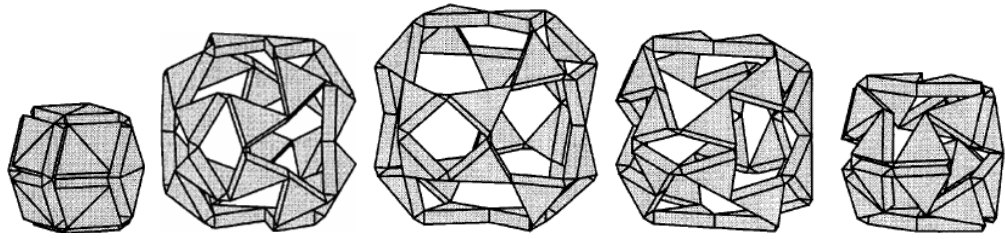


Figure 2.10 The expansion/contraction motion of the Fulleroid between the two limit configurations [26]

Notice that, the Fulleroid seems more likely magnifying a certain polyhedral shape, rather than transforming a polyhedral shape to another one (Figure 2.11).

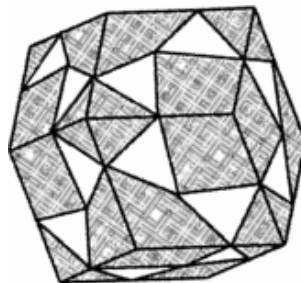


Figure 2.11 Polygonal faces of the Fulleroid on rhombic dodecahedron [26]

A position analysis for the Fulleroid is presented in [26], but an angular displacement is used as the parameter. Instead of making use of this position

data one may make use of the size of a diagonal of a face at the extreme configurations. Since a single parameter suffices to define a continuous magnification, magnification of a face or a line or even a point fully determines the magnification of a spatial object. The minimal and maximal configurations of a pair of links constituting a face is given in [26] as in Figure 2.12.

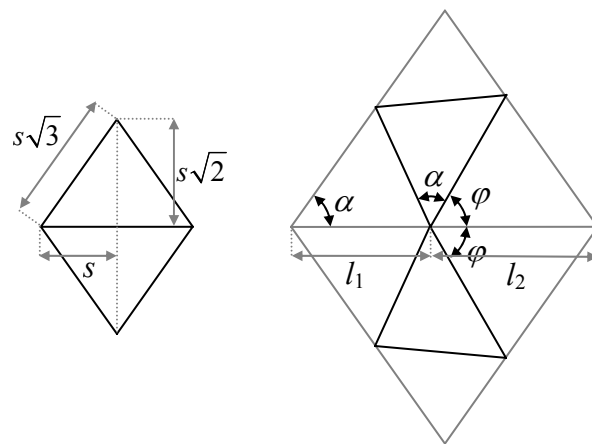


Figure 2.12 A pair of coplanar links at the face of a Fulleroid – at extreme configurations

In [26] the angle between sort diagonal of the rhombic face and a link is calculated as $\varphi = \tan^{-1} \frac{5}{2\sqrt{2}}$, so

$$\sin \varphi = \frac{5}{\sqrt{33}} \quad \text{and} \quad \cos \varphi = \frac{2\sqrt{2}}{\sqrt{33}} \quad (2.8)$$

By sine theorem

$$l_1 = \frac{s\sqrt{3}}{\sin \alpha} \sin \varphi \quad (2.9)$$

$$l_2 = \frac{2s}{\sin \alpha} \sin(\alpha + \varphi) \quad (2.10)$$

$$\sin \alpha = \frac{\sqrt{2}}{\sqrt{3}}, \cos \alpha = \frac{1}{\sqrt{3}}, \text{ hence by (2.8)}$$

$$\sin(\alpha + \varphi) = \sin \alpha \cos \varphi + \sin \varphi \cos \alpha = \frac{3}{\sqrt{11}} \quad (2.11)$$

Then by (2.8), (2.9), (2.10) and (2.11), the total magnification of the short diagonal is

$$\frac{l_1 + l_2}{2s} = \sqrt{\frac{33}{8}} = 2.031 \quad (2.12)$$

Hence the total magnification of the Fulleroid is slightly larger than 2.

2.2.3 Hoberman Designs

Hoberman's success on deployable structures is built upon the discovery of the so called angulated element. In most of the designs angulated elements are the building blocks (Figure 2.13.a), but in some designs gear joints (Figure 2.13.b) or polygonal link groups are used. However, the designs using gear joints (Figure 2.14) are kinematically equivalent to the star transformers of Wohlhart

(See Section 2.4.1) and the designs with polygonal link groups either obtained by variations of angulated elements or are dipolygonoids (Figure 2.15).

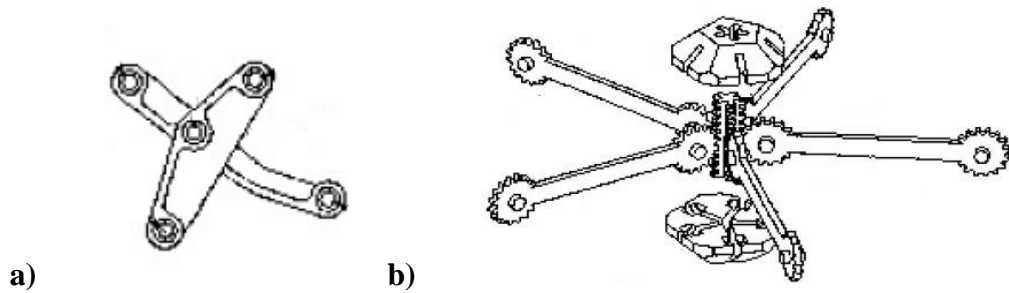


Figure 2.13 a) The scissor elements [27] b) Geared joints [28]

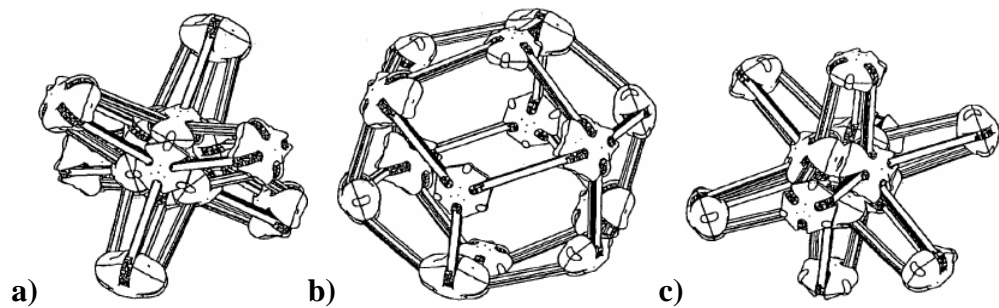


Figure 2.14 An octahedral symmetric linkage with gear joints **a**, **c**) in two possible folded configurations **b**) in an expanded configuration [28]

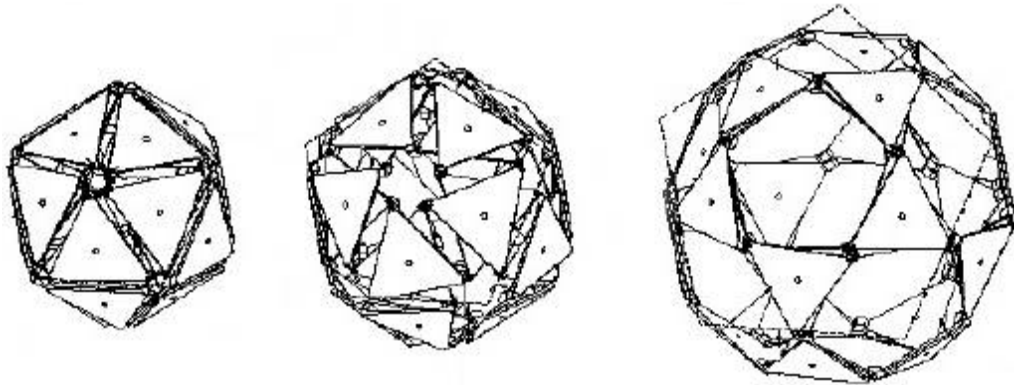


Figure 2.15 A design constructed with polygonal elements [29] – a dipolygonid: $20\{3\} + 20\{3\} | 41^\circ 48' 37''$

An angulated element consists of two bent beams with three kinematic elements on each – two on the ends and one at the bend. The beams are connected via a revolute joint at the bends of the beams and the kinematic elements at the ends are for connection with other angulated elements (Figure 2.15.a). The main feature of the angulated element is that if the four ends of the element is bound to two straight lines, the linkage is movable (Figure 2.16). A mechanism as in Figure 2.17 has $3(3 - 5 - 1) + (1 + 4 \cdot 2) = 0$ dof in general, but for some special link dimensions the mechanism becomes movable. Hoberman states these special dimensions as

$$|AE| = |CE|, |BE| = |DE| \text{ and } \angle AEB = \angle CED = \pi - \alpha \quad (2.13)$$

where, α is the angle between the straight lines being traced (Figure 2.17) [45]. Later, You and Pellegrino showed that a general angulated element can have either of the following proportions [10]:

$$|AE| = |CE|, |BE| = |DE| \quad (2.14)$$

$$|AE| / |CE| = |BE| / |DE| \text{ and } \angle AEB = \angle CED = \pi - \alpha \quad (2.15)$$

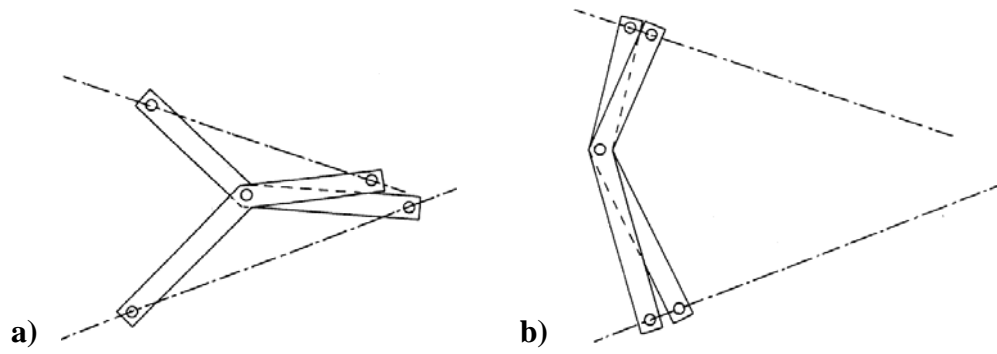


Figure 2.16 A general angulated scissor element in two configurations [8]

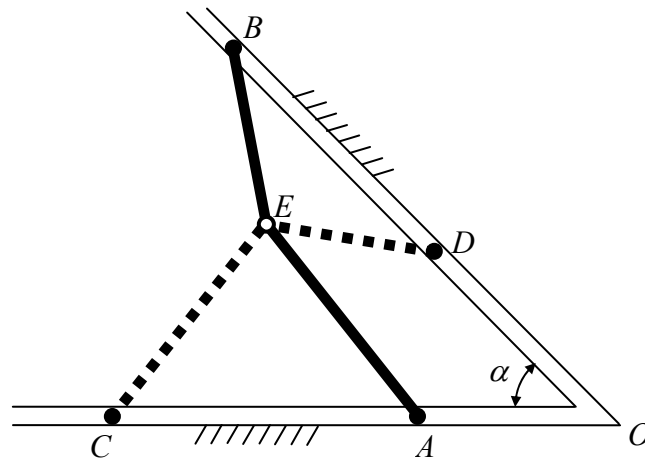


Figure 2.17 A mechanism with an angulated scissor element

As shall be proved in the next chapter, the special dimensions given by (2.13), (2.14) and (2.15) just guarantee the motion of the angulated element through a constant angle but do not provide a magnification, that is $|OB|/|OC|$ varies during the motion. But if all link dimensions are equal as a special case of (2.13), a magnification is realized. Hoberman designed many linkages using angulated elements (Figures 2.18, 2.19).

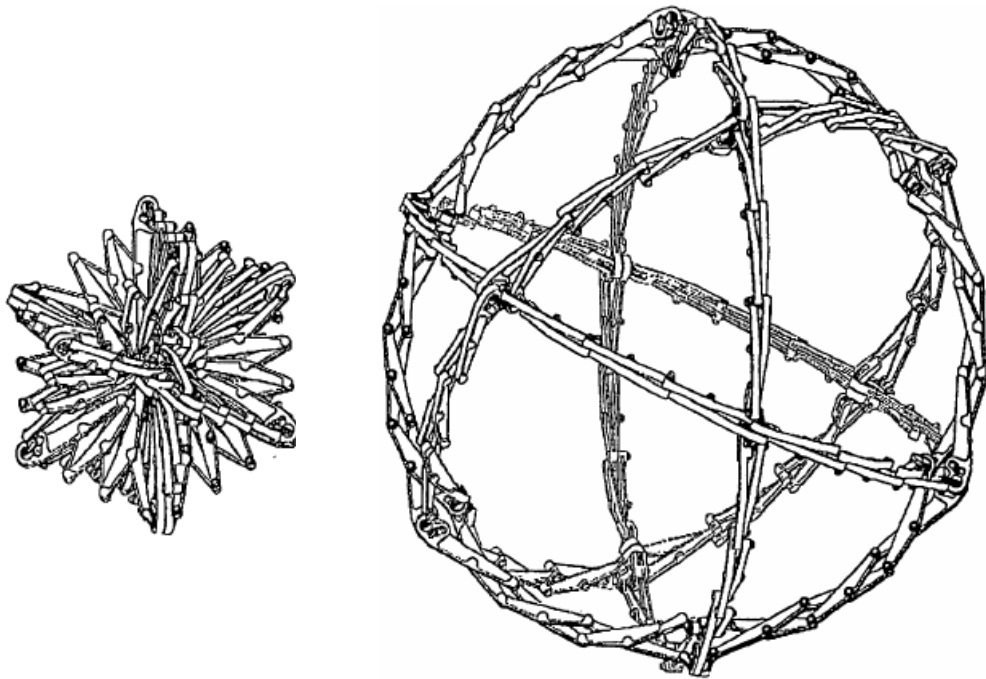


Figure 2.18 The famous Hoberman sphere [27]

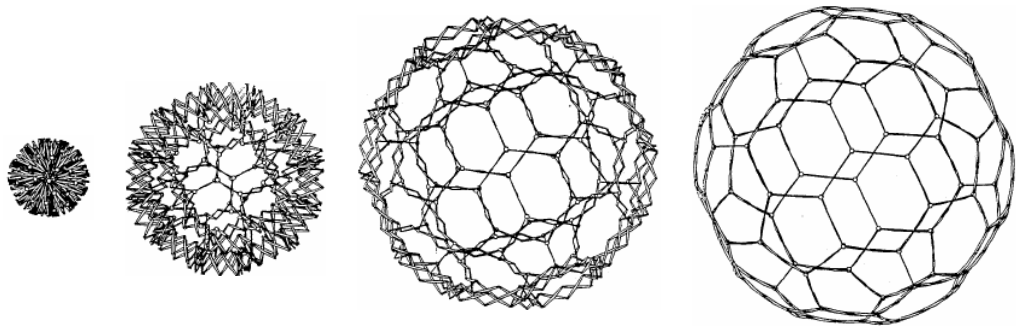


Figure 2.19 A polyhedral linkage making use of angulated elements – magnifies a truncated icosahedron [45]

By the nature of magnification, only an angulated element shall be analyzed for the magnification capability of a polyhedral linkage made up of only one type of angulated element. Consider an angulated element with dimensions $|AE| = |CE| = |BE| = |DE| = l$ and $\angle AEB = \angle CED = \pi - \alpha$. Then the maximum configuration is when C, E and B are collinear as will be proved in the next chapter (Figure 2.20.a). The minimum physically realizable configuration is when A, D and O are coincident, because the angulated element interferes with the other angulated elements after this position (Figure 2.20.b). Then the ratio of magnification between these two extreme configurations is

$$\frac{l / \sin \frac{\alpha}{2}}{2l \cos \frac{\alpha}{2}} = \operatorname{cosec} \alpha \quad (2.16)$$

So the magnification ratio is inversely proportional with $\sin \alpha$, that is a better magnification is achieved for smaller angles. If angulated elements are used as

edges to construct a regular polyhedral linkage, the ratio of magnification is $3\sqrt{2}/4 \cong 1.061$ for a tetrahedron or a cube, $\sqrt{5}/2 \cong 1.118$ for the icosahedron and $3/2 = 1.500$ for the dodecahedron. For the octahedron, these elements cannot be used for magnification purposes, because the ratio of magnification turns out to be 1. For the Hoberman sphere the ratio is 2 and for a truncated icosahedron (Figure 2.19) the ratio is $(29 + 9\sqrt{5})/(6 + 6\sqrt{5}) \cong 2.53$.

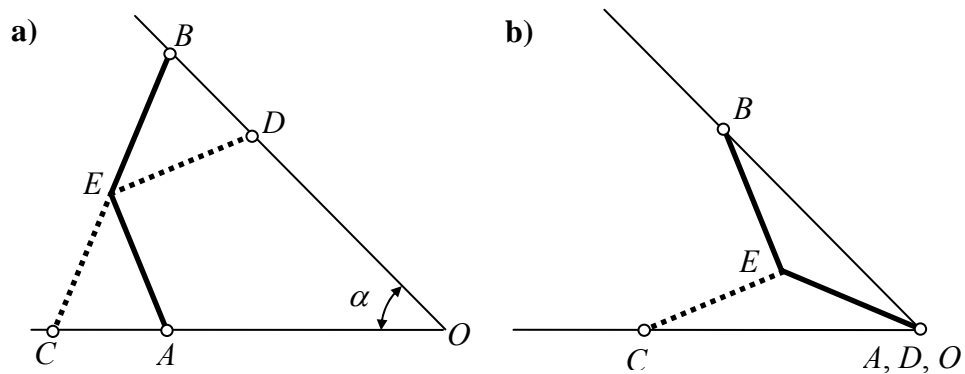


Figure 2.20 The maximal and minimal positions of an angulated element with $|AE| = |CE| = |BE| = |DE| = l$ and $\angle AEB = \angle CED = \pi - \alpha$

2.2.4 Wohlhart Designs

Wohlhart's polyhedral linkage designs involve five types of linkages: polyhedral star-transformers for regular polyhedra, linkages with multiple slider-cranks, linkages with planar link groups that have central links for

double pyramids, linkages with planar link loops for regular polyhedra and polyhedral zigzag linkages.

2.2.4.1 Polyhedral Star-Transformers

Star-transformers of Wohlhart (Figure 2.21) and Hoberman designs with gear joints (Figure 2.22) are kinematically identical designs, hence both designers should be acknowledged. In these linkages, the main aim is not magnification, but some sort of expansion transformation (see Section 1.1). By the nature of the assembly technique used, the faces are necessarily cyclic, hence the resulting polyhedral shape is mostly spherical. It will be proved in the next chapter that a sufficient condition for a polyhedron with cyclic faces to be spherical is that all the vertices have valency 3. In these linkages, two minimal configuration and two maximal configurations exists. If one considers the outward-pointing hubs as vertices of a polyhedral shape (Figure 2.22.a, b), then the two possible small configurations turn out to be the duals of each other, i.e. as if the faces and the vertices of one another are interchanged.

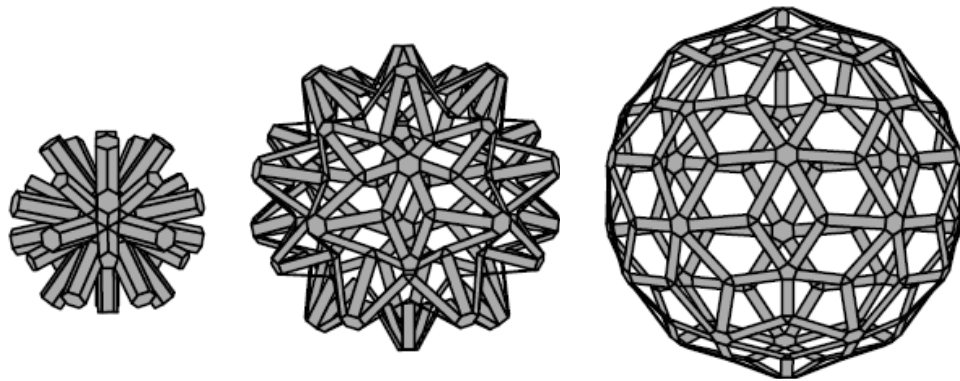


Figure 2.21 Polyhedral star-transformer for the truncated icosahedron [30]

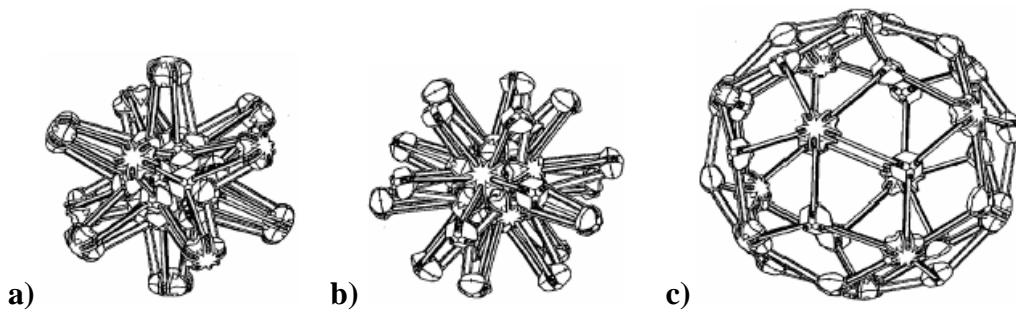


Figure 2.22 A design of Hoberman **a, b**) minimal configurations with (a) 5-valent vertices pointing outward and (b) 3-valent vertices pointing outward **c**) an intermediate configuration between two maximal configurations [28]

The vertex hubs are furthest to the center when the inner hubs become coplanar with the neighboring hubs. This is the fact, because if the inner hubs further move outwards, the vertices start shrinking towards the center. Examples show

that the maximal configuration is not unique. Indeed, for Platonic solids duals with faces having same circumscribing circle radii turn out to have the same circumscribing sphere radius. Whether this is the case for other spherical polyhedra with cyclic faces is an open problem.

The intermediate configurations, as well as the largest configuration belong to the truncation-extension series of dual polyhedra. See [46] for a better understanding of truncation-extension series of polyhedra.

Notice that for both of the smallest configurations among the two possibilities the outer hubs are equally distant to the inner hubs and this distance is the length of a link, being equal to the radius of the circumscribing sphere. For Platonic solids, in the maximal configuration, the link length becomes the radius of a circumscribing circle of a face. Then ratio of magnification is the ratio of the radius of a circumscribing circle of a face to the radius of the circumscribing sphere. This ratio depends on the dihedral angle, γ , and the number of sides of a face, n (Figure 2.23):

$$\begin{aligned}
\frac{|OV|}{|MV|} &= \frac{\sqrt{|OM|^2 + |MV|^2}}{|MV|} = \frac{\sqrt{[|MP| \tan(\gamma/2)]^2 + |MV|^2}}{|MV|} \\
&= \frac{\sqrt{[|MV| \cos(\pi/n) \tan(\gamma/2)]^2 + |MV|^2}}{|MV|} \\
&= \sqrt{[\cos(\pi/n) \tan(\gamma/2)]^2 + 1}
\end{aligned} \tag{2.17}$$

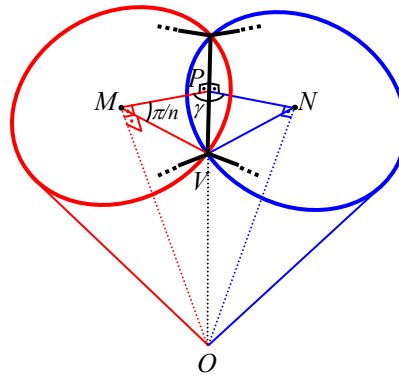


Figure 2.23 Relating circumscribing circle of a face to the circumscribing sphere for a Platonic solid

The total ratio of magnification is $\sqrt{5/4} \cong 1.061$ for the tetrahedron, $\sqrt{3/2} \cong 1.225$ for the cube-octahedron pair and $\sqrt{(15 + 3\sqrt{5})/8} \cong 1.647$ for the dodecahedron-icosahedron pair.

2.2.4.2 Linkages with Multiple Slider-Cranks

These linkages involve multiple slider-cranks on the faces as planar link groups (Figure 2.24). Then these planar link groups can be assembled together via some special gussets to obtain a spatial linkage of any polyhedral shape. For regular faces, if a totally closed form of the polyhedral shape is desired, the lengths of the connecting rods must be the same as a side length of the central link, so that there are no cavities in the minimal configuration. In a general linkage, at any configuration the vertices of the polyhedral shape are realized

as the gussets, while the edges remain blank and faces are realized partially (Figures 2.25-2.27).

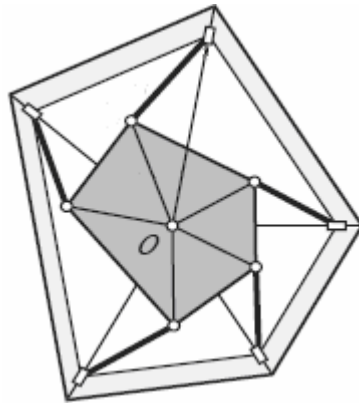


Figure 2.24 A planar link groups for an irregular pentagon [33]

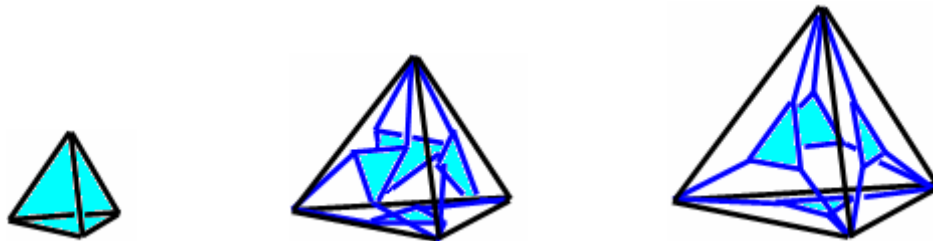


Figure 2.25 The magnification of the vertices are fully realized, but the edges are missing and the faces have blanks

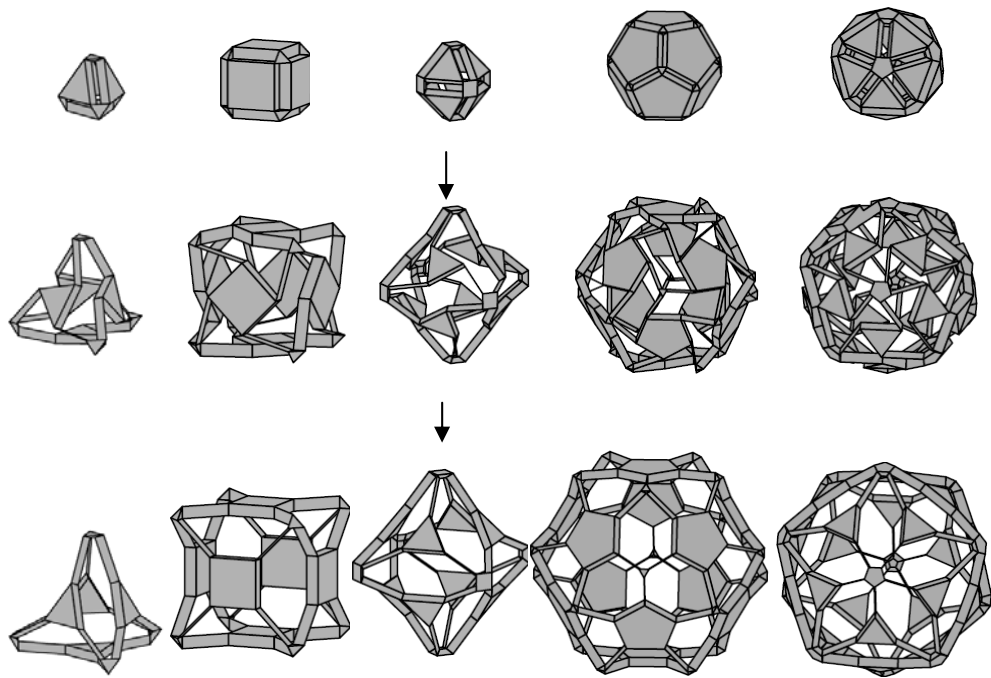


Figure 2.26 Platonic solids by implementing planar link groups with multiple slider cranks on the faces [30]

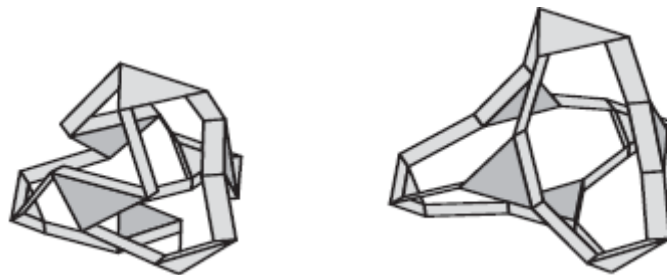


Figure 2.27 An irregular tetrahedral linkage [33]

For the polyhedral linkages with regular faces, i.e. the 5 Platonic solids, the 13 Archimedean solids, the 92 Johnson solids, the regular prisms and the regular antiprisms, the coupler lengths are preferably equal to the crank lengths, hence the total ratio of magnification is 2. For the irregular linkages, the ratio of magnification is bound to the avoidance of the interferences of the gussets with the central links. It is hard to deduce a general statement for the ratio of magnification of all irregular polyhedral shapes, but at least one may guarantee that 2 is an upper bound for the ratio.

2.2.4.3 Linkages with Planar Link Groups for Double Pyramids

A double pyramid, or a dipyrmaid, is obtained by uniting two pyramids with bases of same geometry. So, all the faces of a dipyrmaid are triangular. The linkages for dipyrmaids proposed by Wohlhart comprise planar link groups with 4 links in each link group (Figure 2.28) [34]. The linkages have dextro and leavo parts, hence only dipyrmaids with a base of even number of edges can be magnified. Also, not mentioned in [34], but, since all polygons can be triangulated, these link groups can be used for polyhedral shapes other than dipyrmaids. The triangles can be arbitrarily dissected as in Figure 2.28.a. Notice that this open chain has 4 dofs in a planar affine space, but the three linearity constraints applied on the free vertices of the outer triangles force the chain to have single dof (Figure 2.28.b). The linearity constraint is obtained with assembling the neighboring link groups spatially (Figure 2.29). This dof reducing idea can be used to synthesize many linkages. Indeed, another example is the subject of Section 2.4.4. During the motion of this group of linkages, the vertices remain blank. The edges are realized by two joints and the faces are partially blank (Figure 2.20).

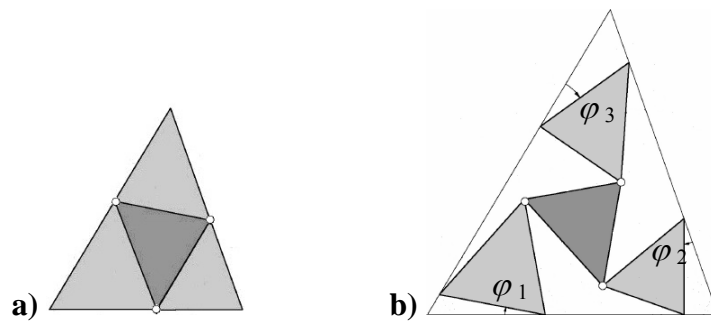


Figure 2.28 The two types of link groups proposed in [34]

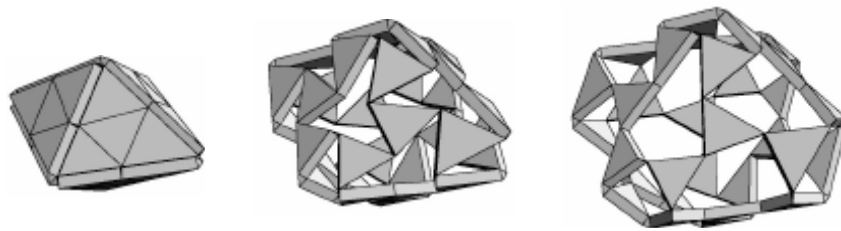


Figure 2.29 An octahedral linkage [34]



Figure 2.30 The edges and faces realized partially [34]

In [34], a set of transcendental equations in terms of angular deviations of the outer triangles from the sides (φ_1 , φ_2 and φ_3 in Figure 2.28.b) are given and numerical solution of these is proposed. Here, another way of position analysis will be proposed.

If a reference frame is fixed at a vertex of the magnifying triangle, an outer triangle experiences a Cardan motion (Figure 2.31). Then, when the outer links are constrained such that a continuous magnification of a triangle is realized, all joints of the central triangle track an ellipse with respect to the moving frames at the vertices of the triangle magnified.

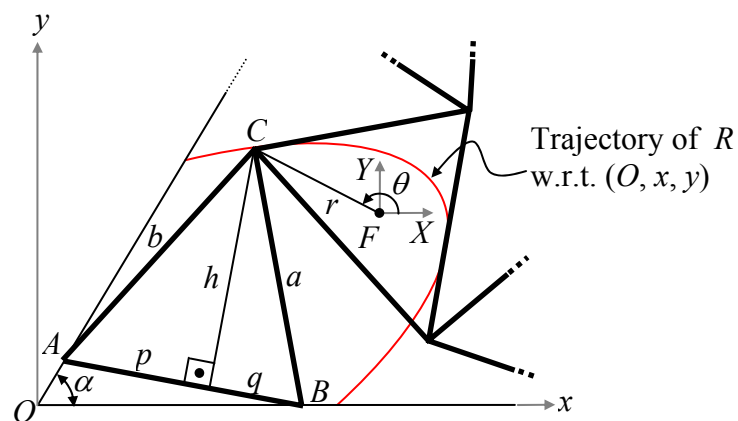


Figure 2.31 The motion of the joint connecting an outer triangle and the central triangle with respect to frame (O, x, y)

As was obtained in the previous chapter, the motion of a joint connecting an outer triangle and the central triangle with respect to a frame located at the corresponding vertex of the magnified triangle is

$$b^2 X^2 + \left[p^2 + \left(h + \frac{c}{\tan \alpha} \right)^2 \right] Y^2 - 2 \left[ph + q \left(h + \frac{c}{\tan \alpha} \right) \right] XY = \left(pq - h^2 - \frac{ch}{\tan \alpha} \right)^2 \quad (2.18)$$

where, a , b , h , p , q and α are as shown in Figure 2.31 and $c = p + q$ (See Section 1.3). Then the elliptic trajectory with respect to (O, x, y) is fully defined by

$$e = \frac{\sqrt{\frac{2(pq - h^2 - dh)^2}{[(a^2 + d^2 + 2dh) - b^2] \sqrt{1 + \frac{4(ch + dq)^2}{[(a^2 + d^2 + 2dh) - b^2]^2} + a^2 + d^2 + 2dh + b^2}}}{\sqrt{1 + \frac{4(ch + dq)^2}{[(a^2 + d^2 + 2dh) - b^2]^2} + a^2 + d^2 + 2dh + b^2}} \quad (2.19)$$

$$f = \frac{\sqrt{\frac{2(pq - h^2 - dh)^2}{[b^2 - (a^2 + d^2 + 2dh)] \sqrt{1 + \frac{4(ch + dq)^2}{[(a^2 + d^2 + 2dh) - b^2]^2} + a^2 + d^2 + 2dh + b^2}}}{\sqrt{1 + \frac{4(ch + dq)^2}{[(a^2 + d^2 + 2dh) - b^2]^2} + a^2 + d^2 + 2dh + b^2}} \quad (2.20)$$

$$\phi = \frac{1}{2} \cot^{-1} \left(\frac{b^2 - a^2 + d^2 + 2dh}{2ch + dq} \right) \quad (2.21)$$

where, $d = c/\tan \alpha$, e and f are the semiminor and semimajor axes lengths and ϕ is the angular displacement of the major axis from horizontal [47].

If the reference frame is translated to the center of the circumscribing circle of the central triangle, i.e. frame (F, X, Y) in Figure 2.13, the position of point R is given by

$$\left[\begin{array}{l} b^2(X - kX_{A,i})^2 + (a^2 + d^2 + 2dh)(Y - kY_{A,i})^2 \\ -2(ch + dq)(X - kX_{A,i})(Y - kY_{A,i}) \end{array} \right] = (pq - h^2 - dh)^2 \quad (2.22)$$

where, $(X_{A,i}, Y_{A,i})$ is the position of A with respect to (F, X, Y) at the minimal configuration and k is the ratio of magnification. Since C tracks a circular path with respect to (F, X, Y) , (2.22) may be written as

$$\left[\begin{array}{l} b^2(r\cos\theta - kX_{A,i})^2 + (a^2 + d^2 + 2dh)(r\sin\theta - kY_{A,i})^2 \\ -2(ch + dq)(r\cos\theta - kX_{A,i})(r\sin\theta - kY_{A,i}) \end{array} \right] = (pq - h^2 - dh)^2 \quad (2.23)$$

where, r is the radius of the circumscribing circle of the central triangle and θ is the inclination of \overline{FC} from positive X . (2.23) involves two variable parameters: k and θ . If (2.23) is rearranged as

$$\begin{aligned} a_2 k^2 + 2a_1 k + a_0 &= 0 && \text{with} \\ a_2 &= b^2 X_{A,i}^2 + (a^2 + d^2 + 2dh) Y_{A,i}^2 - 2(ch + dq) X_{A,i} Y_{A,i} \\ a_1 &= r \left\{ [(ch + dq) Y_{A,i} - b^2 X_{A,i}] \cos\theta + [(ch + dq) X_{A,i} - (a^2 + d^2 + 2dh) Y_{A,i}] \sin\theta \right\} \\ a_0 &= b^2 r^2 \cos^2\theta + (a^2 + d^2 + 2dh) r^2 \sin^2\theta - (ch + dq) r^2 \sin 2\theta - (pq - h^2 - dh)^2 \end{aligned} \quad (2.24)$$

from which k can be solved in terms of θ using the quadratic formula.

For the most simple case consider an equilateral triangle dissected at the midpoints of the sides with one side length 2. Then the fixed parameters are $a = b = c = 1$, $p = q = 1/2$, $h = \sqrt{3}/2$, $r = 1/\sqrt{3}$, $X_{A,i} = -1$, $Y_{A,i} = -1/\sqrt{3}$ and $d = 1/\sqrt{3}$. Then (2.24) yields

$$4k^2 + 2(\sqrt{3}\cos\theta + \sin\theta)k + 4\sin^2\theta - 2\sqrt{3}\sin 2\theta - 6 = 0 \quad (2.25)$$

Hence,

$$k = 2\cos(\theta - \theta_0) \quad (2.26)$$

where, $\theta_0 = 5\pi/6$ is the angle θ at the minimal configuration. (2.26) is plotted using Mathcad 12[®] for the physically realizable motion range and the plot is presented in Figure 2.32. The maximum ratio of magnification is 2.

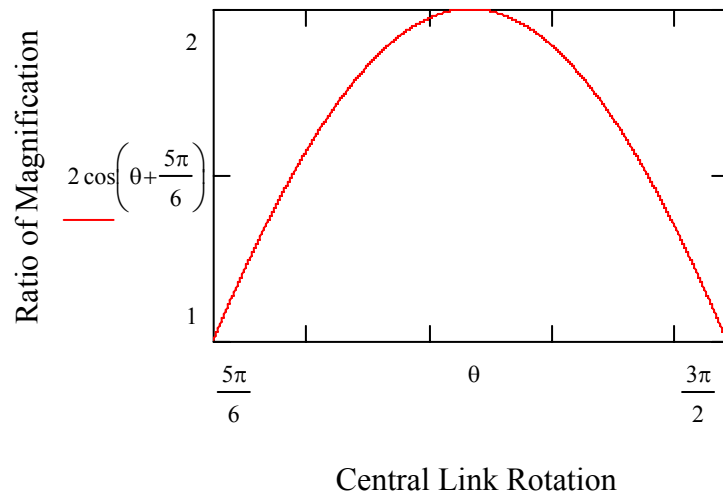


Figure 2.32 Ratio of magnification versus central link rotation for an equilateral triangular linkage

2.2.4.4 Linkages with Planar Link Loops for Regular Polyhedra

These linkages magnify polyhedra with regular faces by means of closed loop planar link groups (Figure 2.33) [32]. Every chain on a face is a single loop and consists of $2n$ identical triangular links connected by $2n$ revolute joints for an n -gon. As was for the linkages of Section 2.4.4, also in these linkages the vertices of the polyhedral shape are blank and the edges and the faces are partially realized (Figure 2.34).

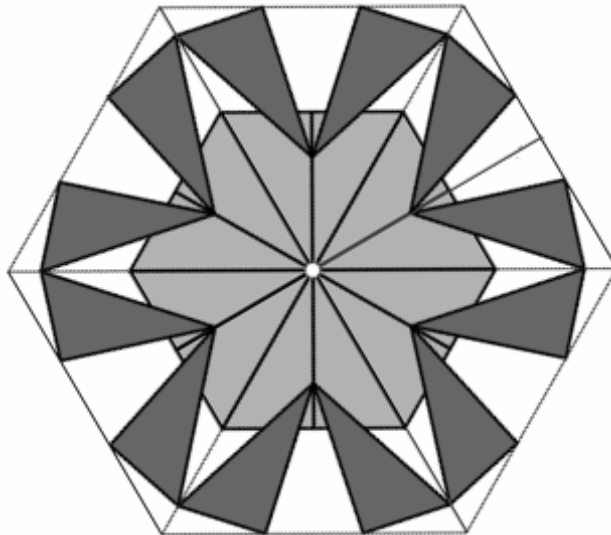


Figure 2.33 Faces magnified as an opening flower [32]



Figure 2.34 Vertices blank, edges through two points, faces partially blank

Again, the Cardan motion plays an important role for these linkages. If the center of the regular polygon is fixed and the inner vertices of the triangular links are linearly constrained, the outer vertices of the links realize a Cardan motion (Figure 2.35).

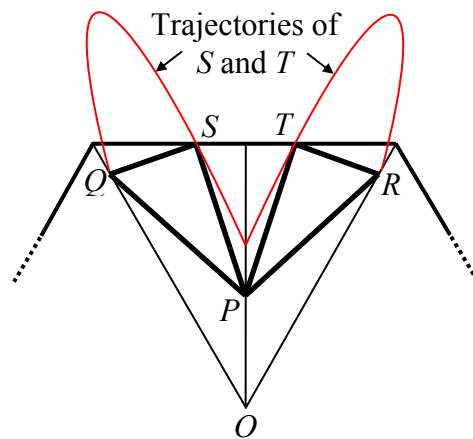


Figure 2.35 The Cardan motion of a link pair

In [32], the maximum ratio of magnification is obtained using geometric relations and found as

$$k = \sqrt{1 + \left[\frac{2}{\sin(2\pi/n)} \right]^2} \quad (2.27)$$

where, n is the number of sides of the regular polygon. Hence, the ratio of magnification is 2.517 for an equilateral triangle, 2.236 for a square, 2.329 for a regular pentagon and 2.517 for a regular hexagon.

2.2.4.5 Polyhedral Zigzag Linkages

This design of Wohlhart is for the five Platonic solids only. The expansion is achieved with the scissor mechanism as well as some special connection mechanisms. These connections, or articulations, are of 4 type (Figures 2.36-2.37). The connection mechanisms are spatial mechanisms with their centers corresponding to the vertices of the polyhedral shape. The torsion of the edges from the vertices is achieved by special gussets. The scissor edges are either towards the center of the polyhedra (as for the tetrahedron, the cube and the icosahedron) or do not interfere the inner part of the polyhedra (as for the octahedron and the dodecahedron). The type of the articulation used for the octahedral and the icosahedral linkages is named by Wohlhart as the flat ring articulation, while the others are named as the rotor shield articulation for the tetrahedral linkage, the parallel plate articulation for the cubic linkage and the coronal articulation for the dodecahedral linkage [35].

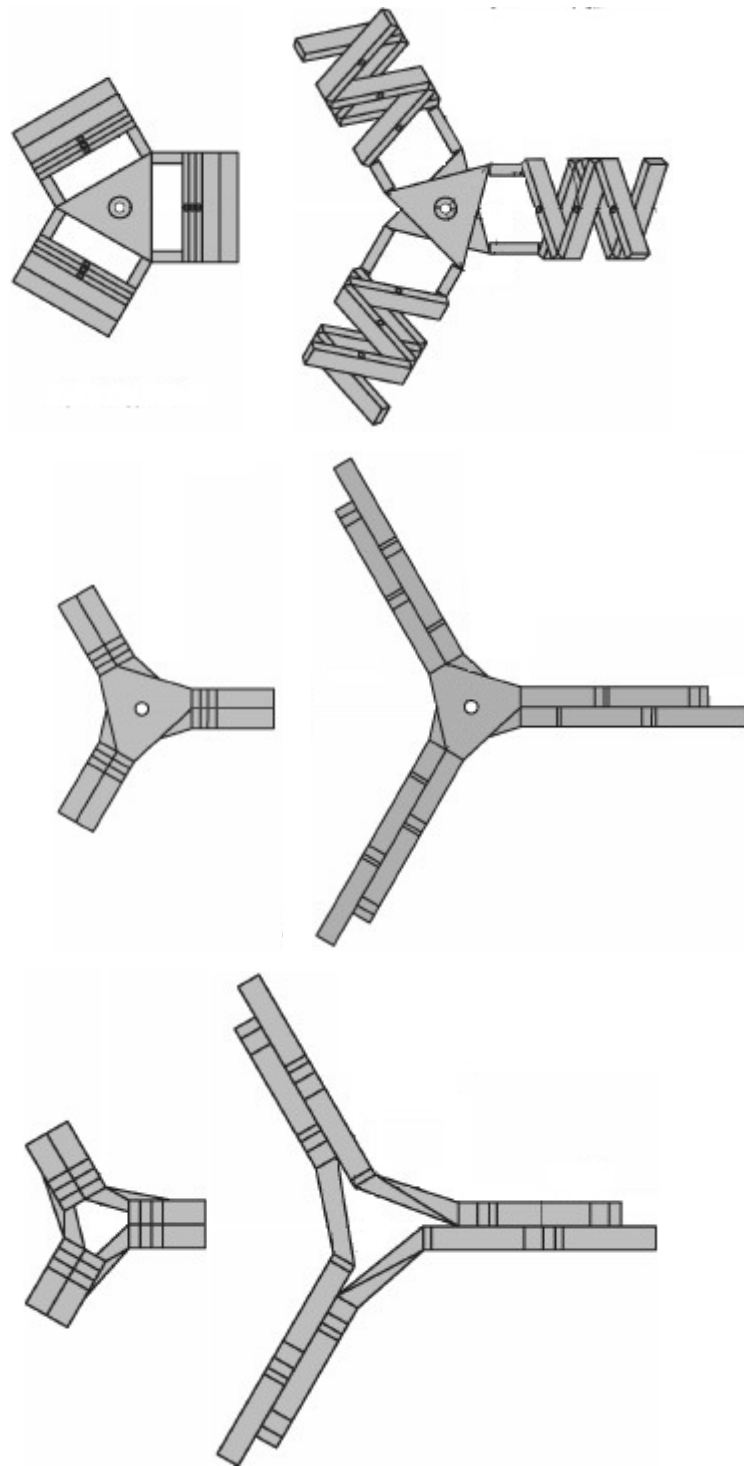


Figure 2.36 Articulations for tetrahedral, cubic, dodecahedral linkages [35]

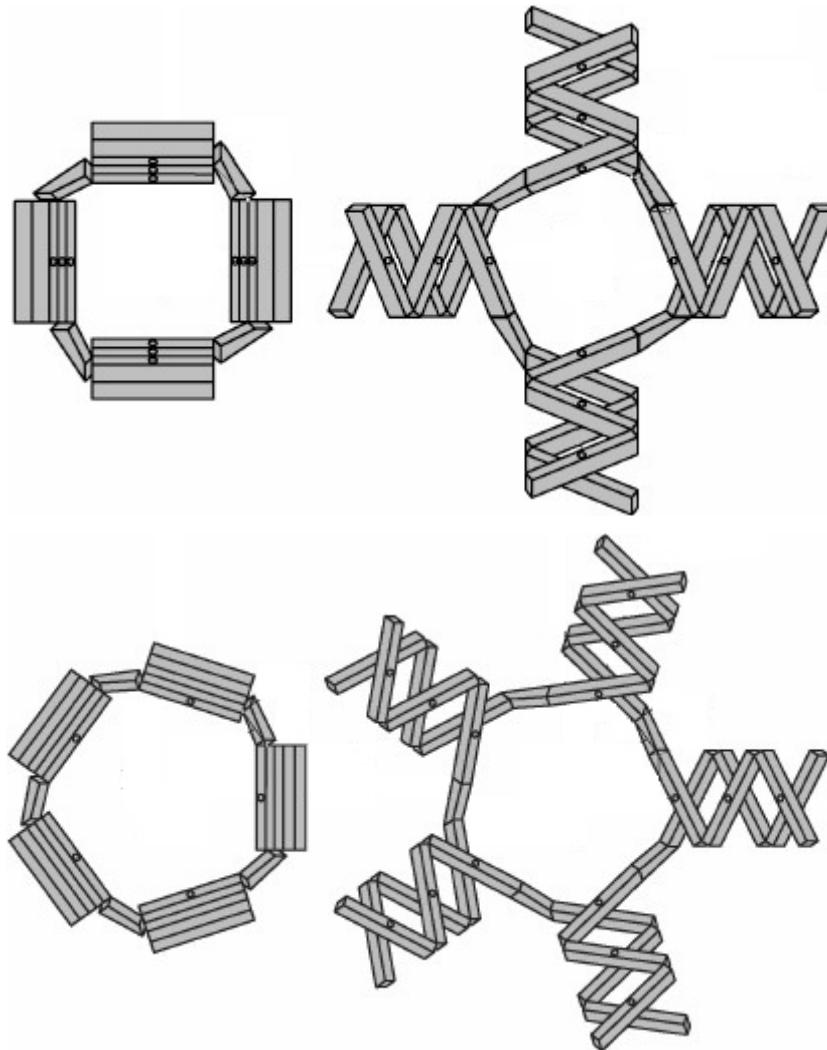


Figure 2.37 Articulations for octahedral and icosahedral linkages [35]

For these linkages, the edges are described by the scissor mechanisms, the vertices are by the articulations, but the faces remain blank.

Neglecting the thicknesses of the scissor elements in the formulae given in [35], the maximum ratio of magnification is 5 for the tetrahedral linkage, 7.544 for the cubic linkage, 2.121 for the octahedral linkage, 2.674 for the dodecahedral linkage and 1.854 for the icosahedral linkage.

2.2.5 Agrawal et. al. Designs

There is not much ingenuity in these designs. The idea is to use prismatic joints along edges of polyhedral shapes while preserving the solid angles rigidly. The very outcomes of this kind of design are that there are less number of kinematic elements when compared to the other designs and the vertices and the edges are realized throughout the expansion process. The resulting linkages are single dof except for some polyhedra. For example, the cube becomes 3-dof when its edges are mobilized by prismatic joints. In this case, Agrawal et al. proposes triangulation of some faces until the mechanism becomes a single dof one (Figure 2.38). Although these designs seem to be advantageous due to the vertices and edges perceived at all configurations, they bring serious problems such as binding due to friction [36].

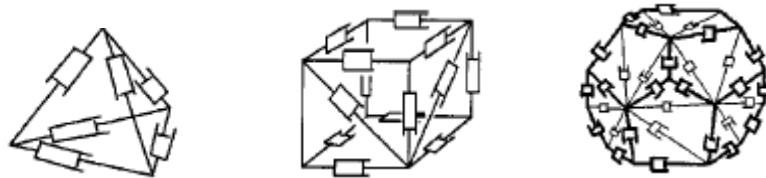


Figure 2.38 The tetrahedral, the cubic and the dodecahedral linkages [36]

The maximum ratio of magnification is less than two if a single prismatic joint is used along the edges. The ratio can be increased if telescoping elements are used, instead. However, in this case, dynamical problems would increase.

2.2.6 Kovács et al. Designs

Kovács et al. use dipolygonoids and a new type of polyhedral linkage, which they call the double link expandohedra, to model the motions of polyhedral viruses (Figure 2.39) [41, 42]. The dipolygonoids used involve a digon and an n -gon. The double link expandohedra look similar to the dipolygonoids but there are two rods instead of one to join the polygonal faces. The double link expandohedra are used for polyhedral shapes with only trivalent vertices. Although [41] and [42] suggest spherical joints, two dof joints shall be used to achieve a single dof linkage. A rod joins the vertex of a polygon with the midpoint of the edge of the adjacent polygon. During the motion, the faces are partially realized, while the edges and the vertices remain blank (Figure 2.40).

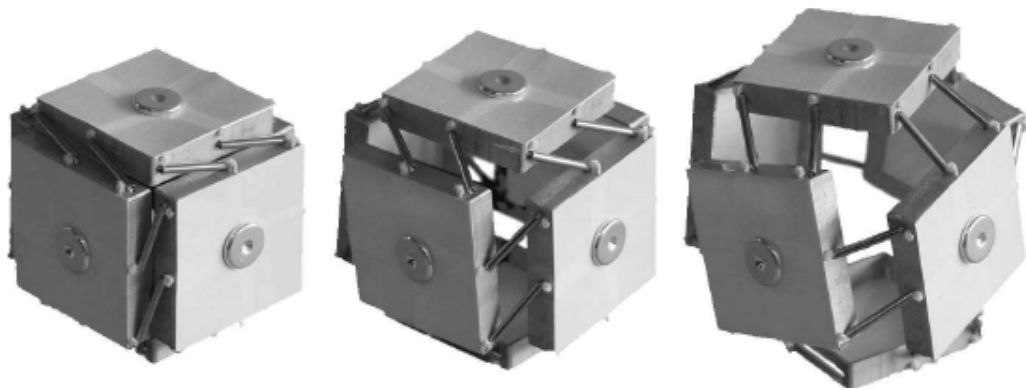


Figure 2.39 A cubic double link expandedhedra [42]

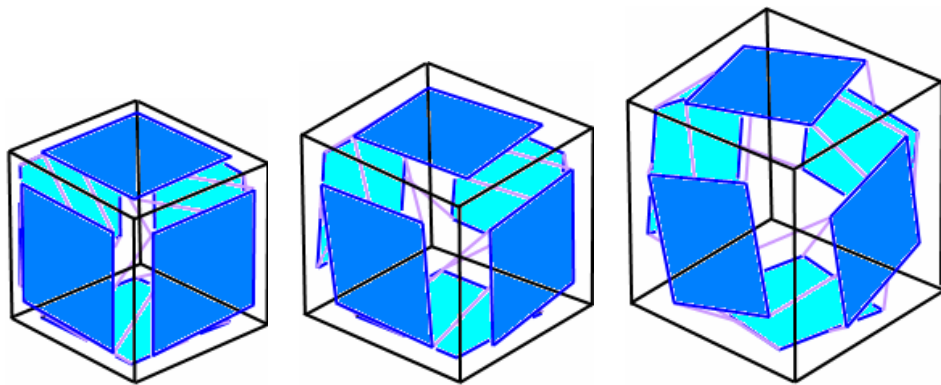


Figure 2.40 Vertices and edges blank, faces partially realized

The motion of the double link expandedhedra also is similar to the motion of a dipolygonid. However, the rotational sense of the polygonal faces does not change as does for the dipolygonids. For the Platonic solids, the maximal configuration is when the opposite vertices of two corresponding edges meet,

hence the ratio of magnification is the ratio of the radius of the circumscribing circle to the inscribing circle, which is equal to $\sec(\pi/n)$ for an n -gonal faces. This ratio is the same for the dipolygonids with same regular faces. The ratio is 2 for the tetrahedron, 1.414 for the cube and 1.236 for the dodecahedron.

2.3 Comparison of the Present Designs

Some properties of the polyhedral linkages covered in this chapter are summarized in Table 2.1. The partially realized and not realized parts of the polyhedral shape being magnified and the maximum ratio of magnification are listed in the table. The ratio for the Fulleroid is for the rhombic dodecahedron, the ratio for the linkages with planar link groups for diyramids is for the octahedron, the ratio range for the double link expandohedra is for the trivalent Platonic solids and the ratio ranges for the other linkages are for the Platonic solids.

Considering the perception of the polyhedral shape, the Hoberman sphere, the polyhedral zigzag linkages and the linkages with prismatic joints are the most effective linkages. However, the linkages with prismatic joints are more likely to malfunction and the Hoberman sphere and the polyhedral zigzag linkages have the most critical clearance effects during the motion. The linkages that have the greatest capability of magnification are the polyhedral zigzag linkages. While the Fulleroid is only for a single polyhedral shape, the linkages with prismatic joints can be used for any polyhedral shape. The less link-requiring linkages are the linkages with prismatic joints with requiring vertex number of links or the dipolygonids with requiring face number of links (not

all the dipolygonids). The most link-requiring linkages are the polyhedral zigzag linkages.

Table 2.1 Summary of some properties of the present polyhedral linkages

Designer	Design Name	Not realized parts	Partially Realized Parts	Maximum Ratio of Mag.
Fuller / Verheyen	Jitterbug / Dipolygonids	Vertices, Edges	Faces	1.24 – 2
Fuller	Fulleroid	Vertices, Edges	Faces	2.03
Hoberman	Hoberman Sphere	Faces	-	1 – 1.5
Wohlhart	Polyhedral Star-Transformer	Edges	Faces	1.06 – 1.65
Wohlhart	Linkages With Multiple Slider-Cranks	Edges	Faces	1.06 – 1.65
Wohlhart	Linkages With Planar Link Groups for Diyamids	Vertices	Edges, Faces	2
Wohlhart	Linkages With Planar Link Loops for Regular Polyhedra	Vertices	Edges, Faces	2.24 – 2.52
Wohlhart	Polyhedral Zigzag Linkages	Faces	-	1.85 – 7.54
Agrawal et. al	Linkages With Prismatic Joints	Faces	-	2
Kovács et al.	Double Link Expandohedra	Vertices, Edges	Faces	1.24 - 2

CHAPTER 3

NEW DESIGN METHODS FOR POLYHEDRAL LINKAGES

In this chapter, new linkage types for resizing polygonal and polyhedral shapes are presented. First, single dof planar linkages are synthesized in order to obtain planar link groups for the faces of polyhedral shapes. The planar linkages involve only revolute joints. Then the polyhedral linkages are assembled by interconnecting the planar linkages with links at the vertices to retain the solid angles of the polyhedral shape of interest.

In the first section, the systematic approach to the problem is given. Then a link group is considered for the required task and a solution is obtained. Afterwards, different types of linkages are derived from the resulting linkages. Finally, the spatial linkages are presented and the linkages are illustrated by examples.

3.1 Sectioning Polyhedra

Using magnifications, it can be shown that scaling (magnifying) a polyhedron is equivalent to scaling its faces with the same scaling factor while preserving the shape, i.e. keeping proper edges of the faces in touch. The scaling problem for a polygon can be simplified into the scaling problem for a triangle, because polygons can be triangulated. Among many possible triangulations, a suitable one for magnification purposes is to choose a point inside the polygon and connect it to the vertices by line segments (Figure 3.1).

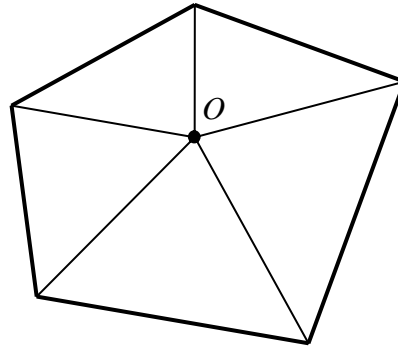


Figure 3.1 A triangulation of a pentagon

Consider an arbitrary triangle ${}^1OP_{\max}R_{\max}$ of side lengths l , p and r (Figure 3.2). Applying a magnification with center O and magnification ratio $k (< 1)$, the triangle is mapped to a new, similar triangle 1OPR (Fig. 2). A linkage that will perform this transformation is to be designed.

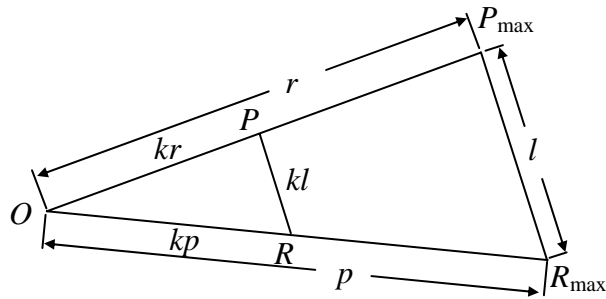


Figure 3.2 Magnification of a triangle centered at one of its vertices

Magnification is a special linear similarity transformation, yet is not an isometry. To physically realize such a transformation by means of linkages, the first thing that comes into mind is to use prismatic joints along the edges of the shape of interest, as investigated by Agrawal et. al. [36]. As stated in [36], use of prismatic joints has practical problems such as binding due to friction. Alternatively, the transformation can be partly realized using revolute joints only. In such systems, one cannot magnify the whole shape of interest, but vertices of the polygon can be scaled. From here on, a triangle, or in general a polygon or a polyhedron, will be considered to be fully defined by its vertices. Of course the connectivity information between the vertices is also necessary to define a polygon or polyhedron, but this aspect is out of concern when similarity transformations are considered. Since the vertices are used to define a polygon, during the design of linkages, the magnification of the sides will be kept out of scope.

Considering the motion of the vertices during a continuous magnification of a triangle, once the magnification center is chosen as one of the vertices, the other two vertices must realize a straight line motion. Consider two slider-crank mechanisms OSQ and OTQ with coupler points P and R on links 2 and 4, respectively (Figure 3.3). There are no sliders along the sides of the triangles, but coupler points P and R must have a linear motion for a continuous magnification of the triangle. The aim is to keep 1OPR similar to ${}^1OP_{\max}R_{\max}$ at any configuration. The location of point Q_{\max} will be discussed in the following sections, but for now, its location can be assumed to be arbitrary on line $P_{\max}R_{\max}$. During the motion, Q will not necessarily be on edge PR .

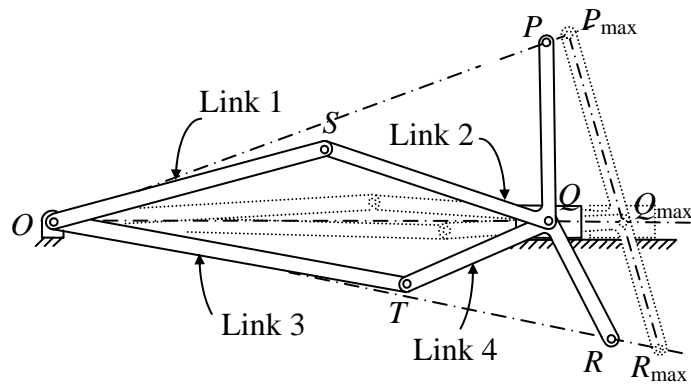


Figure 3.3 A six link kinematic chain which is supposed to scale a triangle

For further simplification of the problem, consider the slider-crank mechanism OSQ only (Figure 3.4). Fictitiously Q is constrained by a slot. Note that the mechanism has a single dof. Dimensional synthesis of such a mechanism to obtain a straight line motion is performed in the following section.

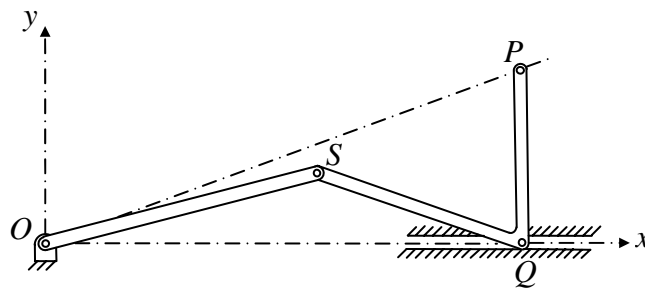


Figure 3.4 Simplified mechanism for half of a triangle

3.2 Synthesizing Linkages for the Triangular Sections

For a triangle ${}^1OP_{\max}Q_{\max}$, let $\angle P_{\max}OQ_{\max} = \alpha$, $|OP_{\max}| = r$ and $|Q_{\max}P_{\max}| = l_P$ (Figure 3.5). For any triangle similar to ${}^1OP_{\max}Q_{\max}$, α and the ratio r/l_P is invariant. $|OS| = a_1$, $|SQ| = a_2$, $|QP| = |Q_{\max}P_{\max}| = l_P$ and $\angle SQP = \gamma$ are the link parameters of the mechanism. θ_1 , θ_2 and s_2 , shown in Figure 3.6, are the joint parameters. a_1 , a_2 and γ are to be determined such that P traces a straight line.

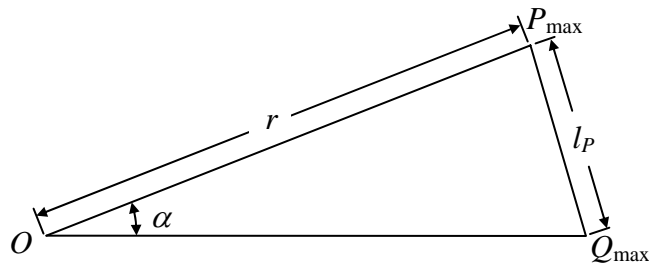


Figure 3.5 The known parameters of the system

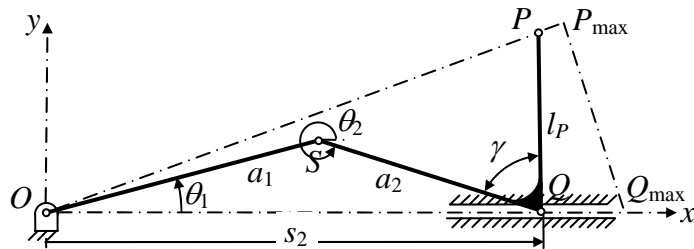


Figure 3.6 The link parameters and the joint parameters of the mechanism

Loop equations for the mechanism can be written as

$$a_1 \cos \theta_1 + a_2 \cos \theta_2 = s_2 \quad (3.1)$$

$$a_1 \sin \theta_1 + a_2 \sin \theta_2 = 0 \quad (3.2)$$

In order for the point P to be on line OP_{\max} , the following must be satisfied

$$P_y = P_x \tan(\alpha) \quad (3.3)$$

Writing x and y components of P

$$P_x = s_2 + l_P \cos(\theta_2 - \pi - \gamma) \quad (3.4)$$

$$P_y = l_P \sin(\theta_2 - \pi - \gamma) \quad (3.5)$$

Substituting (3.4) and (3.5) in (3.3)

$$l_P \sin(\theta_2 - \pi - \gamma) = [s_2 + l_P \cos(\theta_2 - \pi - \gamma)] \tan \alpha \quad (3.6)$$

Manipulating (3.6)

$$l_P \sin(\alpha + \gamma - \theta_2) = s_2 \sin \alpha \quad (3.7)$$

At the extended position of the mechanism, $ds_2/d\theta_2 = 0$, so differentiating (3.7) with respect to θ_2 gives

$$\cos(\alpha + \gamma + \theta_2) = 0 \quad (3.8)$$

For $\theta_2 = 2\pi$, i.e. at the extended position, by (3.8)

$$\gamma = \pi/2 - \alpha \quad (3.9)$$

Also for $\theta_2 = 2\pi$ (3.8) yields $\gamma + \alpha = 3\pi/2$, but since at the extended position α and γ are the inner angles of a triangle, (3.9) is the only realizable solution.

Also, at the extended position, by (3.1), (3.7) and (3.9)

$$\sin \alpha = \frac{l_p}{a_1 + a_2} \quad (3.10)$$

Reconsidering (3.7) for $\theta_2 = 2\pi - \alpha$ and using (3.1), (3.9) and (3.10)

$$(a_1 + a_2)l_p \cos \alpha = l_p(a_1 \cos \theta_1 + a_2 \cos \alpha) \quad (3.11)$$

Using (3.2) and Pythagorean Theorem in (3.11)

$$a_1 \cos \alpha = \sqrt{a_1^2 - a_2^2 \sin^2 \alpha} \quad (3.12)$$

Squaring both sides of (3.12) and using (3.10)

$$a_1 = a_2 = \frac{l_p}{2 \sin \alpha} \quad (3.13)$$

Then by (3.2) and (3.13)

$$\theta_1 + \theta_2 = \pi \quad (3.14)$$

The design parameters are found in terms of the link parameters by (3.9) and (3.13), but still there are some restrictions on these design parameters due to the task requirements. First, $\pi/2$ is an upper bound for $\angle OP_{\max}Q_{\max}$, because at the maximal configuration, $\angle OP_{\max}Q_{\max} < \pi - \alpha - \gamma = \pi/2$ by (3.9). Second, to realize a magnification, one must have $|OP|/|OR|$ constant at any configuration (See Figure 3.3), so location of Q_{\max} cannot be arbitrary. Let $|Q_{\max}R_{\max}| = l_R$. To have $|OP|/|OR|$ constant, one must ensure at $s_2 = 0$

$$\frac{|OP|}{|OR|} = \frac{l_P}{l_R} = \frac{r}{p} \quad (3.15)$$

For $|Q_{\max}R_{\max}| = p$ and $l_P + l_R = |P_{\max}R_{\max}| = l$ (Figure 3.7), by (3.15)

$$l_P = \frac{rl}{p+r} \quad (3.16)$$

and

$$l_R = \frac{pl}{p+r} \quad (3.17)$$

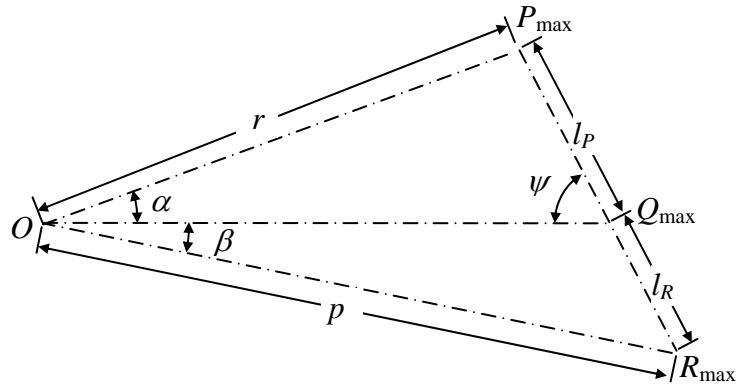


Figure 3.7 The largest desired size of 1OPR

So, the location of point Q is not arbitrary. Also the location of O may depend on system parameters. For O , the most critical configuration is when P , Q and R are collinear, i.e. when P , Q and R are instantaneously coincident with P_{\max} , Q_{\max} and R_{\max} , respectively (Fig. 3.7). Let $\angle R_{\max}OQ_{\max} = \beta$, $\angle OQ_{\max}P_{\max} = \psi$. Writing sine theorem for ${}^1P_{\max}OQ_{\max}$ and ${}^1R_{\max}OQ_{\max}$ and by (3.16) and (3.17):

$$\frac{l_P}{\sin \alpha} = \frac{r}{\sin \psi} \quad (3.18)$$

and

$$\frac{l_R}{\sin \beta} = \frac{r}{\sin(\pi - \psi)} \quad (3.19)$$

Note that $\sin \psi = \sin(\pi - \psi)$ and that $\alpha + \beta < \pi$, so by (3.15), (3.18) and (3.19)

$$\alpha = \beta \tag{3.20}$$

It must be checked whether $|OP|/|OR|$ is kept constant at all configurations. Let $\angle QOS = \theta_P$ (CCW) and $\angle QOT = \theta_R$ (CW) (Figure 3.8). Then by (3.3)

$$\frac{|OP|^2}{|OR|^2} = \frac{(P_y/\tan \alpha)^2 + P_y^2}{(R_y/\tan \alpha)^2 + R_y^2} \tag{3.21}$$

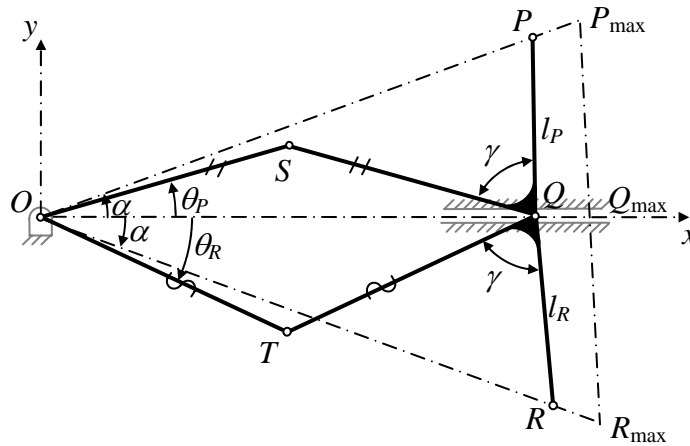


Figure 3.8 The mechanism revised

By (3.15) and (3.21)

$$\frac{|P_y|}{|R_y|} = \frac{l_P}{l_R} \quad (3.22)$$

Considering (3.9) rewriting y-component of P

$$P_y = l_P \sin(\theta_P + \gamma) \quad (3.23)$$

Similarly, the y-component of R can be obtained as

$$R_y = -l_R \sin(\theta_R + \gamma) \quad (3.24)$$

(3.22), (3.23) and (3.24) yield, at all configurations

$$\theta_P = \theta_R \quad (3.25)$$

or

$$\theta_P + \theta_R = 2\alpha \quad (3.26)$$

But, $|OQ| = l_P \cos \theta_P / \sin \alpha = l_R \cos \theta_R / \sin \alpha$, that is θ_R and θ_P have the same sign, hence (3.26) cannot be correct for all configurations. (3.25) yields the correct result.

Next, considering (3.1), (3.13) and (3.14) one obtains

$$|OS| = |OT| = |SQ| = |TQ| = p/2 = r/2 \quad (3.27)$$

(3.27) is quite an important restriction to possible types of triangles that can be scaled by means of the linkage of concern: only isosceles triangles can be scaled by using a linkage as shown in Figure 3.3. Notice that, by this fact, $\angle OQ_{\max}P_{\max} = \angle OQ_{\max}R_{\max} = \pi/2$ and cranks are along the sides OP_{\max} and OR_{\max} at this configuration.

This completes the requirements for the scaling task of a triangle. To summarize, given an isosceles triangle, defined by the angle 2α and side lengths r and l , the link parameters of the mechanism designed that realizes the scaling of a triangle is such that $l_p = l/2$, $\gamma = \pi/2 - \alpha$, $a_1 = a_2 = r/2$ (Figure 3.9).

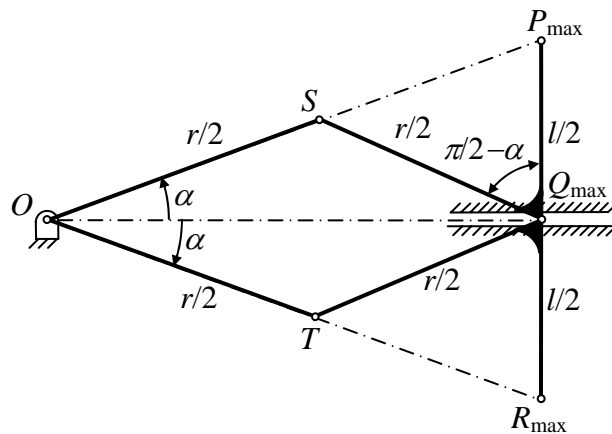


Figure 3.9 The designed scissor linkage for an isosceles triangle $OP_{\max}R_{\max}$

The fixed joint at O and the pin in slot joint Q are hypothetical joints and will not be present when the whole polygonal assembly is constructed. However,

point O will remain stationary in the plane of motion even if it is not connected to a fixed link by a revolute joint. Similarly, in the final system when the slider is removed, point Q will still be on straight line OQ_{\max} .

3.3 On the Motion of the Designed Mechanism

The mechanism in Figure 3.9 is an in-line *isosceles* or *folding* slider-crank mechanism. The coupler link motion is the well known *Cardan Motion* (See Section 1.2). The moving and fixed centrodes of the coupler motion are circles with the moving centrode radius equal to the crank length with center at S and/or T and the fixed centrode of twice the radius of the moving centrode with center at O . Furthermore, a point on the coupler link selected on the circumference of the moving centrode traces a straight line path which passes through O (Figure 3.10). Notice that at the extended position of the slider-crank, the center of the moving centrode is on the slider axis, hence at this configuration $\angle OPQ$ must be $\pi/2$, which can also be obtained using (3.9). As a result, the straight line motion of the vertices P and R can be realized provided that the links containing these points perform Cardan Motion such that the vertices are on the circumference of the respective moving centrodes (Figure 3.10).

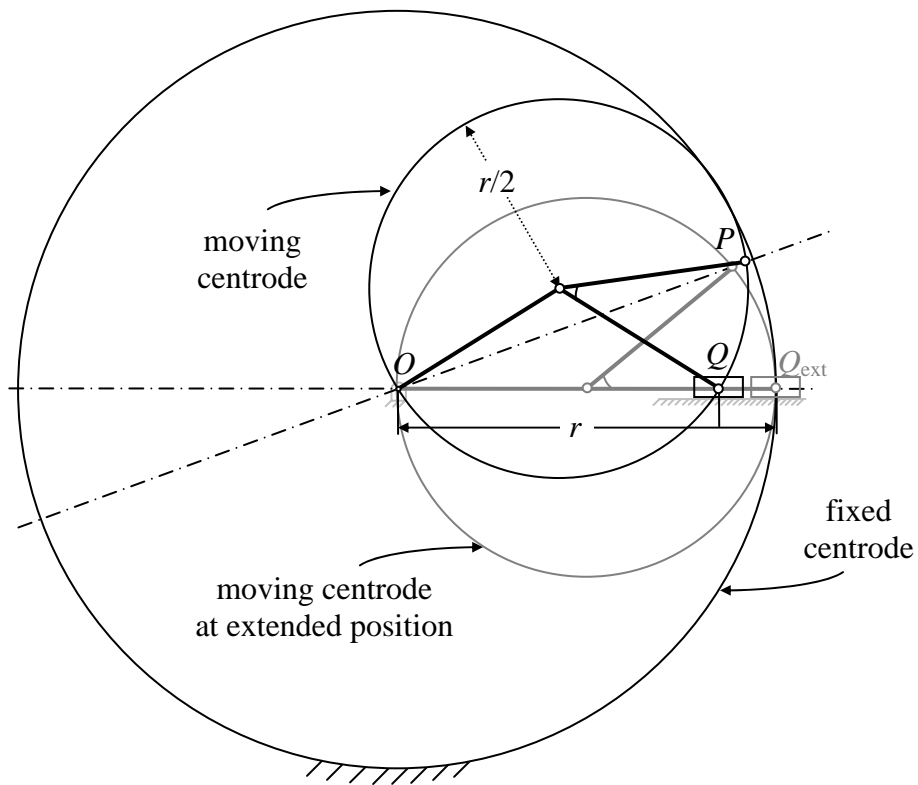


Figure 3.10 Cardan Motion for single slider - The motion of the moving centrode with respect to the fixed centrode

Cardan Motion can also be obtained by a series of isosceles slider-crank mechanisms as shown in Figure 3.11. Notice that, not all isosceles slider-crank mechanisms need to be of the same length. There exists one free design parameter for the mechanism in Fig. 3.11(a), such that $|OS| = |SU| = a_1$, $|UW| = |WQ| = a_2$ and $2a_1 + 2a_2 = r$. In general, $2a_1 + \dots + 2a_n = r$ (Figure 3.11(b)). $s - 1$ free design parameters exist for a multiple slider assembly of s sliders. Below, it is proved that segment PQ makes a Cardan Motion when multiple sliders are used.

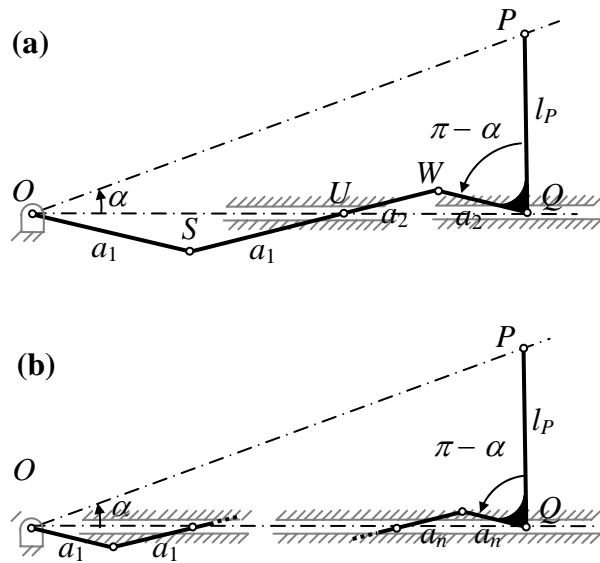


Figure 3.11 Segment PQ makes a Cardan Motion when connected to a multiple slider assembly

Consider a multiple slider assembly as shown in Figure 3.12. Let $|OQ_{\text{ext}}| = 2a_1 + \dots + 2a_n = r$, where Q_{ext} is the position of Q when all the links are collinear. At any configuration, where the crank is rotated by an angle θ , one can draw a circle passing through O and Q with diameter r . Denote this circle by Γ_θ , and let the center of this circle be C_θ . At such a configuration, $|OQ| = 2a_1 \cos \theta + \dots + 2a_n \cos \theta = r \cos \theta$. Since the center of Γ_θ is on the perpendicular bisector of OQ and Γ_θ has radius $r/2$, $\angle QOC_\theta = \angle OQC_\theta = \theta$. Consider point P on Γ_θ located such that $\angle QC_\theta P = 2\alpha$. At any configuration of the mechanism, $\angle QC_\theta P = 2\alpha$, so by the inscribed angle theorem P is on the straight line through O with an inclination of α from OQ , regardless of θ . Therefore, P traces this straight line. Hence Γ_θ is the moving centre of link

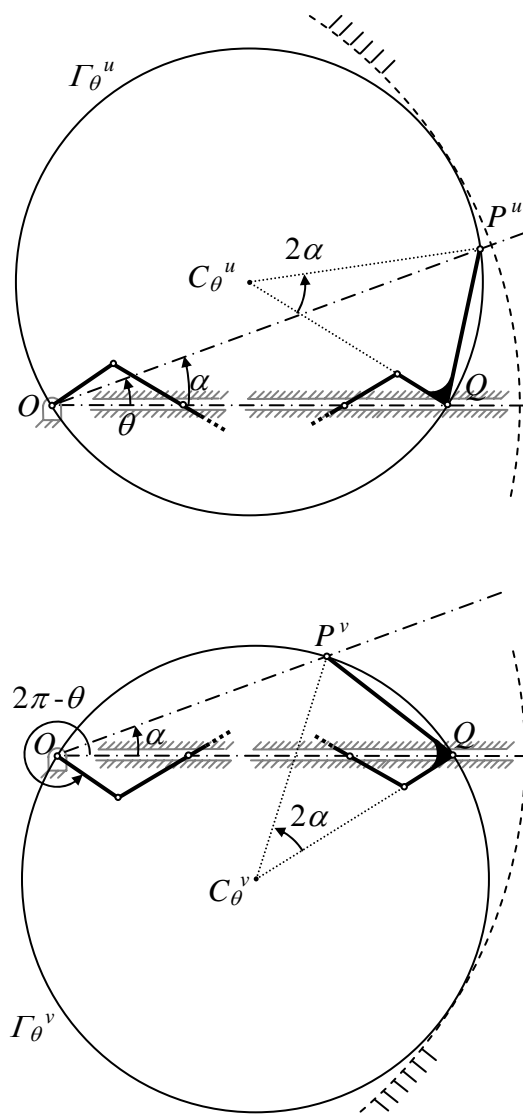


Figure 3.13 Two possible mechanisms to realize a specified straight line coupler path

This short analysis reveals that it is also possible to obtain a straight line motion for the counterclockwise rotation of the segment QP . Assembling symmetrical linkages as in Figure 3.14(a), isosceles triangles can be magnified.

In Figure 14(b) additional coupler points that realize straight line motion are introduced. Actually, the symmetrical coupler links obtained this way are nothing but the “*angulated elements*”, as named by Hoberman [45]. Once these sublinkages are assembled, the resulting polygon scaling linkage will be further redundantly constrained if angulated elements are used. Also the cranks can be removed if the linkages are already constrained by angulated elements [10].

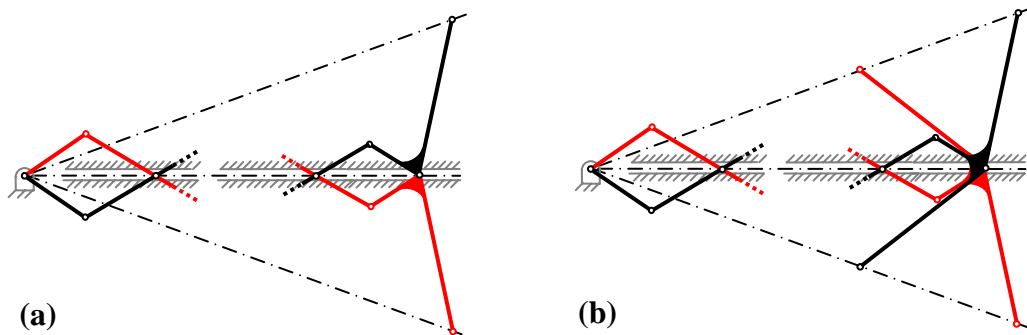


Figure 3.14 Possible constructions for triangle scaling linkages

Another important point is that not only the coupler link realizes the Cardan Motion, but also does the intermediate links. However, obviously, different moving and fixed centrodes correspond to each link. The fixed centrodes appear as concentric circles while the moving centrodes appear in alternating order in terms of being over or under the slider axes and the moving centrodes of the symmetrical slider chains are located mirror symmetrically with respect to the slider axis (Figure 3.15). So, some coupler points may be added to the intermediate links and still the linkage moves with a single dof.

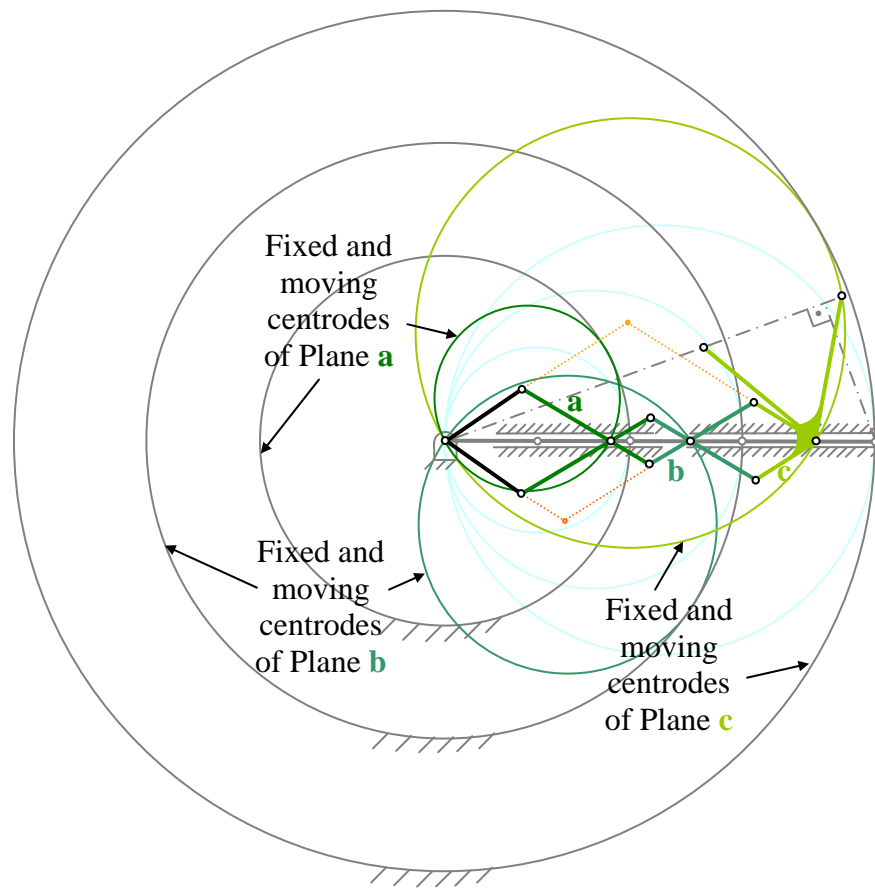


Figure 3.15 The fixed and moving centrodes for the coupler and intermediate links for a three-slider-linkage

3.4 Polygon Scaling

The triangles, which are obtained by triangulating a polygon, can be reassembled to obtain the whole link group representing the polygon. Next, the types of polygons that can be magnified by these link groups shall be investigated.

In order for isosceles triangles to assemble to form a polygon such as in Figure 3.1, all the distances from the selected inner point to the vertices should be equal. Hence only cyclic polygons can be triangulated using isosceles triangles by a triangulation as shown in Figure 3.1. As a result, O cannot be an arbitrary inner point, but must be the center of the circumscribing circle of the cyclic polygon. The converse is obviously true: a cyclic polygon can be triangulated, as in Figure 3.1, such that the triangles are all isosceles. As an example, a regular hexagonal assembly is illustrated in Figure 3.16.

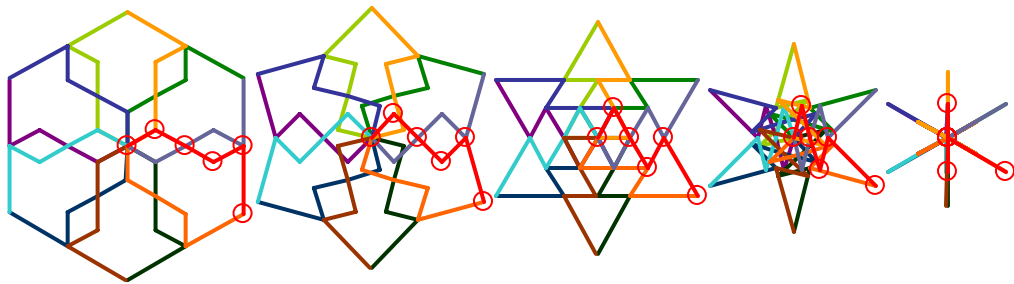


Figure 3.16 Magnification of the vertices of a hexagon

Another form of assembly is when the slider axes pass through the vertices. A similar analysis performed for the linkages with slider axes intersecting the edges reveals that slider axes through vertices also work only for cyclic polygons. In either case, the resulting linkages have a single degree of freedom and the radially assembled sublinkages all realize a Cardan Motion. As an example, a regular hexagonal assembly with slider axes passing through the vertices is illustrated in Figure 3.17.

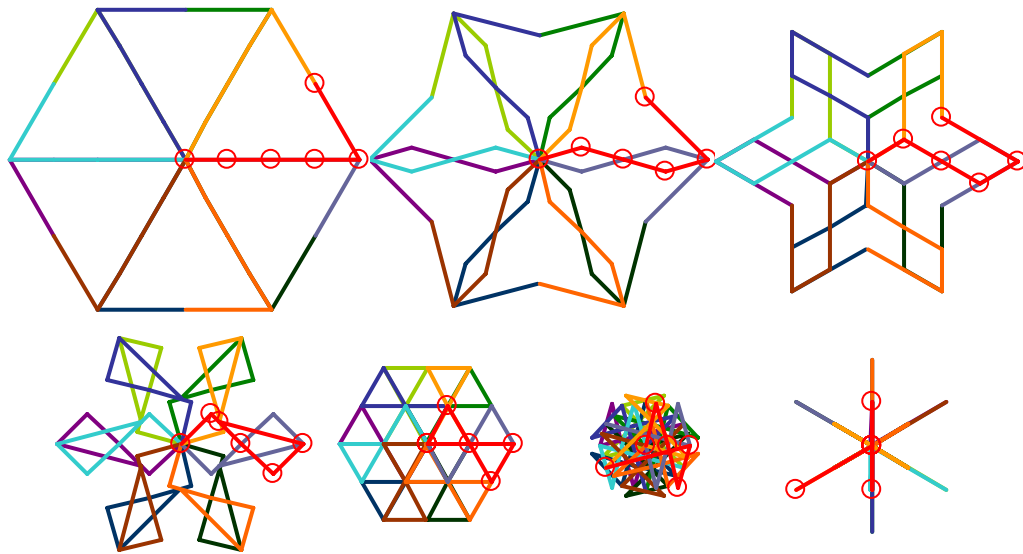


Figure 3.17 Magnification of the vertices of a hexagon by using the linkages with slider axes through the vertices

3.5 Some Modifications – Relations with Existing Polygonal Linkages

Various modifications in the design of the polygon magnifying linkages mentioned in the previous section are possible. As a first modification, consider additional kinematic elements that further constrain the linkages as illustrated in Fig. 3.14(b). Such linkages were designed by Hoberman [56]. Notice that, since clockwise rotating and counter clockwise rotating cranks rotate at the same angular velocity for regular polygons, it is possible to connect these two sets of cranks (Figure 3.18).

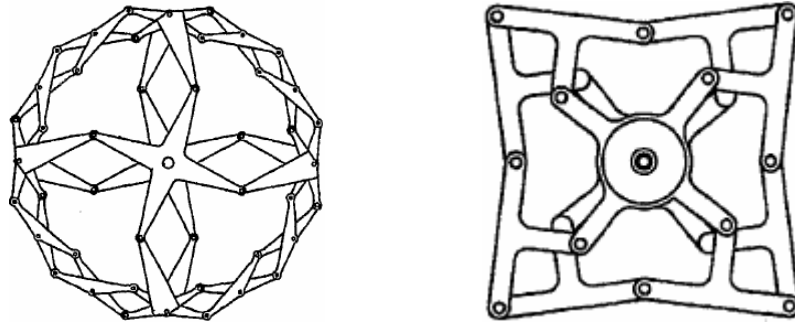


Figure 3.18 Some of Hoberman's designs [48]

Once the additional kinematic pairs are introduced, the sliders can be totally omitted. Such linkages were synthesized by the Deployable Structures Laboratory members of the University of Cambridge [10] (Figure 3.19). The dashed and solid pairs of angulated elements in Figure 3.19 correspond to the gray and black angulated elements in Figure 3.14(b). You, et. al. also introduces additional angulated elements, which can be rigidly connected to each other as illustrated in Figure 3.20. By this modification, concentric rings of rhombi are obtained instead of a single ring of rhombi (Figure 3.20) [10].

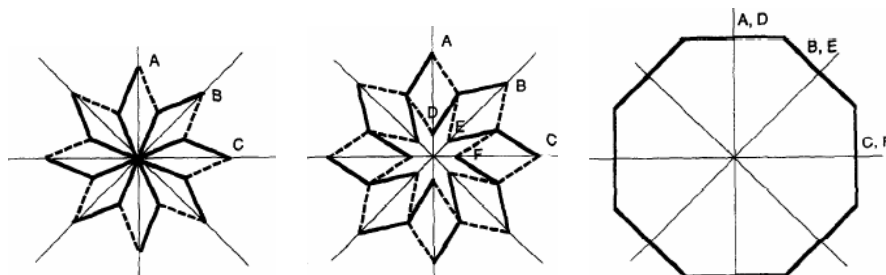


Figure 3.19 Foldable ring structures of You et. al. [10]

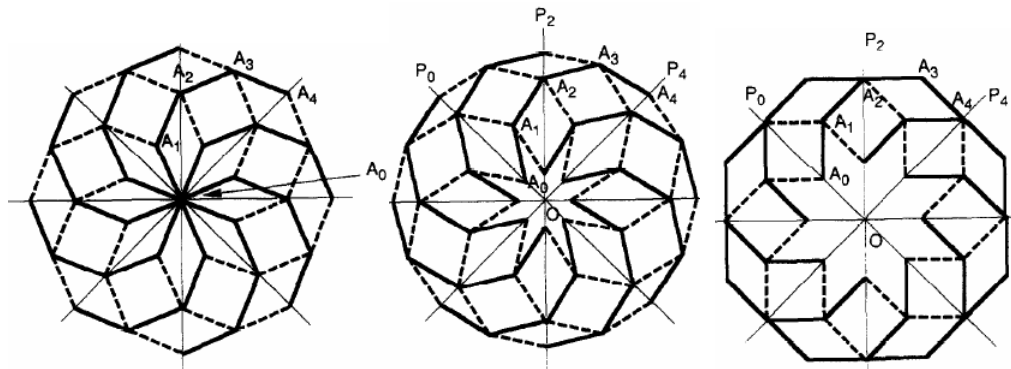


Figure 3.20 Linkages obtained by rigidly connected angulated elements [10]

The polygonal linkages of Wohlhart are interesting in that, not symmetrical parts are used for each subpart of the polygon as in Figure 3.14, but a single slider is used for each subpart (Figure 3.21). The symmetrical parts of Figure 3.14 are, actually, necessary to keep a slider axis, but in Wohlhart's design, the slider axes are kept straight by assembling planar link groups with each other to form a polyhedral shape. In [30], also the cranks are combined in a single link and angulated elements are not used (Figure 3.21(a)). This simplification makes it possible to magnify some irregular polyhedra, because the coupler points are suppressed and hence equation (3.15) is not necessary anymore [33]. In [32], central slider-crank sub-linkages are absent, planar linkage groups are linked at tip points of the angulated elements and these planar link groups are connected to each other at mid points of the angulated elements (Figure 3.21(b)). In all these designs, the common point is that Cardan Motion is used to realize the straight line motion of a coupler point.

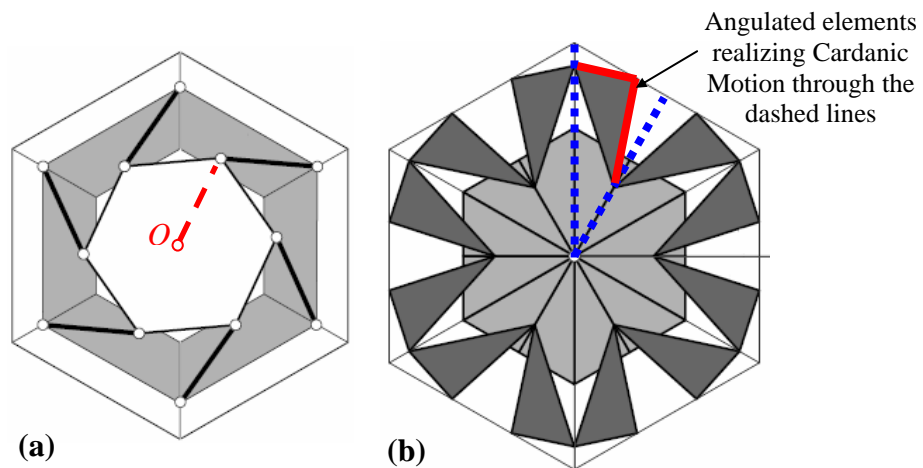


Figure 3.21 Wohlhart's linkages [30, 32]

3.6 Cover Plates for Planar Linkages

The links constituting the planar linkages can be designed such that the area spanned by the linkage is covered at some or all configurations. One possible construction for a two-slider-linkage is to arrange the linkages as shown in Figure 3.22. Of course, various other designs are possible ([5] presents such a design). Also, geometric optimization must be considered in cover element design ([14] optimizes the geometry of the cover plates proposed in [5]). As an example, a linkage, scaling a square with these extensions is illustrated in Figure 3.23. Also a linkage for a square with single sliders is constructed and is shown in Figure 3.24.

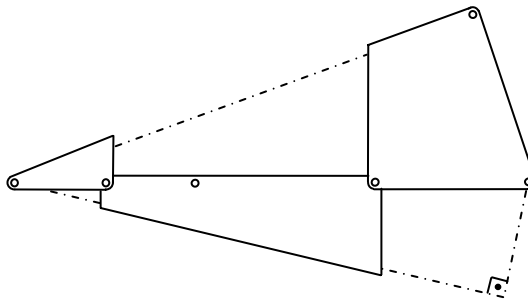


Figure 3.22 Some extensions for the links to cover the faces

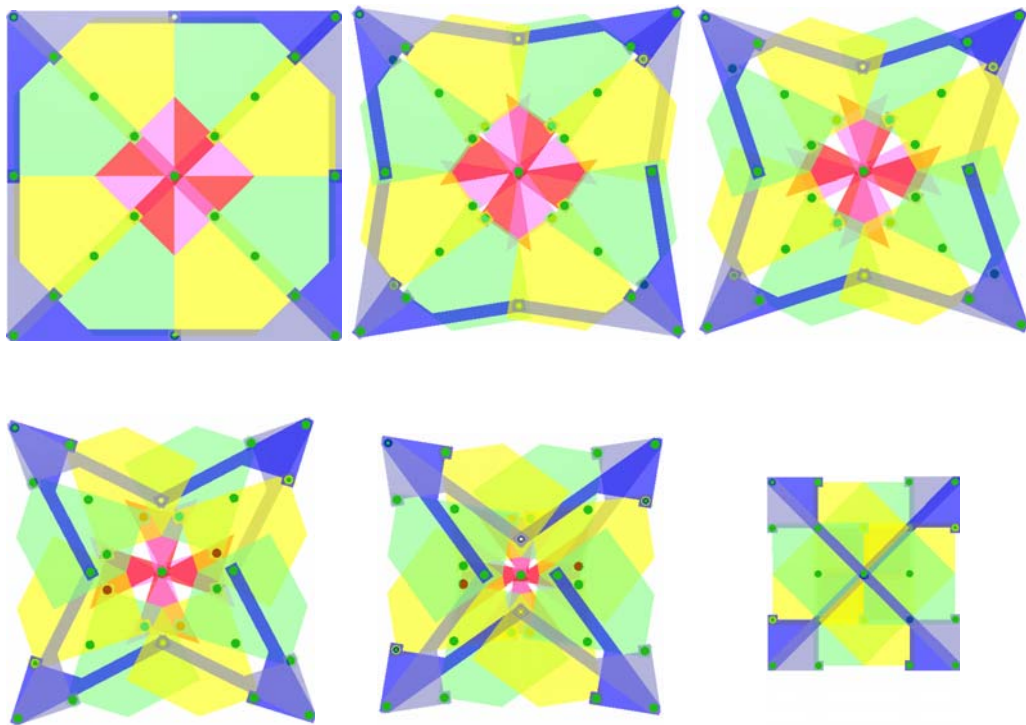


Figure 3.23 Phases of magnification of a square with links covering the surface fully at the maximal and the minimal configurations (simulation prepared using MSC.visualNastran 4D 2002)

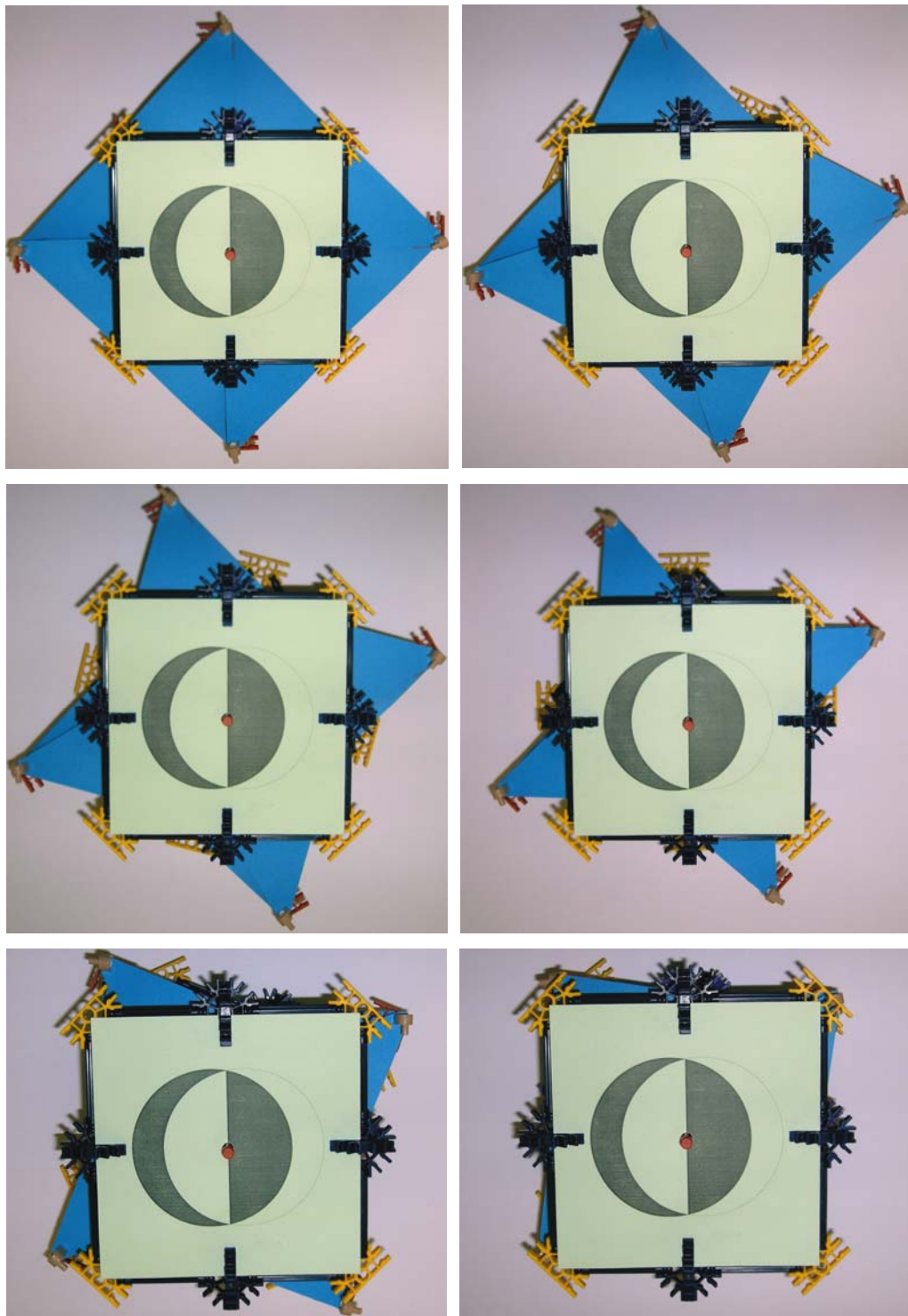


Figure 3.24 A K'nex[®] model of a linkage magnifying a square

3.7 Solid Angle Preserving Links and Polyhedron Scaling

The planar linkages can be assembled in order to obtain a desired polyhedral shape of concern. One may simply use a link at each vertex constituting n kinematic elements for a vertex of valency n . Such a link can be realized by means of a solid base which has the shape of the part of the polyhedron in the neighborhood of the vertex of concern and n pins coming out of the small scale faces of the base (Figure 3.25). The resulting linkage has a single dof, because, continuous magnification is a single dof process.

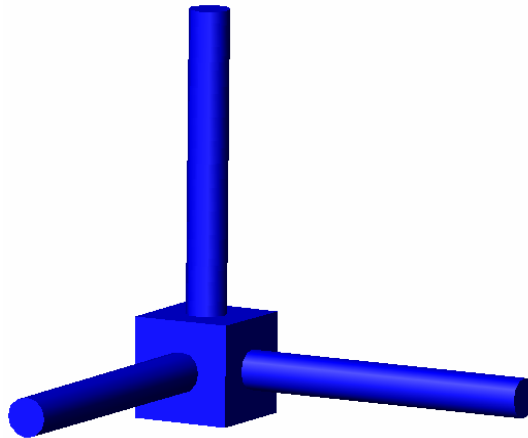


Figure 3.25 A link that can be used to connect a cubic vertex

As an example, a linkage for scaling a cube is given in Figure 3.26.

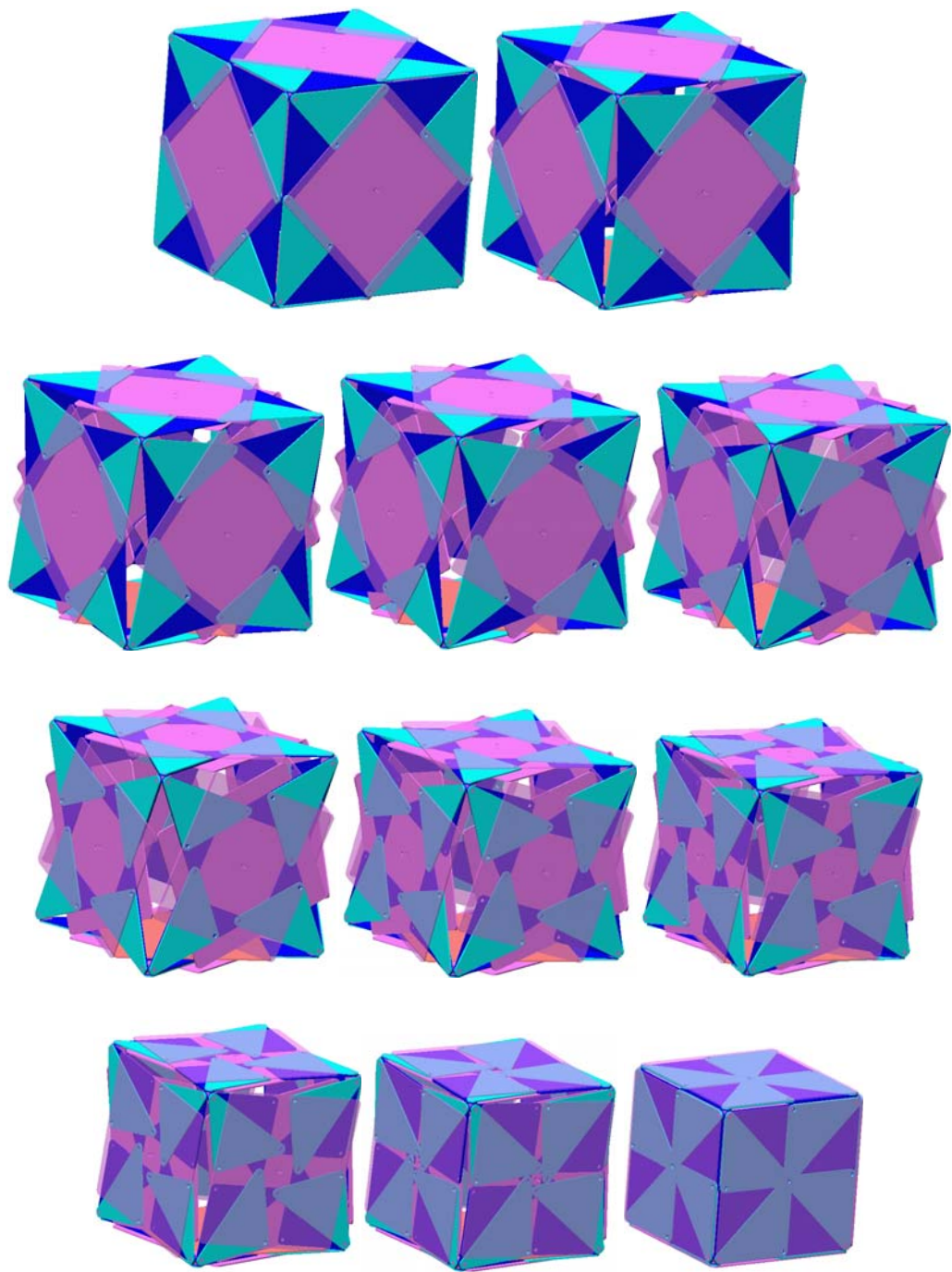


Figure 3.26 A cubic linkage (simulation prepared using MSC.visualNastran 4D 2002)

A necessary condition for a polyhedron to be magnified by means of the linkages proposed is that the polygonal faces of the polyhedron should have a circumscribing circle. For polyhedra with cyclic polygonal faces, limited information shall be given here. It can be proven that polyhedra with cyclic polygonal faces are circumscribed by a sphere, i.e. all the vertices of the polyhedron lie on a sphere if all the vertices are 3-valent. The outline of the proof is as follows: consider two neighboring cyclic polygons, sharing an edge. The perpendiculars drawn at the circumcenters intersect at a point, say O . For a 3-valent vertex, the perpendiculars corresponding to the three pairs of neighboring faces intersect at a common point (Figure 3.27). If all the vertices are 3-valent, the proof can be concluded by induction. For polyhedra having vertices with valency greater than 3, the polyhedron needs not be circumscribed by a sphere. An obvious counter example is the gyro-elongated square dipyramid (Figure 3.28).

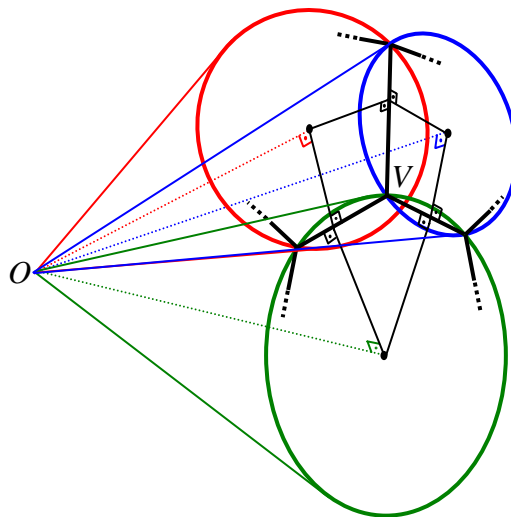


Figure 3.27 Right cones intersecting at the tip for a 3-valent vertex

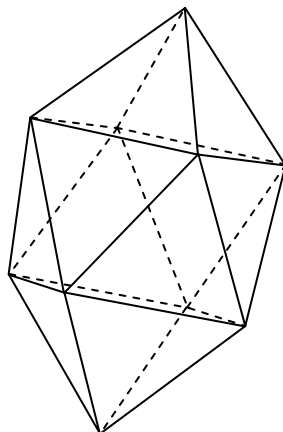


Figure 3.28 The gyro-elongated square dipyramid

Trivially, the maximum ratio of magnification of the linkages given in this chapter is the same as Hoberman's linkages with the angulated elements. The ratio is $\operatorname{cosec} \alpha$ for α being the minimum of the central angles on the faces.

CHAPTER 4

DISCUSSION AND CONCLUSIONS

This thesis work mainly deals with developing design methods for polyhedral linkages, which is the main subject of the Chapter 3. Chapter 1 is an introductory chapter including some basic definitions and theory together with the description of some previous studies related to the deployable structures. Chapter 2 focuses on polyhedral linkages, analyses the motion characteristics of them, determines the maximum ratio of magnification for each type of linkage and finally gives a comparison between the linkages.

Some of the analysis methods in Chapter 2 are new. First of all, in a big class of deployable structures, the motion of certain links are found to be the Cardan Motion, and this idea is totally new as far as polyhedral linkages are considered. Specifically, Cardan motion can be encountered in the motion of Wohlhart's linkages with planar link groups for double pyramids (Section 2.2.4.3) and linkages with planar link loops for regular polyhedra (Section 2.2.4.4) as specified in Chapter 2 and in Hoberman's linkages with angulated elements (Section 2.2.3) as revealed in the Chapter 3. The Cardan motion also can be visualized in the other designs as well, but this kind of approach was not included in Chapter 2, lacking the necessity in the analyses. Since the edges of the polyhedral shapes are magnified, if one fixes a frame at the vertices, the motion of the links moving along the edges would be a Cardan motion, as in the dipolygonids (Section 2.2.1), the Fulleroid (Section 2.2.2), Wohlhart's linkages with multiple slider-cranks (Section 2.2.4.2). The Cardan motion appears as the motion of the radially deploying/expanding links in the polyhedral star-transformers (Section 2.2.4.1).

Also, some of the linkage types presented in Chapter 2 can be considered to be the members of a family of linkages. The linkages of Wohlhart with multiple slider-cranks, planar link groups for double pyramids and planar link loops for regular polyhedra can be considered to be synthesized by constraining $n + 1$ dof linkages spatially for n -gonal faces. Many other linkages can be synthesized using the same idea, but this is behind the scope of this thesis.

Chapter 3 presents planar linkages to magnify polygonal shapes. These planar linkages are assembled spatially to obtain polyhedral linkages. In the other polyhedral linkages constructed by implementing planar linkages on the faces (the Fulleroid and the linkages of Wohlhart with multiple slider-cranks, planar link groups for double pyramids and planar link loops for regular polyhedra) all have multi-dof planar link groups, but the planar linkages presented in Chapter 3 are single dof. This fact increases the overconstrainedness of the linkages, but provides the opportunity to design the links such that the whole surfaces of the polyhedral linkages are covered at all or some configurations.

The linkages of Chapter 3 are not much successful in magnifying the polyhedral shapes in large scales. However, these linkages are advantageous in that the vertices are realized at all configurations and the edges and the faces are fully or partially realized at all configurations. It can be said that these linkages are the most successful linkages resembling the polyhedral shape of interest.

Although the planar linkages synthesized are used as the faces of the polyhedral linkages, they can be used individually for certain tasks, as well. Since the linkages of Hoberman and DSL of the University of Cambridge (Section 1.3) appear as a special case of the linkages synthesized in Chapter 3, the other types can be used in similar applications as for the existing linkages.

The linkages can either be used as planar linkages or can be projected on some surface, depending on the application. These applications include retractable roofs, satellite reflectors and toys.

The most critical contribution of this thesis work to deployable structures is the introduction of Cardan motion in the analysis and synthesis of the linkages. Although only a certain type of mechanism, i.e. the isosceles slider-crank mechanism, is used as a starting point in the synthesis of the new type of linkages in this thesis, many different mechanisms realizing the Cardan motion can be used to synthesize deployable structures. The Cardan motion can be used in planar linkages, as was done in Chapter 3, but the Cardan motion can also be used in spherical-symmetric structures as well. Research on such designs can be counted as the further possible studies for this thesis.

REFERENCES

1. Pelegrino, S., Guest, S.D., *Deployable Structures: Theory and Applications, Proc. of IUTAM-IASS Symp. Cambridge, U.K*, Kluver Akad. Publ., London, 1998.
2. *McGraw-Hill Dictionary of Scientific and Technical Terms*, 2nd Ed., McGraw-Hill, New York, 2003.
3. Söylemez, E., “Centroides of Plane Motion Mechanisms” §1.1 in *ME519 Lecture Notes*, Middle East Technical University, Ankara, 2002.
4. Department of Engineering – University of Cambridge, Deployable Structures Laboratory, <http://www-civ.eng.cam.ac.uk/dsl>, last access date: 21.08.2006.
5. Jensen, F. V., *Cover Elements for Retractable Roof Structures*, First-year report submitted to the University of Cambridge on the progress of Ph.D.-work, Darwin College, 2001.
6. Escrig, F., Brebbia, C., *Mobile and Rapidly Assembled Structures II*, First ed. Computational Mechanics Publications, Southampton, UK, 1996.
7. Hoberman Designs, Inc. and Hoberman Associates, Inc., 40 Worth Street, Suite 1680, New York, 10068, USA, <http://www.hoberman.com>, last access date: 21.08.2006.
8. Hoberman, C., *Radial Expansion/Retraction Truss Structures*, US Patent 5,024,031, 1991.
9. Hoberman, C., *Retractable Structures Comprised of Interlinked Panels*, USA Patent no. 6,739,098, 2003.
10. You, Z., Pellegrino, S., *Foldable Bar Structures*, International Journal of Solid Structures, Vol. 34-15, pp.1825-1844, 1997.
11. Kovács, F., Tarnai, T., *Foldable Bar Structures*, 2nd International PhD Symposium in Civil Engineering, Budapest, 1998.
12. Kokawa, T., *Proposal of Retractable Loop-Dome*, IASS Nagoya Symposium, 2001.

13. Kokawa, T., *Cable Scissors Arch-Marionettic Structure*, IASS Structural Morphology, 1997.
14. Buhl, T., Jensen, F. V., Pellegrino, S., *Shape Optimization of Cover Plates for Retractable Roof Structures*, Computers & Structures, Vol. 82-16, pp. 1227-1236, 2004.
15. Guest, S. D., *Tensegrities and rotating rings of tetrahedra: a symmetry viewpoint of structural mechanics*, Phil. Trans. R. Soc. Lond. A. 358, pp. 229-243, 2000.
16. Tibert, A. G., Pellegrino, S., *Deployable Tensegrity Masts*, American Institute for Aeronautics and Astronautics, 2003 - 1978.
17. Tibert, A. G., Pellegrino, S., *Furlable Reflector Concept for Small Satellites*, American Institute for Aeronautics and Astronautics, 2001 - 1261.
18. Pellegrino, S. Green, C., Guest, S.D., Watt, A., *SAR Advanced Deployable Structure*, CUED/D-STRUCT/TR191, November, 2000.
19. De Focatiis, D. S. A., Guest, S. D., *Deployable Membranes Designed From Folding Tree Leaves*, Phil. Trans. R. Soc. Lond. A, 2002.
20. Perez, A., McCarthy, J. M., *Dimensional Synthesis of Bennett Linkages*, ASME Journal of Mechanical Design, 125(1), pp. 98-104, March 2003.
21. Chen, Y., You, Z., *Mobile Assemblies Based on The Bennett Linkage*, Proc. of the Royal Society (2005) 461, pp. 1229-1245.
22. Chen, Y., You, Z., *Deployable Structures Based on the Bricard Linkages*, 45th AIAA/ASME/ASCE/AHS/ASC Structures, Structural Dynamics & Materials Conference, Palm Springs, California, 19 - 22 April 2004.
23. Department of Architecture – Massachusetts Institute of Technology, Kinetic Design Group, <http://www.robotecture.com/kdg/>, last access date: 21.08.2006.
24. Greenberg, M., *Polyhedral Linkages*, National Mathematics Magazine, Vol. 16-7, pp. 323-332, 1942.
25. Verheyen, H. F., *The Complete Set of Jitterbug Transformers and the Analysis of Their Motion*, The International Journal of Computers and Mathematics With Applications, Vol. 17, No. 1-3, pp. 203-250, 1989.

26. Wohlhart, K., *Kinematics and Dynamics of the Fulleroïd*, Multibody System Dynamics, Vol.1, No.2, pp. 241-258, Kluwer Academic Publisher, 1997.
27. Hoberman, C., *Connections to Make Foldable Structures*, US Patent 2,002,083,675, 2002.
28. Hoberman, C., *Geared Expanding Structures*, US Patent 2,004,134,157, 2004.
29. Hoberman, C., *Reversibly Expandable Structures Having Polygon Links*, US Patent 6,219,974, 2001.
30. Wohlhart, K., *Regular Polyhedral Linkages*, In: Proc. of the Second Workshop on Computational Kinematics, Seoul, Korea, 2001, pp. 239-248.
31. Wohlhart, K., *Deformable Cages*, Proceedings of the 10th World Congress on Theory of Machines and Mechanisms, Vol. 2, pp. 683-688, Oulu, Finland, 1999.
32. Wohlhart, K., *New Regular Polyhedral Linkages*, In: Proc. of SYROM, Bucharest, Rumania, pp. 365-370, 2001.
33. Wohlhart, K., *Irregular Polyhedral Linkages*, In: Proc. of 11th World Congress in Mechanism and Machine Sciences, Tianjin, China, pp. 1083-1087, April 1-4 2004.
34. Wohlhart, K., *Double Pyramidal Linkages*, the 11th International Symposium on Theory of Machines and Mechanisms, Vol. 1, pp. 293-300, Bucharest, Rumania, 2005.
35. Wohlhart, K., *Polyhedral Zig-Zag Linkages*, 9th International Symposium on Advances in Robot Kinematics, pp.351-360, 2004.
36. Agrawal, S. K., Kumar, S., Yim, M., *Polyhedral Single Degree-of-Freedom Expanding Structures: Design and Prototypes*, Journal of Mechanical Design, Vol. 124, pp. 473-478, 2002.
37. Kovács, F., Tarnai, T., *An Expandable Dodecahedron*, In: Bridge Between Civil Engineering and Architecture, Proceedings of the 4th International Colloquium on Structural Morphology. Delft University of Technology, Delft, pp. 227-234, 2000.

38. Fowler, P. W., Steer, J. I., *The Leapfrog Principle: a Rule for Electron Counts of Carbon Clusters*, Journal of the Chemical Society Chemical Communications, pp. 1403–1405, 1987.
39. Kovács, F., Tarnai, T., Fowler, P. W., Guest, S. D., *A Class of Expandable Polyhedral Structures*, International Journal of Solids and Structures, Vol. 41, pp. 1119-1137, 2004.
40. Baker, J. E., Tarnai, T., *On Modeling an Expandable Virus*, In: Proc. of 11th World Congress in Mechanism and Machine Sciences, Tianjin, China, pp. 1295-1299, April 1-4 2004.
41. Guest, S.D., Kovács, K., Tarnai, T. and Fowler, P. W., *Construction of a Mechanical Model for the Expansion of a Virus*, in Proceedings, IASS-2004, Montpellier, France, September 20–24, 2004.
42. Kovács, F., Tarnai, T., Guest, S. D., Fowler, P. W. *Double-link Expandohedra: A Mechanical Model for Expansion of a Virus*, Proceedings of the Royal Society: Mathematical, Physical & Engineering Sciences, Vol. 461(2051), pp. 3191-3202, November 8 2004.
43. Coxeter, H. S. L., Greitzer, S. M., "A Genealogy of Transformations" §4.9 in *Geometry Revisited*, Washington, DC: Math. Assoc. Amer., pp. 100-101, 1967.
44. Cromwell, P. R., *Polyhedra*, Cambridge University Press, 1997.
45. Hoberman, C., *Reversibly Expandable Doubly-Curved Truss Structure*, US Patent 4,492,700, 1990.
46. Starck, M., *Truncation's and Extension's Sequences*, http://www.ac-noumea.nc/maths/amc/polyhedr/sequences_.htm, 27.07.2006.
47. Weisstein, E. W., *Ellipse*, from MathWorld - A Wolfram Web Resource. <http://mathworld.wolfram.com/Ellipse.html>, 14.07.2006.
48. Hoberman, C., *Loop Assemblies Having a Central Link*, Patent WO02063111, 2002.

APPENDIX

SYMMETRY GROUPS OF POLYHEDRA

A rotation of $2\pi/n$ is called an *n-fold rotation*. An axis of *n-fold rotational symmetry* is an *n-fold axis*. For $n = 1$, the *identity symmetry* is obtained (identity symmetry can also be obtained by repeated reflections) [44].

Rotational symmetries also have subcategories: *cyclic symmetries* (C_n – isomorphic to the cyclic group), *dihedral symmetries* (D_n – isomorphic to the dihedral group), *tetrahedral symmetries* (T – isomorphic to the alternating group A_4), *octahedral symmetries* (O – isomorphic to the symmetric group S_4), *icosahedral symmetries* (I – isomorphic to the alternating group A_5). The details of these symmetries will not be discussed here, but it should be noted that these are the only rotational symmetries [44].

Reflection symmetries are subdivided into *bilateral symmetry* (C_s), *prismatic symmetries* (D_{nh} , D_{nv} , D_n , C_{nh} , C_{nv} , C_n ; h is for horizontal mirror planes, v is for vertical mirror planes), *compound symmetries* (S_{2n} , C_i), *cubic symmetries* (O_h , O , T_h , T_d , T) and *icosahedral symmetries* (I_h , I). An asymmetric polyhedron is denoted by C_1 . A polyhedron shall have one of these 17 types of symmetries [44]. Cromwell gives an algorithm to determine the symmetry of a polyhedron:

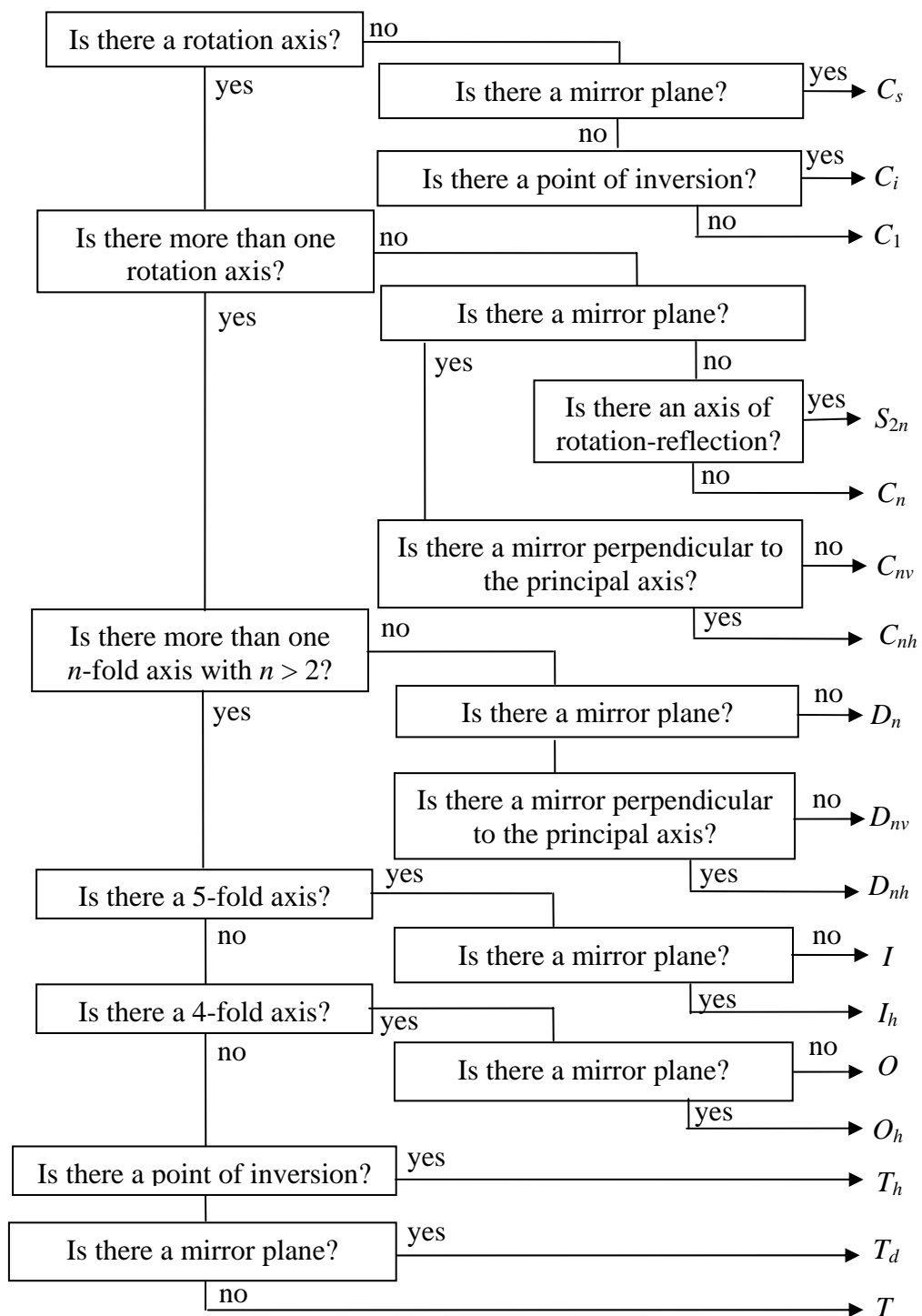


Figure A.1 An algorithm to find the symmetry group of a polyhedron [44]